Accepted Manuscript

Design, chemical synthesis of 3-(9*H*-fluoren-9-yl)pyrrolidine-2,5-dione derivatives and biological activity against enoyl-ACP reductase (InhA) and *Mycobacterium tuberculosis*

Tetiana Matviiuk, Frédéric Rodriguez, Nathalie Saffon, Sonia Mallet-Ladeira, Marian Gorichko, Ana Luisa de Jesus Lopes Ribeiro, Maria Rosalia Pasca, Christian Lherbet, Zoia Voitenko, Michel Baltas

PII: S0223-5234(13)00622-3

DOI: 10.1016/j.ejmech.2013.09.041

Reference: EJMECH 6444

To appear in: *European Journal of Medicinal Chemistry*

Received Date: 16 May 2013

Revised Date: 18 September 2013

Accepted Date: 20 September 2013

Please cite this article as: T. Matviiuk, F. Rodriguez, N. Saffon, S. Mallet-Ladeira, M. Gorichko, A.L. de Jesus Lopes Ribeiro, M.R. Pasca, C. Lherbet, Z. Voitenko, M. Baltas, Design, chemical synthesis of 3-(9*H*-fluoren-9-yl)pyrrolidine-2,5-dione derivatives and biological activity against enoyl-ACP reductase (InhA) and *Mycobacterium tuberculosis*, *European Journal of Medicinal Chemistry* (2013), doi: 10.1016/j.ejmech.2013.09.041.

Graphical Abstract

Design, chemical synthesis of 3-(9*H*-fluoren-9-yl)pyrrolidine-2,5-dione derivatives and biological activity against enoyl-ACP reductase (InhA) and *Mycobacterium tuberculosis*

Tetiana Matviiuk, Frédéric Rodriguez, Nathalie Saffon, Sonia Mallet-Ladeira, Marian Gorichko, Ana Luisa de Jesus Lopes Ribeiro, Maria Rosalia Pasca, Christian Lherbet, Zoia Voitenko, Michel Baltas

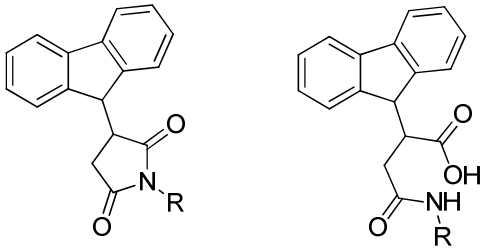

- Inhibition of InhA up to 95% at 50 μM
- Activities against TB and MDR-TB up to 2 μg/mL (5 μM)

Highlights

- A series of 3-(9*H*-fluoren-9-yl)pyrrolidine-2,5-dione derivatives were synthesized.
- Several compounds displayed good inhibitory activity against InhA.
- Some of them exhibited promising activities against *M. tuberculosis* and multi-drug resistant *M. tuberculosis* strains.

Design, chemical synthesis of 3-(9*H*-fluoren-9-yl)pyrrolidine-2,5-dione derivatives and biological activity against enoyl-ACP reductase (InhA) and *Mycobacterium tuberculosis*

Tetiana Matviiuk,[a,b,e] Frédéric Rodriguez,[a,b] Nathalie Saffon,[c] Sonia Mallet-Ladeira,[c] Marian Gorichko,[e] Ana Luisa de Jesus Lopes Ribeiro,[d] Maria Rosalia Pasca,[d] Christian Lherbet,[a,b*] Zoia Voitenko,[e] Michel Baltas[a,b*]

[a] CNRS; Laboratoire de Synthèse et Physico-Chimie de Molécules d'Intérêt Biologique, LSPCMIB, UMR-5068; 118 Route de Narbonne, F-31062 Toulouse cedex 9, France

[b.] Université de Toulouse; UPS; Laboratoire de Synthèse et Physico-Chimie de Molécules d'Intérêt Biologique, LSPCMIB; 118 route de Narbonne, F-31062 Toulouse cedex 9, France

[c.] Université de Toulouse, UPS and CNRS, ICT FR2599, 118 route de Narbonne, 31062 Toulouse cedex 9, France

[d.] University of Pavia; Dipartimento di Biologia e Biotecnologie "Lazzaro Spallanzani", via Ferrata 1, 27100 Pavia, Italy.

[e.] Taras Shevchenko National University of Kyiv, Department of Chemistry, 64 str. Volodymyrska, Kyiv, 01033, Ukraine

Fax: 33 (0)5 61556011; Tel: 33 (0)5 61556289; E-mail : lherbet@chimie.ups-tlse.fr; baltas@chimie.ups-tlse.fr

Keywords: *Mycobacterium tuberculosis*, InhA, inhibition, 3-(9*H*-fluoren-9-yl)pyrrolidine-2,5-dione, succinimide

Abstract

We report here the discovery, synthesis and screening results of a series of 3-(9*H*-fluoren-9-yl)pyrrolidine-2,5-dione derivatives as a novel class of potent inhibitors of *Mycobacterium tuberculosis* H37Rv strain as well as the enoyl acyl carrier protein reductase (ENR) InhA. Among them, several compounds displayed good activities against InhA which is one of the key enzymes involved in the type II fatty acid biosynthesis pathway of the mycobacteria cell wall. Furthermore, some exhibited promising activities against *M. tuberculosis* and multi-drug resistant *M. tuberculosis* strains.

1. Introduction

Tuberculosis (TB) is the leading cause of worldwide mortality alongside malaria and AIDS with about two million deaths every year [1]. Today, nearly one third of the global population is infected, their location being mainly in developing countries. Tuberculosis is caused by *Mycobacterium tuberculosis* (*M. tuberculosis*), and current chemotherapeutic treatments are based on the use of antibiotics, the most important being isoniazid (INH), rifampicin, pyrazinamide, ethambutol and streptomycin. The effectiveness of current anti-tuberculosis drugs to combat this infection is severely compromised by the emergence of multi- and extensively drug-resistant tuberculosis (MDR-TB [2,3] and XDR-TB [4]). Therefore, more new drugs are required to raise the probability of stopping short all forms of drug-resistant TB. It is in this context that many studies target the cell wall of mycobacteria and in particular mycolic acid biosynthesis which involves several successive enzymatic cycles and especially two related but distinct Fatty Acid Synthase (FAS) systems, FAS I and II [5]. The InhA protein (ENR, EC number: 1.3.1.9) is part of FAS II and shows an NADH-dependent enoyl-ACP reductase activity. InhA is an essential enzyme of *M. tuberculosis* and thus a good target in addition to the fact that the FAS II system is present in bacteria but is absent in humans.

We previously described the synthesis of potential inhibitors of InhA, bearing a triazole as a central core to mimick the phenolic group of triclosan [6,7]. In the course of our studies on the Michael reaction on maleimide [8,9], we focused on the succinimide fragment as a core structure of newly designed inhibitors. Molecules containing succinimide as a structural fragment have been employed numerous times in drug design. For example, 2,5-pyrrolidinediones are core structural units in naturally occurring substances and also in some approved drugs and clinical drug candidates. [10-13]. Since Komura and co-workers in 1987 reported the isolation of Andrimide as a new and highly specific antibiotic, 1,3-substituted and 3,4-disubstituted succinimides emerged as a new class of natural products with high biological activity [14]. Andrimide and Moiramide B (Fig 1) exhibit potent antibacterial activity against methicillin-resistant *Staphylococcus aureus* and a range of other antibiotic-resistant human pathogens. These natural antibiotics have been described to target the FAS system that is also the primary target for antitubercular drugs [15]. Moreover, Hirsutellone A, a natural molecule bearing a succinimide ring (Fig. 1) displayed a significant growth inhibitory activity against *M. tuberculosis* H37Rv [16]. Furthermore, the hydrophobic fluorenyl moiety has received much attention as a pharmacophore for the inhibition of InhA [17,18]. Indeed, it has already played the role of an anchor in the binding site of InhA, for example in GEQ inhibitor (Genz-10850) and is responsible for extensive hydrophobic interactions (Fig. 1).

Based on these data, we first performed *in silico* screening of the database of virtual compounds based on the succinimide core fragment as promising pharmacophore moiety. From docking studies, 3-(9*H*-fluoren-9-yl)pyrrolidine-2,5-dione was identified for the development of new antitubercular agents (Fig. 1). We report herein the synthesis and evaluation of 3-(9*H*-fluoren-9-yl)pyrrolidine-2,5-dione derivatives as inhibitors of InhA and *M. tuberculosis*.

2. Results and discussion

2.1. Chemistry

The compounds described in Table 1 were prepared by multi-step synthesis through two important intermediates **2** and **9** (Schemes 1 and 4). Compound **2** is accessible by three different methods (methods A, B C, Scheme 1). As shown in Scheme 1, the first step is the condensation of fluorenone with succinonitrile in the presence of *t*BuOK to obtain 3-(9*H*-fluoren-9-ylidene)pyrrolidine-2,5-dione **1** in good yield, as described before [19]. Two different methods were then used to reduce the double bond. Generally, reduction of unsaturated succinimides is accomplished by catalytic hydrogenation in the presence of 10% Pd/C in high yields or by using the $NiCl_2/NaBH_4$ couple [20]. In our hands, reduction of the double bond by $NiCl_2$ (7 eq) and $NaBH_4$ (8 eq) afforded compound **2** in only 40% yield (method A, Scheme 1). So, a second method was applied combining zinc powder and acetic acid under reflux conditions, leading to target compound **2** in excellent yield (97%, method B) [21]. The third method (method C, Scheme 1) used diacid **3** as an intermediate. Compound **3** was synthesized in 74% yield by fusion, from commercially available fluorene condensed with maleic anhydride, followed by aqueous basic treatment for several hours before acidification and recrystallization of the solid formed [22,23]. Then succinimide **2** was formed in 73% yield from **3** upon treatment with ammonium hydroxide at high temperature [24].

GEQ analogue **6** bearing a succinimide and an indole moiety was synthesized in three steps. First, compound **5** was synthesized in two steps starting from **2**, using a known procedure [21,25], followed by its condensation with indole-5-carboxylic acid in the presence of EDC affording **6** in 83% yield [26].

Synthesis of compounds **7a-c** and **8a-d** was performed as outlined in Scheme 3. Coupling of the succinimide intermediate **2** with acyl chloride or alkyl bromide derivatives, respectively, afforded compounds **7a-c** and **8a-d** in good yields. Note that two methods were applied to obtain compounds **8a-d** depending on the base used. When potassium hydride in DMF was used, higher yields were obtained. Both enantiomers for racemic compounds **7a** and **8a** were obtained under supercritical fluid chromatography separation, in order to compare their activities in the presence of InhA.

Another strategy was used to gain access to succinimide derivatives **11a-d** through succinic anhydride **9** (Scheme 4) obtained by treatment of diacid **3** with acetic anhydride under reflux. Compound **9** was then allowed to react with different primary amines affording amides **10a-d**. When THF is used as solvent at room temperature, good β-regioselectivity was observed. Indeed, reactions performed with *p*-F-aniline, 3,4,5-trimethoxyaniline and tryptamine afforded mixtures of α- and β-anilides in ratios of 85:15, 60:40 and 70:30 respectively, as measured by ^{1}H NMR on the crude product. Pure β-isomers

were obtained by recrystallization of the mixtures for compounds **10a** and **10c** and flash chromatography for **10b**. The same reaction was also carried out in CH_3CN to afford **10a** but in this case, a 1/1 mixture (α/β regioselectivity) as measured by ^{1}H NMR was observed. Cyclisation was then performed in acetic anhydride to afford the corresponding succinimide derivatives **11a-c** and **11e** in good yields except for hydrazinamide compound **10d** which is the result of the condensation of the front-line antitubercular drug isoniazid with succinic anhydride **9**. Attempts to cyclize it afforded a complex mixture.

2.2. Biology

2.2.1. InhA inhibition assay

Recombinant *M. tuberculosis* InhA was expressed in *E. coli* and subsequently purified according to a previously reported procedure [6]. The synthetic compounds were evaluated *in vitro* for the inhibition of InhA from *M. tuberculosis* at 50 μM by applying a commonly used method [6]. The results are shown in Table 2.

Three different series of molecules can be compared in Table 2, a first series with the succinimide ring bearing an acyl group (compounds **6, 7a-7c**), a second for succinimide substituted with an alkyl or aromatic group (compounds **8a-8d** and **11a-11e**) and a third possessing the β–amide frame (compounds **10a-10d**).

In the first series, all compounds tested presented similar activities against InhA, varying between 50% and 73% of inhibition at 50 μM, with the lowest value for the indole derivative **6** and the highest for compound **7b** bearing a C_8-alkyl chain. No notable differences were observed in the activities of each enantiomer of **7a**.

The second series presented more promising results. For compounds where an aryl ring is directly attached to the nitrogen atom of the succinimide (**11a, 11b, 11e**), the 3,5-dichloroanilide derivative **11b** emerges as an excellent InhA inhibitor (>95% inhibition at 50 μM), while the two other compounds **11a, 11e** are rather weak inhibitors. For compounds where a methylene group is first attached to the nitrogen atom (**8a-8d** and **11c**) compound **8a** is a weak inhibitor while **8b** and **8d** present moderate activities (56% and 59% respectively). The last two compounds **8c** and **11c** emerge as the best inhibitors of this series with inhibition values of 86% and 79% at 50 μM respectively. It is noteworthy that compound **8c** presents a C_8-alkyl chain, as does the best active compound (**7b**) in the first series, while compound **11c** presents a tryptamine group in comparison to the 5-indole carbonyl derivative **6** of the first series which is a moderate inhibitor.

Finally, in the third series (β–amide derivatives **10a-10d**), only compound 10c possessing the tryptamine group presents a good inhibition activity (60% at 50 μM) while the three other derivatives are inactive or weak inhibitors.

2.2.2. Bacterial growth inhibition experiments with M. tuberculosis *H37Rv strain*

All the synthesized compounds were evaluated by determining the minimal inhibitory concentration (MIC) on *M. tuberculosis* H37Rv strain (Table 3). Triclosan and GEQ were used for comparison.

The majority of the compounds displayed higher activities than GEQ. A MIC of above 40 μM was found for GEQ

which is consistent with the literature (>125 μM) [17]. Ortiz de Montellano *et al.* suggested that this high MIC could be due to a poor membrane permeability. Indeed, by replacing the piperazine moiety by a succinimide ring, GEQ analogue **6** showed a higher inhibition (MIC 39 μM). This could be due to an increased membrane permeability.

In the first series, compounds **6, 7b** and **7c** presented the same moderate activities while compound **7a** strongly inhibited *M. tuberculosis* growth (MIC 5.4 μM). In the second series, again most of the compounds are moderately active only compound **11b**, possessing a 3,5-dichloromethyl substitution on the nitrogen atom, presented a good MIC value of 19.6 μM. Finally, in the third series, compounds **10b** bearing the same 3,5-dichlorophenyl pattern and **10d** bearing the isoniazide pharmacophore emerged as very potent with MIC values of 4.7 μM and 10.0 μM respectively.

Considering the biological effects of the compounds evaluated, derivatives **7a** and **11b** might be considered as inhibitors affecting both InhA protein (though perhaps not exclusively) and *M. tuberculosis* growth. Compounds **7b**, **8c** and **11c** are the ones that affected InhA protein most but have weak effects on *M. tuberculosis* growth.

Finally, for compounds **10b** and **10d** of the third series the lack of inhibition on InhA combined with low MIC suggests that InhA is not the target. In addition, when compound **10b was** tested against multi-drug-resistant *M. tuberculosis* strains, it exhibited the same level of efficiency as for the H37Rv strain (Table 4). These results confirmed that InhA, inhibited by the adduct INH-NAD, is not the target for **10b** [27].

2.3. Docking

Compound **11b**, showing the best InhA inhibition activity, was chosen and studied using molecular docking methods. The active site of InhA is known to be flexible with states corresponding to major or minor portal opening and loop reordering (residues 195-210) [28-30]. Recently, methods were developed in the field of ligand or structure based design, which tried to take InhA's features into account [31-33] in order to improve the correlation of rankings obtained by calculation and by experimental methods. Nevertheless, it is still often difficult to correlate simulated results with relevant biological ones, in particular in the case of screening libraries including a limited number of compounds. Consequently we used molecular docking to prove the concept of modeling the hypothetical binding conformation of compound **11b** in the active site, relative to the conformation of GEQ in the same protein structure (PDB 1P44 entry) [18].

The predicted binding mode of **11b** (carbons in violet) with the best scoring results obtained from the docking studies is shown in **Fig. 2** superimposed on the crystallographic conformation of Genz-10855 (carbons in green). The inhibitor fits the binding pocket of InhA in the same manner as GEQ inhibitor. Hydrogen bonding with Tyr158 residue is highly conserved and other residues of the binding site (i.e. Met161, Phe149) showed minor fluctuations. In contrast to the GEQ position, hydrogen bonds between **11b** and cofactor NAD^+ are not observed. This corresponds to the position of the carbonyl groups of the pyrrolidine-2,5-dione ring (displaced in the direction of the minor portal, on the right in the figure) and rotation flexibility of Phe149 from the binding pocket of InhA. Finally, while the opposite configuration of **11b** is able to form hydrogen bonds with Tyr158 but also with NAD^+, it exhibits lower docking scores despite a similar orientation of the fluorene ring.

3. Conclusion

A series of 3-(9*H*-fluoren-9-yl)pyrrolidine-2,5-dione derivatives was prepared and assayed for the inhibition of InhA and *M. tuberculosis* growth. Among them, three molecules **11b**, **11c** and **8c** displayed interesting activities against InhA. Furthermore, replacing the piperazine ring of GEQ for a succinimide core led to increased activities against *M. tuberculosis* H37Rv strains with activities of up to 5 μM (compound **7a**). Finally, β–amide derivative **10b** with a MIC of 4.7 μM, was evaluated against MDR-strains and presented the same level of efficiency. Because of the ability of these new compounds to strongly affect InhA protein and/or *M. tuberculosis* growth, they could represent new leads for the development of candidate drugs.

4. Experimental

4.1. Material

Kinetic studies were performed on a Cary Bio 100. All chemicals were obtained from Aldrich or Acros Organics and used without further purification. Nuclear magnetic resonance spectra were recorded on a Bruker AC 300 spectrometer (^{1}H and ^{13}C NMR), solvent residue signals were used for calibration of spectral data. Mass spectrometry (MS) data were obtained on a ThermoQuest TSQ 7000 spectrometer. High-resolution mass spectra (HRMS) were recorded on a ThermoFinnigan MAT 95 XL spectrometer using electrospray ionization (ESI) methods. Optical rotations were measured using a sodium D line on a P-2000 series Jasco, PTC-262 polarimeter. Melting points were measured on a Mettler Toledo MP50 melting point system and are uncorrected.

Crystallographic data for compounds **2**, **8a** and **10a** were collected at a temperature of 193(2)K on a Bruker-AXS Quazar APEX II diffractometer (**2** and **8a**) using a 30 W air-cooled microfocus source (ImS) with focusing multilayer optics or on a Bruker-AXS SMART APEX II diffractometer (**10a**), with MoKα radiation (wavelength = 0.71073 Å). Phi- and omega-scans were used. The data were integrated with SAINT [34], and an empirical absorption correction with SADABS [34] was applied. The structures were solved by direct methods, using SHELXS-97 and refined using the least–squares method on F^2 [35]. All non-H atoms were treated anisotropically. The H atoms were fixed geometrically and treated as a riding model. For compound **2**, the H atom attached to nitrogen was located on a difference Fourier map and refined without any restraints. For **10a**, H atoms attached to nitrogen and to oxygen atoms were located on difference Fourier map and refined with distance restraints of N-H 0.88(1) Å and O-H 0.84(1) Å.

Full crystallographic data for the structures have been deposited with the Cambridge Crystallographic Data Centre under registration numbers CCCDC 934383 (**2**), CCDC 934384 (**8a**) and CCDC 934385 (**10a**) [36]. GEQ compound (genz-10850) was synthesized according to the literature procedure [18].

4.2. Synthesis and Characterizations

4.2.1. 3-(9H-Fluoren-9-ylidene)pyrrolidine-2,5-dione (1). To a solution of potassium *tert*-butoxide (4.70 g, 41.6 mmol) in *tert*-butanol at 50° C under nitrogen atmosphere, a solution of 9-fluorenone (5.00 g, 27.7 mmol) and succinonitrile (2.22 g, 27.7 mmol) in *t*-BuOH was added dropwise in 15 minutes. After completion the addition, the resulting mixture was

refluxed under nitrogen atmosphere for 2 h, allowed to cool and acidified with 6M hydrochloric acid (20 mL). The solution was evaporated under reduced pressure and distilled water (50 mL) was added. The crude product was extracted three times with EtOAc (3 × 30 mL). The combined organic layers were dried over Na_2SO_4, filtered and evaporated under reduced pressure. The residue was crystallized using a mixture of *i*PrOH : EtOH (3:1) to afford the desired product as a lightly green powder (6.00 g, 84%). Mp: 178–179 ^{0}C. ^{1}H NMR (300 MHz, DMSO-d_6): δ = 4.01 (s, 2H), 7.31–7.50 (m, 4H), 7.75–7.88 (m, 3H), 9.29 (d, *J* = 7.8 Hz, 1H), 11.68 (br s, 1H); ^{13}C NMR (75 MHz, DMSO-d_6): δ = 38.4, 127.4, 119.6, 120.0, 127.1, 127.9, 128.9, 130.2, 130.4, 135.3, 137.8, 140.7, 140.9, 141.3, 141.7, 171.2, 174.7; HRMS (TOF MS Cl$^+$) m/z (M+H$^+$) calculated for $C_{17}H_{12}NO_2$ 262.0868; found 262.0869.

4.2.2. 3-(9H-Fluoren-9-yl)pyrrolidine-2,5-dione (2)

Method A: 3-(9*H*-Fluoren-9-ylidene)pyrrolidine-2,5-dione **1** (0.52 g, 2 mmol) was added in one portion to a solution of $NiCl_2.6H_2O$ (3.32 g, 14 mmol) in MeOH – THF (3:1) 15 mL at 4 $^\circ$C. Then $NaBH_4$ (0.61 g, 16 mmol) was added portionwise over 30 min and the resulting black slurry was stirred overnight at room temperature. The reaction mixture was neutralized by 1M HCl to pH = 7. The black slurry was filtered through a short pad of Florisil® and washed three times with CH_2Cl_2 (3 × 15 mL). The solution was dried over $MgSO_4$, filtered and evaporated under reduced pressure. The product was further purified by flash chromatography (PE/EtOAc – 8:2) to afford white crystals (211 mg, 40%). Mp: 177-178 $^\circ$C. IR (ν, cm^{-1}) 1783, 1448, 1352; ^{1}H NMR (300 MHz, $CDCl_3$): δ = 1.45 (dd, *J* = 5.4 Hz, *J* = 18.6 Hz, 1H), 2.24 (dd, *J* = 9 Hz, *J* = 18.6 Hz, 1H), 3.77 (ddd, *J* = 3.6 Hz, *J* = 5.4 Hz, *J* = 9 Hz, 1H), 4.69 (d, *J* = 3.6 Hz, 1H), 7.23–7.50 (m, 6H), 7.77 (d, *J* = 7.5 Hz, 2H), 8.54 (br s, 1H); ^{13}C NMR (75 MHz, $CDCl_3$): δ = 30.6, 44.7, 46.2, 120.4, 120.6, 123.8, 124.9, 127.8, 127.9, 128.2, 128.6, 141.3, 141.4, 142.3, 144.1, 176.1, 179.1. HRMS (TOF MS Cl$^+$) m/z (M+H$^+$) calculated for $C_{17}H_{14}NO_2$ 264.1025; found 264.1031.

Method B: To a solution of 3-(9*H*-fluoren-9-ylidene)pyrrolidine-2,5-dione (**1**) (300 mg, 1.15 mmol) in acetic acid (10 mL, 166.7 mmol), zinc powder (225.5 mg, 3.45 mmol) was added. The reaction mixture was refluxed for 90 min. After the reaction had cooled to room temperature, the solvent was evaporated under reduced pressure and then water (15 mL) was added and stirred for 15 min. The precipitate was filtered and purified by flash chromatography (PE/EtOAc – 7:3) to afford the desired product (294 mg, 97%).

4.2.3. 2-(9H-Fluoren-9-yl)succinic acid (3). Fluorene (15.00 g, 90 mmol) and maleic anhydride (8.84 g, 92 mmol) were mixed in a round bottom flask fitted with a condenser. The mixture was stirred at 200 $^\circ$C for 6 hours. Then the reaction mixture was cooled and dissolved in a saturated solution of sodium bicarbonate. Insoluble material was filtered. Acidification of the filtrate gave 2-(9*H*-fluoren-9-yl)succinic acid, which was then recrystallized from diluted acetic acid (40% in distilled water). Yield: 18.8 g, 74%. Mp: 186–187 ^{0}C. IR (ν, cm^{-1}) 1701, 1451, 1408, 1240; ^{1}H NMR (300 MHz, DMSO-d_6): δ = 1.21 (dd, *J* = 3 Hz, *J* = 16.8 Hz, 1H), 1.93 (dd, *J* = 11.1 Hz, *J* = 16.8 Hz, 1H), 3.65 (ddd, *J* = 3 Hz, *J* = 6 Hz, *J* = 11.1 Hz, 1H), 4.46 (d, *J* = 3 Hz, 1H), 7.28–7.44 (m, 5 H), 7.66 (d, *J* = 7.2 Hz, 1H), 7.86–7.91 (m, 2H), 12.46 (br. s, 2H); ^{13}C NMR (75 MHz, DMSO-d_6): δ = 29.8, 42.8, 47.6, 120.0, 120.3, 124.3, 124.6, 127.1, 127.5, 127.7, 140.7, 141.0, 143.1, 144.5, 172.9, 174.6.

4.2.4. Method C: Synthesis of 3-(9H-fluoren-9-yl)pyrrolidine-2,5-dione (2) from 2-(9H-fluoren-9-yl)succinic acid (3). 2-To a dispersed mixture of (9*H*-Fluoren-9-yl)succinic acid **5** (3.00 g, 10.63 mmol) in 50 mL of distilled water, 9 mL of 25 % aqueous solution of ammonia (64 mmol of NH_4OH) was added gradually. The mixture was heated in an oil bath with simultaneous distillation of water. The cyclization reaction was continued at 190 ^{0}C for 2 h with transmittance of gaseous ammonia in the reaction mixture. Crude product was dispersed in saturated solution of sodium bicarbonate and extracted 3 times with ETOAc (3 × 40 mL). The organic phase was dried with $MgSO_4$, filtered and the solvent evaporated. The residue was chromatographed with elution system of EtOAC/PE – 3:7 to afford the desired product (2.00 g, 73 %).

4.2.5. Synthesis of 3-(9H-Fluoren-9-yl)-1-(1H-indol-5-ylcarbonyl)-2,5-pyrrolidinedione (6).

4.2.5.1. tert-Butyl 3-(9H-fluoren-9-yl)-2,5-dioxopyrrolidine-1-carboxylate (4). To a mixture of amide **2** (158 mg, 0.6 mmol) and DMAP (7.4 mg, 0.06 mmol) in acetonitrile, di-*tert*-butyl dicarbonate (0.16 mL, 0.7 mmol) was added dropwise at 0 $^\circ$C. The mixture was stirred at 4 $^\circ$C for 30 min and then at room temperature for 3 h (reaction progress monitored by TLC). After completion of the reaction, the solvent was evaporated and the crude product purified by flash chromatography (PE/CH_2Cl_2 – 6:4) to afford light brown crystals (124 mg, 57%). Mp: 156 °C (decomposition). ^{1}H NMR (300 MHz, $CDCl_3$): δ = 1.56 (dd, *J* = 5.7 Hz, *J* = 18.6 Hz, 1H) , 1.58 (s, 9H), 2.33 (dd, *J* = 9.3 Hz, *J* = 18.6 Hz, 1H), 3.86 (ddd, *J* = 3.9 Hz, *J* = 5.7 Hz, *J* = 9.3 Hz, 1H), 4.73 (d, *J* = 3.9 Hz, 1H), 7.14–7.50 (m, 6H), 7.17 (d, *J* = 7.5 Hz, 2H).

4.2.5.2 3-(9H-Fluoren-9-yl)-1-hydroxypyrrolidine-2,5-dione (5). To a solution of *N-Boc*-succinimide **4** (124 mg, 0.34 mmol) in acetonitrile an excess of aqueous solution of hydroxylamine (0.14 mL, 50% wt. 2.0 mmol) was added. After stirring the mixture overnight at room temperature the aqueous phase was saturated with brine and extracted three times with EtOAc (3 × 20 mL). The organic layer was dried with sodium sulfate and then evaporated under reduced pressure. The crude product was purified by flash chromatography (CH_2Cl_2/EtOAc/THF – 90:10:5) to afford compound **5** (81 mg, 85%). Mp: 149-150 °C (decomposition). ^{1}H NMR (300 MHz, DMSO-d_6): δ = 1.33 (d, *J* = 18 Hz, 1H), 2.23 (d, *J* = 18 Hz, 1H), 3.73 (s, 1H), 4.68 (s, 1H), 7.14–7.50 (m, 6H), 7.17 (t, *J* = 7.5 Hz, 2H), 8.13 (br. s, 1H).

4.2.5.3. 3-(9H-Fluoren-9-yl)-1-(1H-indol-5-ylcarbonyl)pyrrolidine-2,5-dione (6). N-Hydroxysuccinimide **5** (81 mg, 0.29 mmol) was added to a suspension of indole-5-carboxylic acid (56 mg, 0.35 mmol) in anhydrous CH_2Cl_2, then the mixture was cooled to 4 $^\circ$C and stirred for 15 minutes. Thereafter *N*-(3-dimethylaminopropyl)-*N'*-ethylcarbodiimide (EDC, 54 mg, 0.35 mmol) was added and the reaction mixture was stirred for 63 h. The reaction progress was monitored by TLC. Then the solvent was evaporated and the residue was washed with water and filtered. The brown solid was recrystallized from the mixture of *i*-PrOH/MeOH (5:1) to afford **6** as a white powder (66 mg, 56 %). Overall yield in 3 steps: 32%. Mp: 236–237 °C (decomposition). IR (ν, cm^{-1}) 3401; 1758; 1725, 1615; ^{1}H NMR (300 MHz, $CDCl_3$): δ = 1.62 (br. s, 2H), 2.38 (dd, *J* = 9.3 Hz, *J* = 18.3 Hz, 1H), 3.91 (br. s, 1H), 4.81 (s, 1H), 6.69 (s, 1H), 7.32–7.98 (m, 10H), 8.54 (s, 2H); ^{13}C NMR (75 MHz, DMSO-d_6): δ = 26.9, 103.2, 112.1, 112.3, 114.5, 120.3, 122.4, 122.8, 124.4, 124.5, 127.6, 127.7, 128.1, 128.2, 128.4, 139.6, 140.7, 141.2, 141.7, 143.5, 162.6, 169.1, 172.2. HRMS (TOF MS Cl$^+$) m/z (M+H$^+$) calculated for $C_{26}H_{18}N_2O_3$ 407.1390; found 407.1373.

4.2.6. General procedure for the acylation of 3-(9H-fluoren-9-yl)pyrrolidine-2,5-dione (7) A dispersion of NaH in mineral oil (0.4 mmol) was added to a solution of amide **2** (0.2 mmol) in THF under argon atmosphere. After 20 minutes, the

mixture was cooled to 4 °C and a solution of acyl chloride (0.3 mmol) in THF was added. The reaction mixture was stirred for 4 h at room temperature. After evaporation of solvent, the resulting residue was mixed with distilled water (30 mL) and extracted 3 times with CH_2Cl_2 (3 × 20 mL). The organic layer was dried over $MgSO_4$ and then concentrated under reduced pressure. The product was further purified by flash chromatography.

4.2.6.1. 1-Benzoyl-3-(9H-fluoren-9-yl)- 2,5-pyrrolidinedione (7a) The product was purified by flash chromatography (PE/EtOAc – 7:3) to give a light yellow amorphous solid (35 mg, 47%). Mp: 60-61 °C. IR (ν, cm^{-1}) 1787; 1717, 1697; 1448; ^{1}H NMR (300 MHz, $CDCl_3$): δ = 1.64 (dd, *J* = 5.7 Hz, *J* = 18.9 Hz, 1H), 2.40 (dd, *J* = 9.3 Hz, *J* = 18.9 Hz, 1H), 3.94 (ddd, *J* = 3.6 Hz, *J* = 5.7 Hz, *J* = 9.3 Hz, 1H), 4.80 (d, *J* = 3.6 Hz, 1H), 7.32–7.84 (m, 13H); ^{13}C NMR (75 MHz, $CDCl_3$): δ = 30.2, 44.5, 46.5, 120.6, 120.7, 123.9, 125.3, 127.9, 128.0, 128.4, 128.9, 129.1, 130.8, 131.4, 135.3, 141.2, 141.4, 142.5, 143.8, 167.6, 173.9, 176.6. HRMS (TOF MS Cl^+) m/z ($M+H^+$) calculated for $C_{24}H_{18}NO_3$ 368.1287; found 368.1300. $[\alpha]_D^{20} = +222.0$ (*c* 0.3, $CHCl_3$, ee 100 %), $[\alpha]_D^{20} = -216.0$ (*c* 0.25, $CHCl_3$, ee 97.2%). Chiral preparative SFC, Chiralpak OJ-H 5µM (10□250 mm) cellulose *tris*(4-methylbenzoate) with 15% CH_3CN, 40 °C, P=120 bar, flow rate 12 mL/min t_R *d*-enantiomer 3.27 min, *l*-enantiomer 4.40 min.

4.2.6.2. 3-(9H-Fluoren-9-yl)-1-nonanoyl-2,5-pyrrolidinedione (7b) The crude product was purified by flash chromatography (PE/EtOAc – 9:1) to give the final product as a colorless oil (50 mg, 62%). IR (ν, cm^{-1}) 1759, 1721, 1699, 1538, 1448; ^{1}H NMR (300 MHz, $CDCl_3$): δ = 0.86–0.91 (m, 5H), 1.27–1.36 (m, 5H), 1.58–1.75 (m, 4H), 2.26 (t, *J* = 9.6 Hz, 1H), 2.35 (t, *J* = 7.5 Hz, 2H), 2.88 (td, *J* = 0.9 Hz, *J* = 7.2 Hz, 2H), 3.75 (ddd, *J* = 3.6 Hz, *J* = 5.7 Hz, *J* = 9.6 Hz, 1H), 4.75 (d, *J* = 3.6 Hz, 1H), 7.23–7.50 (m, 6H), 7.78 (dd, *J* = 2.7 Hz, *J* = 7.5 Hz, 2H); ^{13}C NMR (75 MHz, $CDCl_3$) : δ = 14.3, 22.8, 23.9, 24.8, 29.1, 29.7, 31.9, 33.9, 39.3, 43.6, 46.6, 120.5, 120.7, 123.9, 124.8, 127.9, 128.4, 128.8, 141.0, 141.4, 143.8, 172.9, 173.5, 176.4. LRMS (DCI/NH_3) [$M+NH_4^+$] calculated for $C_{26}H_{33}N_2O_3$ 421.3; found 421.2.

4.2.6.3. 3-(9H-Fluoren-9-yl)-1-(2-phenylacetyl)-2,5-pyrrolidinedione (7c). The product was purified by flash chromatography (PE/EtOAc – 8:2) to give a colorless amorphous solid (30.5 mg, 40%). Mp: 52 °C. IR (ν, cm^{-1}) 1769; 1700, 1408; ^{1}H NMR (300 MHz, $CDCl_3$): δ = 1.44 (dd, *J* = 6.0 Hz, *J* = 18.6 Hz, 1H), 2.23 (dd, *J* = 9.6 Hz, *J* = 18.6 Hz, 1H), 3.68 (ddd, *J* = 3.6 Hz, *J* = 6.0 Hz, *J* = 9.6 Hz, 1H), 4.27 (s, 2H), 4.70 (d, *J* = 3.6 Hz, 1H), 7.07–7.44 (m, 11H), 7.76 (t, *J* = 7.8 Hz, 2H); ^{13}C NMR (75 MHz, DMSO-d_6): δ = 30.6, 41.2, 43.3, 46.1, 120.5, 120.6, 123.9, 124.9, 127.5, 127.8, 128.2, 128.6, 129.0, 129.8, 131.2, 133.4, 141.3, 142.7, 167.9, 174.2, 177.5. HRMS (TOF MS Cl^+) m/z ($M+H^+$) calculated for $C_{25}H_{20}NO_3$ 382.1438; found 382.1433.

4.2.7. General procedure of alkylation of 3-(9H-fluoren-9-yl)pyrrolidine-2,5-dione (8) Method A: Anhydrous potassium carbonate (110 mg, 0.8 mmol) was dispersed in dry acetone, then amide **2** (50 mg, 0.2 mmol) was added. The mixture was stirred for 20 min at room temperature. Then a solution of alkyl bromide (0.3 mmol) in acetone was added. The reaction mixture was stirred for 5 h and monitored by TLC. After completion of the reaction, the solution was filtered and the solvent evaporated under reduced pressure. The resulting residue was purified by flash chromatography. *Method B*: To a solution of 3-(9*H*-fluoren-9-yl)pyrrolidine-2,5-dione **2** (50 mg, 0.2 mmol) in dry DMF, potassium hydride (50% in paraffin) (15 mg, 0.3 mmol) was added. Then the reaction mixture was cooled to 4 °C and alkyl bromide (0.3 mmol) was

added. The reaction mixture was stirred for 3 h and filtered. The precipitate was washed with CH_2Cl_2. The filtrate was concentrated under reduced pressure and the crude product was purified by flash chromatography.

4.2.7.1. 3-(9H-Fluoren-9-yl)-1-(phenylmethyl)- 2,5-pyrrolidinedione (8a). The desired product was synthesized according to Method A and was purified by flash chromatography (PE/EtOAc – 8:2) to give **8a** as white crystals (49 mg, 69%). Mp: 159 °C. IR (ν, cm^{-1}) 1769, 1701, 1491, 1401; ^{1}H NMR (300 MHz, $CDCl_3$): δ = 1.37 (dd, *J* = 4.8 Hz, *J* = 18.6 Hz, 1H), 2.22 (dd, *J* = 9.0 Hz, *J* = 18.6 Hz, 1H), 3.67 (ddd, *J* = 3.6 Hz, *J* = 4.8 Hz, *J* = 9 Hz, 1H), 4.64–4.81 (m, 3H), 6.70–6.86 (m, 2H), 7.29–7.49 (m, 9H), 7.69–7.75 (m, 2H); ^{13}C NMR (75 MHz, $CDCl_3$): δ = 29.4, 43.6, 44.2, 46.8, 100.5, 107.2, 120.3, 123.8, 124.9, 127.6, 127.7, 128.1, 128.3, 137.7, 141.2, 141.3, 142.1, 144.2, 161.1, 176.0, 178.9; HRMS (TOF MS Cl^+) m/z ($M+H^+$) calculated for $C_{24}H_{20}NO_2$ 354.1481; found 354.1487.

$[\alpha]_D^{20} = +249.0$ (*c* 0.3, $CHCl_3$, ee 100 %), $[\alpha]_D^{20} = -256.0$ (*c* 0.25, $CHCl_3$, ee 98.5%). Chiral preparative SFC, Chiralpak OJ-H 5µM (10□250 mm) cellulose *tris*(4-methylbenzoate) with 25% CH_3CN, 40 °C, P=120 bar, flow rate 12 mL/min t_R *d*-enantiomer 2.50 min, *l*-enantiomer 5.27 min.

4.2.7.2. 1-(3,5-Dimethoxybenzyl)-3-(9H-fluoren-9-yl)-2,5-pyrrolidinedione (8b). The desired product was synthesized according to Method B and was purified by flash chromatography (PE/CH_2Cl_2 – 7:3) to give **8b** as a lightly yellow solid (60 mg, 73%). Mp: 140 °C. IR (ν, cm^{-1}) 1773; 1699, 1607, 1597, 1432; ^{1}H NMR (300 MHz, $CDCl_3$): δ = 1.37 (dd, *J* = 4.8 Hz, *J* = 18.6 Hz, 1H), 2.22 (dd, *J* = 9.3 Hz, *J* = 18.6 Hz, 1H), 3.67 (ddd, *J* = 3.6 Hz, *J* = 4.8 Hz, *J* = 9.3 Hz, 1H), 3.79 (s, 6H), 4.58 (d, *J* = 13.7 Hz, 1H), 4.67 (d, *J* = 3.6 Hz, 1H), 4.71 (d, *J* = 13.7 Hz, 1H), 6.45 (t, *J* = 2.4 Hz, 1H), 6.60 (d, *J* = 2.4 Hz, 2H), 6.79–6.83 (m, 1H), 6.92 (td, *J* = 1.2 Hz, *J* = 7.5 Hz, 1H), 7.28–7.49 (m, 4H), 7.72 (t, *J* = 7.8 Hz, 2H); ^{13}C NMR (75 MHz, $CDCl_3$): δ = 29.4, 42.8, 42.9, 46.6, 55.5, 100.5, 107.2, 120.3, 123.8, 124.9, 127.6, 127.7, 128.1, 128.3, 137.7, 141.2, 141.3, 142.1, 144.2, 161.1, 176.0, 178.9. HRMS (TOF MS Cl^+) m/z ($M+H^+$) calculated for $C_{26}H_{24}NO_4$ 414.1705; found 414.1721.

4.2.7.3. 3-(9H-Fluoren-9-yl)-1-nonyl-2,5-pyrrolidinedione (8c). The desired product was synthesized according to Method A and was purified by flash chromatography (PE/EtOAc – 9:1) to give **8c** as lightly yellow oil (37 mg, 71%). IR (ν, cm^{-1}) 2922, 2851, 1770, 1699, 1689, 1409; ^{1}H NMR (300 MHz, $CDCl_3$): δ = 0.86–0.95 (m, 5H), 1.24–1.41 (m, 9H), 1.50–1.65 (m, 4H), 2.19 (dd, *J* = 9.1 Hz, *J* = 18.6 Hz, 1H), 3.55 (t, *J* = 7.5 Hz, 1H), 3.67 (ddd, *J* = 3.6 Hz, *J* = 5.1 Hz, *J* = 9.1 Hz, 1H), 4.73 (d, *J* = 3.6 Hz, 1H), 7.17–7.24 (m, 2H), 7.31–7.51 (m, 4H), 7.76 (d, *J* = 7.5 Hz, 2H); ^{13}C NMR (75 MHz, $CDCl_3$): δ = 14.3, 22.8, 27.1, 27.9, 29.38, 29.41, 29.6, 32.0, 39.2, 43.2, 46.4, 120.4, 120.5, 123.9, 124.8, 127.6, 127.8, 128.1, 128.5, 141.3, 141.5, 142.3, 144.4, 176.5, 179.3; LRMS (DCI/NH_3) [$M+NH_4^+$] calculated for $C_{26}H_{35}N_2O_2$ 407.5; found 407.2.

4.2.7.4. 3-(9H-Fluoren-9-yl)-1-(2-oxo-2-phenylethyl)-2,5-pyrrolidinedione (8d). The product was synthesized according to Method B and was purified by flash chromatography (PE/EtOAc – 7:3) to afford **8d** as a white powder (72 mg, 94%). Mp: 186 °C. IR (ν, cm^{-1}) 2923, 1775, 1707, 1699, 1420; ^{1}H NMR (300 MHz, $CDCl_3$): δ = 1.57 (dd, *J* = 5.7 Hz, *J* = 18.6 Hz, 1H), 2.36 (dd, *J* = 9.3 Hz, *J* = 18.6 Hz, 1H), 3.90 (ddd, *J* = 3.6 Hz, *J* = 5.7 Hz, *J* = 9.3 Hz, 1H), 4.79 (d, *J* = 3.6 Hz, 1H), 4.97 (d, *J* = 17.1 Hz, 1H), 5.05 (d, *J* = 17.1 Hz, 1H), 7.30–8.03 (m, 13H); ^{13}C NMR (75 MHz, $CDCl_3$): δ = 29.6, 43.6, 44.9, 46.2, 120.4, 123.9, 125.3, 127.8, 127.9, 128.2, 128.3, 128.5, 129.1, 134.2, 134.6, 141.4, 142.2, 144.4, 175.8, 178.7, 190.1; HRMS (TOF MS Cl^+) m/z ($M+H^+$) calculated for $C_{25}H_{20}NO_3$ 382.1443; found 382.1453.

4.2.8. General procedure for the synthesis of fluorene succinamic acid derivatives (10a-d). 2-(9*H*-Fluoren-9-yl)succinic acid **3** 200 mg (0.71 mmol) was dissolved in 5 mL of acetic anhydride (49 mmol) and refluxed for 2 h 30 min. Then solvent was evaporated and residue dried under oil vacuum pump. Dried 2-(9*H*-fluoren-9-yl)succinic anhydride **9** was dissolved in 7-10 mL of dry THF and 1 equivalent of amine was added. The mixture was stirred at room temperature overnight. Thereafter solvent was evaporated and residue dissolved in saturated solution of sodium hydrocarbonate, filtered and acidified with 1M HCl. Precipitate was filtered and purified by flesh chromatography or recrystalized from ethanol to afford the product.

4.2.8.1. 3-(9H-fluoren-9-yl)dihydro-2,5-furandione (9). The product was dried under vacuum and used without further purification. A small amount was recrystallized for analysis from glacial acetic acid to give a white powder (187 mg, quantitative yield). Mp: 168°C. ^{1}H NMR (300 MHz, $CDCl_3$): δ = 1.69 (dd, *J* = 6.3 Hz, *J* = 19.2 Hz, 1 H), 2.47 (dd, *J* = 9.9 Hz, *J* = 19.2 Hz, 1 H), 3.99 (ddd, *J* = 3.6 Hz, *J* = 6.3 Hz, *J* = 9.9 Hz, 1 H), 4.70 (d, *J* = 3.6 Hz, 1 H), 7.30–7.51 (m, 6 H), 7.77–7.81 (m, 2H). ^{13}C NMR (75 MHz, DMSO-d_6): δ = 29.2, 44.1, 46.2, 120.5, 120.6, 123.7, 124.6, 127.9, 128.3, 128.5, 129.0, 140.2, 142.2, 143.1, 143.8, 169.3, 173.2.

4.2.8.2. 2-(9H-Fluoren-9-yl)-4-(4-fluoroaniline)-4-oxobutanoic acid (10a). The product was crystallized from EtOH to give a white powder (113 mg, 86%). Mp: 171 °C decomposition. IR (ν, cm^{-1}) 3317, 1702, 1669, 1620, 1557, 1510; ^{1}H NMR (300 MHz, DMSO-d_6): δ = 1.28 (d, *J* = 15.6 Hz, 1 H), 2.15 (dd, *J* = 11.4 Hz, *J* = 15.9 Hz, 1 H), 3.85 (d, *J* = 10.5 Hz, 1 H), 4.52 (br. s, 1 H), 6.90–8.05 (m, 12 H), 9.70 (br. s, 1 H), 12.86 (br. s, 1 H). ^{1}H NMR (300 MHz, CD_3OD): δ = 1.41 (dd, *J* = 3.6 Hz, *J* = 15.9 Hz, 1 H), 2.21 (dd, *J* = 10.5 Hz, *J* = 15.9 Hz, 1 H), 3.94 (ddd, *J* = 3.9 Hz, *J* = 6.6 Hz, *J* = 10.5 Hz, 1 H), 4.60 (d, *J* = 3.6 Hz, 1 H), 6.87–7.86 (m, 12 H) ; ^{13}C NMR (75 MHz, $CDCl_3$): δ = 32.6, 44.3, 49.4, 115.8, 116.1, 120.9, 121.1, 122.8, 122.9, 125.4, 126.1, 128.1, 128.6, 128.8, 128.9, 136.0, 142.6, 143.1, 144.7, 146.0, 160.0 (d, *J* = 241.8 Hz), 172.5, 177.2. HRMS (TOF MS Cl$^+$) m/z (M+H$^+$) calculated for $C_{23}H_{19}NO_3F$ 376.1349; found 376.1360. ^{19}F NMR (300 MHz, DMSO-d_6): δ = -116.0.

4.2.8.3. 4-(3,5-Dichloroanilino)-2-(9H-fluoren-9-yl)-4-oxobutanoic acid (10b). The crude product was crystallized from EtOAc to afford light brown crystals (140 mg, 69%). Mp: 98–99 °C (decomposition). IR (ν, cm^{-1}) 1705, 1670, 1586, 1539, 1447, 1410; ^{1}H NMR (300 MHz, DMSO-d_6): δ = 1.29 (dd, *J* = 3.0 Hz, *J* = 16.5 Hz, 1H), 2.11 (dd, *J* = 11.1 Hz, *J* = 16.5 Hz, 1H), 3.82 (ddd, *J* = 3.0 Hz, *J* = 6.3 Hz, *J* = 11.1 Hz, 1H), 4.52 (d, *J* = 3.0 Hz, 1H), 7.17 (t, *J* = 1.9 Hz, 1H), 7.31–7.47 (m, 7H), 7.63–7.68 (m, 1H), 7.90 (t, *J* = 7.2 Hz, 2H), 9.98 (s, 1H), 12.93 (br. s, 1H); ^{13}C NMR (75 MHz, DMSO-d_6): δ = 31.8, 42.2, 47.5, 116.8, 120.1, 122.1, 124.3, 124.7, 127.2, 127.6, 127.7, 133.9, 140.7, 141.1, 141.3, 143.3, 144.5, 170.2, 174.8; HRMS (TOF MS Cl$^+$) m/z (M+H$^+$) calculated for [$C_{23}H_{18}NO_3Cl_2$] 426.0664; found 426.0656.

4.2.8.4. 2-(9H-Fluoren-9-yl)-4-{[2-(1H-indol-3-yl)ethyl]amino}-4-oxobutanoic acid (10c). The product was purified by crystallization from mixture i-PrOH /EtOH – 3:1 to give brown crystals (160 mg, 83%). Mp: 123 °C decomposition. IR (ν, cm^{-1}) 1709, 1618, 1535, 1448; ^{1}H NMR (300 MHz, $CDCl_3$): δ = 1.20 (dd, *J* = 2.4 Hz, *J* = 15.9 Hz, 1H), 1.94 (dd, *J* = 10.8 Hz, *J* = 15.9 Hz, 1H), 2.76 (t, *J* = 6.6 Hz, 2H), 3.26–3.45 (m, 2H), 3.68–3.74 (m, 1H), 4.67 (d, *J* = 2.1 Hz, 1H), 5.32 (t, *J* = 6.0 Hz, 1H), 6.80 (s, 1H), 6.99–7.55 (m, 10H), 7.69 (d, *J* = 7.5 Hz, 2H), 8.14 (br. s, 1H); ^{13}C NMR (75 MHz, $CDCl_3$): δ = 24.9, 31.6, 40.0, 44.0, 48.0, 111.4, 112.2, 118.6, 119.6, 120.0, 122.3, 122.4, 124.3, 125.9, 127.2, 127.5, 127.6, 127.9, 136.4,

141.5, 141.7, 143.3, 144.6, 173.2, 176.6; HRMS (TOF MS Cl^+) m/z ($M+H^+$) calculated for [$C_{27}H_{25}N_2O_3$] 425.1865; found 425.1869.

4.2.8.5. 2-(9H-Fluoren-9-yl)-4-(2-isonicotinoylhydrazino)-4-oxobutanoic acid (10d). The product was crystallized from a mixture of *i*-PrOH – MeOH (8:2) to give a white powder. (100 mg, 58 %). Mp: 158 °C. IR (ν, cm^{-1}) 1704, 1651, 1450; ^1H NMR (300 MHz, $CDCl_3$): δ = 1.56 (dd, *J* = 5.4 Hz, *J* = 18.6 Hz, 1H), 2.40 (dd, *J* = 9.0 Hz, *J* = 18.6 Hz, 1H), 3.91 (ddd, *J* = 3.6 Hz, *J* = 5.4 Hz, *J* = 9.0 Hz, 1H), 4.76 (d, *J* = 3.6 Hz, 1H), 7.17–7.80 (m, 12H), 8.73 (br. s, 2H), 9.43 (s, 1H); ^{13}C NMR (75 MHz, DMSO-d_6): δ = 28.8, 42.1, 47.7, 120.1, 120.4, 122.5, 124.4, 124.7, 127.2, 127.6, 127.8, 140.8, 141.1, 141.7, 143.4, 144.6, 148.1, 163.0, 170.0, 174.6; HRMS (TOF MS Cl^+) m/z ($M+H^+$) calculated for $C_{23}H_{18}N_3O_3$ 384.1348; found 384.1343.

4.2.9. General procedure for cyclization of fluorene succinamic acid derivatives (11a-c-11e). 2-(9*H*-Fluoren-9-yl)succinamic acid **10** (0.7 mmol) was dissolved in acetic anhydride (39 mmol, 4 mL). The solution was refluxed for 30 minutes. Then the solvent was evaporated under reduced pressure. To the crude product, a saturated solution of sodium hydrocarbonate ($NaHCO_3$, 10 mL) was added and the resulting solution was extracted 3 times with EtOAc (3 × 20 mL). The combined organic layers were dried with magnesium sulfate and the solvent was evaporated under reduced pressure. Crude products were purified by flesh chromatography.

4.2.9.1. 3-(9H-Fluoren-9-yl)-1-(4-fluorophenyl)-2,5-pyrrolidinedione (11a) The crude product was purified by flash chromatography (PE/EtOAc – 7:3) to give a white powder (80 mg, 87%). Mp: 231 °C decomposition. IR (ν, cm^{-1}) 1778, 1705, 1506, 1447, 1391; ^1H NMR (300 MHz, $CDCl_3$): δ = 1.56 (dd, *J* = 5.1 Hz, *J* = 18.9 Hz, 1H), 2.38 (dd, *J* = 9.1 Hz, *J* = 18.9 Hz, 1H), 3.87 (ddd, *J* = 3.9 Hz, *J* = 5.1 Hz, *J* = 9.1 Hz, 1H), 4.80 (d, *J* = 3.9 Hz, 1H), 7.18–7.55 (m, 10H), 7.78–7.82 (m, 2H); ^{13}C NMR (75 MHz, $CDCl_3$): δ = 29.6, 43.3, 46.7, 116.3, 116.6, 120.5, 120.7, 123.9, 124.7, 127.7, 127.9, 128.3, 128.4, 128.5, 128.8, 141.3, 141.4, 142.5, 144.1, 163.5 (d, *J* = 248.7 Hz), 175.3, 178.1. HRMS (TOF MS Cl^+) m/z ($M+H^+$) calculated for $C_{23}H_{17}NO_2F$ 358.1243; found 358.1259. ^{19}F NMR (300 MHz, $CDCl_3$): δ = -116.8.

4.2.9.2. 1-(3,5-Dichlorophenyl)-3-(9H-fluoren-9-yl)-2,5-pyrrolidinedione (11b). The product was purified by flash chromatography (PE/EtOAc – 65:35) to give a lightly brown powder (45 mg, 83%). Mp: 196 °C decomposition. IR (ν, cm^{-1}) 1780, 1713, 1704, 1576, 1448, 1381; ^1H NMR (300 MHz, $CDCl_3$): δ = 1.51 (dd, *J* = 5.1 Hz, *J* = 18.9 Hz, 1H), 2.32 (dd, *J* = 9.3 Hz, *J* = 18.9 Hz, 1H) 3.79 (ddd, *J* = 3.9 Hz, *J* = 5.1 Hz, *J* = 9.3 Hz, 1H), 4.71 (d, *J* = 3.9 Hz, 1H), 7.19–7.47 (m, 9H), 7.71–7.75 (m, 2H); ^{13}C NMR (75 MHz, $CDCl_3$): δ = 29.6, 43.3, 46.7, 116.4, 116.7, 120.5, 120.7, 123.9, 124.7, 127.7, 127.9, 128.3, 128.4, 128.5, 128.8, 141.3, 141.4, 142.5, 144.1, 160.8, 164.1, 175.3, 178.1; HRMS (TOF MS Cl^+) m/z ($M+H^+$) calculated for $C_{23}H_{16}NO_2Cl_2$ 408.0558; found 408.0569.

*4.2.9.3. 3-(9H-Fluoren-9-yl)-1-[2-(1H-indol-3-yl)ethyl]-2,5-pyrrolidinedione (11c). T*he product was purified by flash chromatography (CH_2Cl_2/EtOAc/THF – 85:15:5) to give purple crystals (39 mg, 75%). Mp: 182 °C decomposition. IR (ν, cm^{-1}) 3341, 1766, 1687, 1450, 1436, 1333; ^1H NMR (300 MHz, $CDCl_3$): δ = 1.37 (dd, *J* = 5.1 Hz, *J* = 18.6 Hz, 1H), 2.17 (dd, *J* = 9.0 Hz, *J* = 18.6 Hz, 1H), 3.12 (m, 2H), 3.61 (ddd, *J* = 3.6 Hz, *J* = 5.1 Hz, *J* = 9.0 Hz, 1H), 3.91 (t, *J* = 7.8 Hz, 2H),

4.71 (d, *J* = 3.6 Hz, 1H), 7.00 (td, *J* = 1.2 Hz, *J* = 7.5 Hz, 1H), 7.12–7.49 (m, 9H), 7.73–7.77 (m, 3H), 8.01 (br. s, 1H); ^{13}C NMR (75 MHz, $CDCl_3$): δ = 23.6, 29.5, 39.5, 43.1, 46.4, 111.3, 112.4, 118.9, 119.8, 1120.4, 120.5, 122.2, 122.4, 123.9, 124.7, 127.6, 127.7, 128.5, 136.0, 136.4, 141.4, 142.2, 144.3, 176.4, 179.2; HRMS (TOF MS Cl^+) m/z ($M+H^+$) calculated for [$C_{27}H_{23}N_2O_2$] 407.1760; found 407.1759.

4.2.9.4. 3-(9H-Fluoren-9-yl)-1-(3,4,5-trimethoxyphenyl)-2,5-pyrrolidinedione (11e). The product was purified by flash chromatography (CH_2Cl_2/EtOAc – 9 : 1) to give a white powder (49 mg, 83%). Mp: 166–167 ^{0}C decomposition. IR (ν, cm^{-1}) 1719, 1658, 1586, 1538, 1441, 1410; ^{1}H NMR (300 MHz, $CDCl_3$): δ = 1.58 (dd, *J* = 5.1 Hz, *J* = 18.9 Hz, 1H), 2.39 (dd, *J* = 9.3 Hz, *J* = 18.9 Hz, 1H), 3.88 (s, 10 H), 4.80 (d, *J* = 3.9 Hz, 1 H), 6.48 (s, 2H), 7.28–7.83 (m, 8H); ^{13}C NMR (75 MHz, $CDCl_3$): δ = 29.7, 43.2, 46.8, 56.4, 61.0, 104.4, 120.5, 120.8, 123.9, 124.9, 127.4, 127.9, 128.3, 128.8, 141.4, 142.6, 144.0, 153.8, 175.5, 178.3; HRMS (TOF MS Cl^+) m/z ($M+H^+$) calculated for $C_{26}H_{24}NO_5$ 430.1654; found 430.1647.

4.3. Biology

4.3.1. InhA expression and purification.

The production and purification were performed as described [6].

4.3.2. Inhibition Kinetics

Stock solutions of all compounds were prepared in DMSO such that the final concentration of this co-solvent was constant at 5% v / v in a final volume 1 mL for all kinetic reactions. Kinetic assays using *trans*-2-dodecenoyl-Coenzyme A (DD-CoA) and wild-type InhA were performed as described [6]. Reactions were initiated by addition of InhA (100 nM final) to solutions containing DD-CoA (50 μM final), inhibitor, and NADH (250 μM final) in 30 mM PIPES, 150 mM NaCl, pH 6.8, buffer. Control reactions were carried out with the same conditions as described above but without inhibitor. The inhibitory activity of each derivative was expressed as the percentage inhibition of InhA activity (initial velocity of the reaction) with respect to the control reaction without inhibitor. All activity assays were performed in triplicate.

4.3.3. Growth conditions

M. tuberculosis H37Rv strain was grown either in Middlebrook 7H9 broth (Difco) supplemented with 0.05% Tween 80, or on Middlebrook 7H11 agar (Difco) supplemented with 0.5% glycerol, both supplemented with 10% (vol/vol) OADC. All compounds were dissolved in dimethyl sulfoxide (DMSO). Mycobacterial cultures were usually grown at 37°C without shaking.

4.3.4. MIC determinations

A single colony of *M. tuberculosis* strain was used to inoculate complete Middlebrook 7H9. The cultures were incubated at 37°C until exponential growth phase (~10^8 CFU/mL) was reached, corresponding to an OD_{600nm} ranging from 0.8 and 1.0. Cultures were diluted to the final concentration of about 10^7 CFU/mL; 1 μL of the diluted cultures was then streaked onto plates containing two-fold serial dilutions of appropriate compound. MIC values were scored as the lowest drug concentrations inhibiting bacterial growth. All assays were repeated three times.

M. tuberculosis clinical isolates and drug susceptibility testing. Three *M. tuberculosis* MDR isolates were collected at the Sondalo Division of the Valtellina and Valchiavenna, Italy, hospital authority in the 2012. Their resistance profile is shown in Table 3. All clinical isolates were grown in BACTEC™ MGIT™ 960 and Lowenstein–Jensen slants. Drug susceptibility testing for all first-line antitubercular drugs was performed with the BACTEC™ MGIT™ 960 System (Becton-Dickinson Diagnostic Systems, Sparks, Maryland). MIC determination to second-line drugs was also performed by the MGIT™ 960 System.

4.3.5. Molecular docking studies

Molecular graphics and some analyses were performed with the UCSF Chimera package. Chimera is developed by the Resource for Biocomputing, Visualization, and Informatics at the University of California, San Francisco (supported by NIGMS P41-GM103311). The Protein structures were prepared (structure checks, rotamers, hydrogenation) using Accelrys Discovery Studio 3.0 client and UCSF Chimera 1.6.2 or 1.7 (Dock Prep without minimization). The Ligand structures were extracted (SciTE text editor) from aligned protein structure or sketched using ChemAxon Marvin 5.5 and prepared (hybridization, hydrogenation) using Discovery Studio 3.0 client.

The entry 1P44 (chain A, X-ray, 2.7 Å resolution) [18] from Protein Data Bank [37] includes NAD^+/NADH and GEQ in the active site and was chosen as InhA molecular structure.

We used Molegro Virtual Docker 5.5 software (CLC Bio, Aarhus, Denmark) for docking studies. The cavity detection algorithm implemented in MVD was used to optimize the definition of a 15 Å (radius) potential binding site but not for constraining results to the cavity. The corresponding crystallographic NAD^+ molecules were used as cofactor using the MVD features and no water molecules were taken into account. The side chains around compound 11b (16 residues) were set flexible in calculation. A combination of different calculation (Moldock SE, Moldock Optimizer) schemes and scoring schemes (Moldock, Plants) was used [38,39] giving similar best poses for GEQ and **11b**. After calculation, minimization steps (global, lateral chain, ligands) and optimization of H bonds, were done using MVD default features followed by clustering. Using these conditions the crystallographic conformation of GEQ was reproduced with a good accuracy (less than 0.7 Å of RMSD with reference structure 1P44a) and nearly no fluctuation of flexible residues including Tyr158 was recorded. Subsequently these parameters were applied to compound **11b** and the best (GEQ like, Moldock and Rerank scores) poses were retained for further analysis.

Acknowledgments

We thank the CNRS and University Paul Sabatier for financial support. T. M. was supported by the French Embassy in Kiev (Ukraine), the investigations having been performed within the framework of the GDRI (Groupement de recherche Franco-Ukrainien en Chimie Moléculaire).

References and Notes.

[1] World Health Organization : http://www.who.int/tb/publications/global_report/2010/en/index.html

[2] M.H. Cynamon, Y. Zhang, T. Harpster, S. Cheng, M.S. DeStefano, High-dose isoniazid therapy for isoniazid-resistant murine *Mycobacterium tuberculosis* infection, Antimicrob. Agents Chemother. 43 (1999) 2922-2924.

[3] P. Bemer-Melchior, A. Bryskier, H.B. Drugeon, Comparison of the in vitro activities of rifapentine and rifampicin against *Mycobacterium tuberculosis* complex, J. Antimicrob. Chemother. 46 (2000) 571-576.

[4] A. Jain, R. Mondal, Extensively drug-resistant tuberculosis: current challenges and threats, FEMS Immunol. Med. Microbiol. 53 (2008) 145-150.

[5] H. Marrakchi, F. Bardou, M.-A. Lanéelle, M. Daffé, The Mycobacterial Cell Envelope, D. Mamadou and J.M. Reyrat, eds. (2008**)** 41-62. ASM Press, Washington, DC; (b) Bloch, K. Adv. Enzymol. Relat. Areas Mol. Biol. 45 (1977) 1-84.

[6] C. Menendez, S. Gau, C. Lherbet, F. Rodriguez, C. Inard, M.R. Pasca, M. Baltas, Synthesis and biological activities of triazole derivatives as inhibitors of InhA and antituberculosis agents, Eur. J. Med. Chem. 46 (2011) 5524-5531.

[7] C. Menendez, A. Chollet, F. Rodriguez, C. Inard, M.R. Pasca, C. Lherbet, M. Baltas, Chemical synthesis and biological evaluation of triazole derivatives as inhibitors of InhA and antituberculosis agents, Eur. J. Med. Chem. 52 (2012) 275-283.

[8] T.V. Matviiuk, O.M. Silenko, Z. Voitenko, Catalytic Michael reaction in heterocyclic systems, Bulletin of Kiev National Taras Shevchenko University 47 (2008) 31–33.

[9] T. Matviiuk, M. Gorichko, A. Kysil, S. Shishkina, O. Shishkin, Z.Voitenko, Catalysis by lithium perchlorate enables double-conjugate addition of electron-deficient maleimides to 2-aminopyridines and 2-aminothiazoles, Synth. Comm. 42 (2012) 3304–3310.

[10] H.S. Snyder, Drugs and the Brain; Scientific American Library: New York, 1986.

[11] A.M. Crider, T.M. Kolczynski, K.M. Yates, Synthesis and anticancer activity of nitrosourea derivatives of phensuximide, J. Med. Chem. 23 (1980) 324–326.

[12] Y. Ando, E. Fuse, W.D. Figg, Thalidomide metabolism by the CYP2C subfamily, Clin. Cancer Res. 8 (2002) 1964–1973.

[13] C. Freiberg, H.P. Fischer, N.A. Brunner, Discovering the mechanism of action of novel antibacterial agents through transcriptional profiling of conditional mutants, Antimicrob. Agents Chemother. 49 (2005) 749 –759.

[14] A. Fredenhagen, S. Y. Tamura, P. T. M. Kenny, H. Komura, Y. Naya, K. Nakanishi, K. Nishiyama, M. Sugiura, H. Kita, Andrimid, anew peptide antibiotic produced by an intracellular bacterial symbiont isolated from a brown planthopper, J. Am. Chem. Soc. 109 (1987) 4409 –4411.

[15] C. Freiberg, N.A. Brunner, G. Schiffer, T. Lampe, J. Pohlmann, M. Brands, M. Raabe, D. Häbich, K. Ziegelbauer, Identification and characterization of the first class of potent bacterial acetyl-CoA carboxylase inhibitors with antibacterial activity, J. Biol. Chem. 279 (2004) 26066.

[16] M. Isaka, N. Rugseree, P. Maithip, P. Kongsaeree, S. Prabpai, Y. Thebtaranonth, Hirsutellones A-E, antimycobacterial alkaloids from the insect pathogenic fungus *Hirsutella nivea* BCC 2594, Tetrahedron 61 (2005) 5577–558.

[17] X. He, A. Alian, P.R. Ortiz de Montellano, Inhibition of the Mycobacterium tuberculosis enoyl acyl carrier protein reductase InhA by arylamides, Bioorg. Med. Chem. 15 (2007) 6649–6658.

[18] M.R. Kuo, H.R. Morbidoni, D. Alland, S.F. Sneddon, B.B. Gourlie, M.M. Staveski, M. Leonard, J.S. Gregory, A.D. Janjigian, C. Yee, J.M. Musser, B. Kreiswirth, H. Iwamoto, R. Perozzo, W.R. Jacobs Jr., J.C. Sacchettini, D.A. Fidock, Targeting tuberculosis and malaria through inhibition of enoyl reductase: compound activity and structural data, J. Biol. Chem. 278 (2003) 20851–20859.

[19] M.L. Lopez-Rodrıguez, J.M. Morcillo, T.K. Rovat, E. Fernandez, B. Vicente, A.M. Sanz, M. Hernandez, L. Orensanz, Synthesis and structure-activity relationships of a new model of arylpiperazines. 4. 1-[omega-(4-Arylpiperazin-1-yl)alkyl]-3-(diphenylmethylene) - 2, 5-pyrrolidinediones and -3-(9H-fluoren-9-ylidene)-2, 5-pyrrolidinediones: study of the steric requirements of the terminal amide fragment on 5-HT1A affinity/selectivity, J. Med. Chem. 42 (1999) 36–49.

[20] R. Ballini, G. Bosica, G. Cioci, D. Fiorini, M. Petrini, Conjugate addition of nitroalkanes to *N*-substituted maleimides. Synthesis of 3-alkylsuccinimides and pyrrolidines, Tetrahedron 59 (2003) 3603–3608.

[21] C.-F. Cheng, Z-C. Lai, Y.-J. Lee, Total synthesis of (±)-camphorataimides and (±)-himanimides by $NaBH_4/Ni(OAc)_2$ or Zn/AcOH stereoselective reduction, Tetrahedron 64 (2008) 4347–4353.

[22] E. Bergman, M. Orchin, Synthesis of Fluoranthene and its Derivatives, J. Am. Chem. Soc. 71 (1949) 1917-1918.

[23] A. Sieglitz, H. Troester, P. Boehme, Über 3-Hydroxy-fluoranthen-carbonsäuren-(1), -(2) und -(10), Chemische Berichte 95(1962) 3013-3029.

[24] J. Obniska, I. Chlebek, J. Pichor, M. Kopytko, K. Kaminski, Synthesis, physicochemical and anticonvulsant properties of new *N*-[(4-arylpiperazin-1-yl)alkyl]-3-phenyl- and 3-(3-methyl-phenyl)-pyrrolidine-2,5-diones, Acta Pol. Pharm. 66 (2009) 639–647.

[25] C. Einhorna, J. Einhorna, C. Marcadal-Abbadi, Mild and convenient one pot synthesis of *N*-hydroxyimides from *N*-unsubstituted imides, Synth. Comm. 31 (2001) 741–748.

[26] E. Palma, J.D.G. Correia, A. Domingos, I. Santos, New mixed-ligand Re^{V} complexes with bis(2-mercaptoethyl) sulfide and functionalized thioimidazolyl ligands, Eur. J. Inorg. Chem. (2002) 2402–2407.

[27] R. Rawat, A. Whitty, P.J. Tonge, The isoniazid-NAD adduct is a slow, tight-binding inhibitor of InhA, the *Mycobacterium tuberculosis* enoyl reductase: Adduct affinity and drug resistance, PNAS 100 (2003) 13881-13886.

[28] D.A. Rozwarski, C. Vilcheze, M. Sugantino, R. Bittman, C. Sacchettini. Crystal Structure of the Mycobacterium tuberculosis Enoyl-ACP Reductase, InhA, in Complex with NAD+ and a C16 Fatty Acyl Substrate, J. Biol. Chem. (1999) 274, 15582–15589.

[29] J.S. Freundlich, F. Wang, C. Vilcheze, G. Gulten, R. Langley, G.A. Schiehser, D.P. Jacobus, W.R. Jr Jacobs, J.C. Sacchettini, Triclosan derivatives: towards potent inhibitors of drug-sensitive and drug-resistant Mycobacterium tuberculosis, Chem. Med. Chem. 4 (2009) 241–248.

[30] S.R. Luckner, N. Liu, C.W. am Ende, P.J. Tonge, C. Kisker, A Slow, Tight Binding Inhibitor of InhA, the Enoyl-Acyl Carrier Protein Reductase from *Mycobacterium tuberculosis*, J. Biol. Chem. 285 (2010) 14330-14337.

[31] R.C. Barros, A.T. Winck, K.S. Machado, M.P. Basgalupp, A. de Carvalho, D.D. Ruiz, O.N de Souza., Automatic design of decision-tree induction algorithms tailored to flexible-receptor docking data, BMC Bioinformatics 13 (2012) 310-323.

[32] S.L Kinnings, N. Liu, P.J. Tonge, R.M. Jackson, L Xie, P.E. Bourne, A machine learning-based method to improve docking scoring functions and its application to drug repurposing, J. Chem. Inf. Model. 51 (2011) 408–419.

[33] J.L. Stigliani, V. Bernardes-Génisson, J. Bernadou, G. Pratviel, Cross-docking study on InhA inhibitors: a combination of Autodock Vina and PM6-DH2 simulations to retrieve bio-active conformations, Org. Biomol. Chem. 10 (2012) 6341-6349.

[34] Bruker, (2006) SAINT and SADABS. Bruker AXS Inc., Madison, Wisconsin, USA

[35] G.M. Sheldrick, A short history of SHELX, Acta Cryst. A64 (2008) 112-122.

[36] Copy of the data can be obtained, free of charge, on application to CCDC, 12 Union Road, Cambridge CB2 1EZ, UK (fax: +44 1223336033 or email: deposit@ccdc.cam.ac.uk).

[37] H.M. Berman, J. Westbrook, Z. Feng, G. Gilliland, T.N. Bhat, H. Weissig, I.N. Shindyalov, P.E. Bourne, The Protein Data Bank, Nucl. Acids Res. 28 (2000) 235-242 (www.pdb.org).

[38] R. Thomsen, M.H. Christensen, MolDock: A new technique for high-accuracy molecular docking, J. Med. Chem. 49 (2006) 3315–3321.

[39] O. Korb, T. Stützle, T.E. Exner, Empirical Scoring Functions for Advanced Protein-Ligand Docking with PLANTS, J. Chem. Inf. Model. 49 (2009) 84-96.

Table 1. Synthesized compounds.

Cpds	Structure	Yield (%)	Cpds	Structure	Yield (%)
2	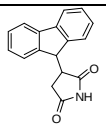	40 (Method A) 97 (Method B) 73 (Method C)	**8c**	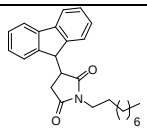	71
3	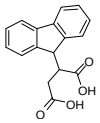	74	**8d**	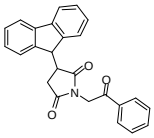	94
4	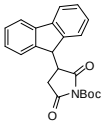	57	**10a**	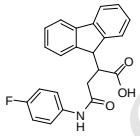	86
5	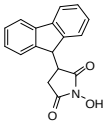	84	**10b**	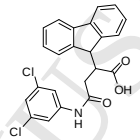	69
6	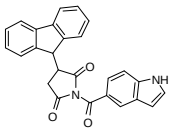	56	**10c**	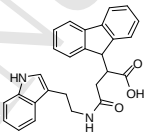	83
7a	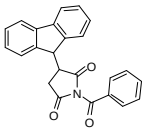	47	**10d**	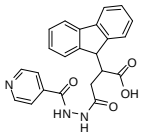	58
7b	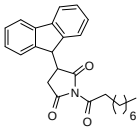	62	**11a**	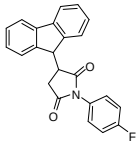	87
7c	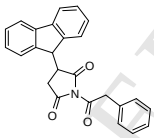	40	**11b**	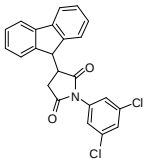	83
8a	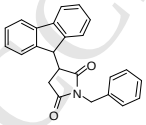	69	**11c**	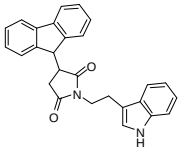	75
8b	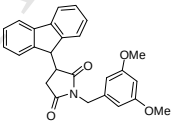	73	**11e**	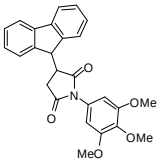	83

Table 2. Enzyme inhibition values. Results are expressed as a percentage of InhA inhibition.

Compound	% Inhibition at 50 μM	Compound	% Inhibition at 50 μM
Triclosan	>99	**GEQ**	>99
2	14	**8d**	59
3	56	**10a**	6
6	50	**10b**	8
7a	65	**10c**	60
7a (*l*) / 7a(*d*)	71/62		
7b	73	**10d**	30
7c	63	**11a**	23
8a	25	**11b**	>95 (31 at 5 μM)
8a (*l*) / 8a(*d*)	20/27		
8b	56	**11c**	79
8c	86	**11e**	34

Table 3 Compounds tested as inhibitory agents of *M. tuberculosis* growth.

Comp	MIC (μg/mL) / (μM)	Comp	MIC (μg/mL) / (μM)
Triclosan	10 / 34.5	**GEQ**	>16 / >40.7
2	8 / 30.4	**8d**	>16 / >41.9
3	8 / 28.3	**10a**	16 / 42.6
6	16 / 39.4	**10b**	2 / 4.7
7a	2 / 5.4	**10c**	16 / 37.7
7b	16 / 39.7	**10d**	4 / 10.0
7c	16 / 41.9	**11a**	>16 / >44.8
8a	16 / 45.3	**11b**	8 / 19.6
8a (*l*) / 8a(*d*)	16 (45.3) / 16 (45.3)		
8b	>16 / >38.7	**11c**	>16 / >39.4
8c	16 / 41.1	**11e**	16 / 37.3

Table 4. Activities against multi-drug-resistant *M. tuberculosis* strains.

Compound	MIC			
	***M. tuberculosis* H37Rv (μg/mL / μM)**	***M. tuberculosis* clinical isolates**		
		IC1[a] (μg/mL / μM)	**IC2[a] (μg/mL / μM)**	**IC3[a] (μg/mL / μM)**
10b	2 / 4.7	2 / 4.7	2 / 4.7	2 / 4.7

[a]*Mtb* clinical isolate: IC1 : drug resistance profile: resistant to streptomycin, isoniazid (INH), rifampicin, ethambutol; IC2 : drug resistance profile: resistant to streptomycin, isoniazid (INH), rifampicin, ethambutol, pyrazinamide, ethionammide, capreomicin; IC3 : drug resistance profile: resistant to streptomycin, isoniazid (INH), rifampicin, ethambutol, pyrazinamide, ethionammide.

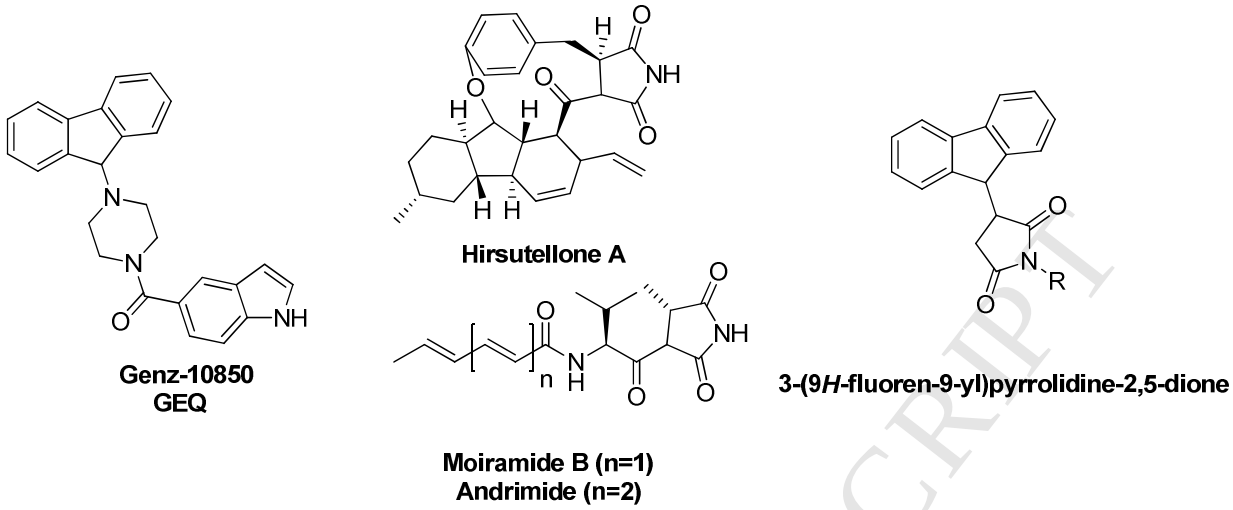

Figure 1. GEQ, a potent inhibitor of InhA; Structure of natural antibiotics (Moiramide B and Andrimide) and antimycobacterial alkaloid Hirsutellone A; Structure of inhibitors developed herein.

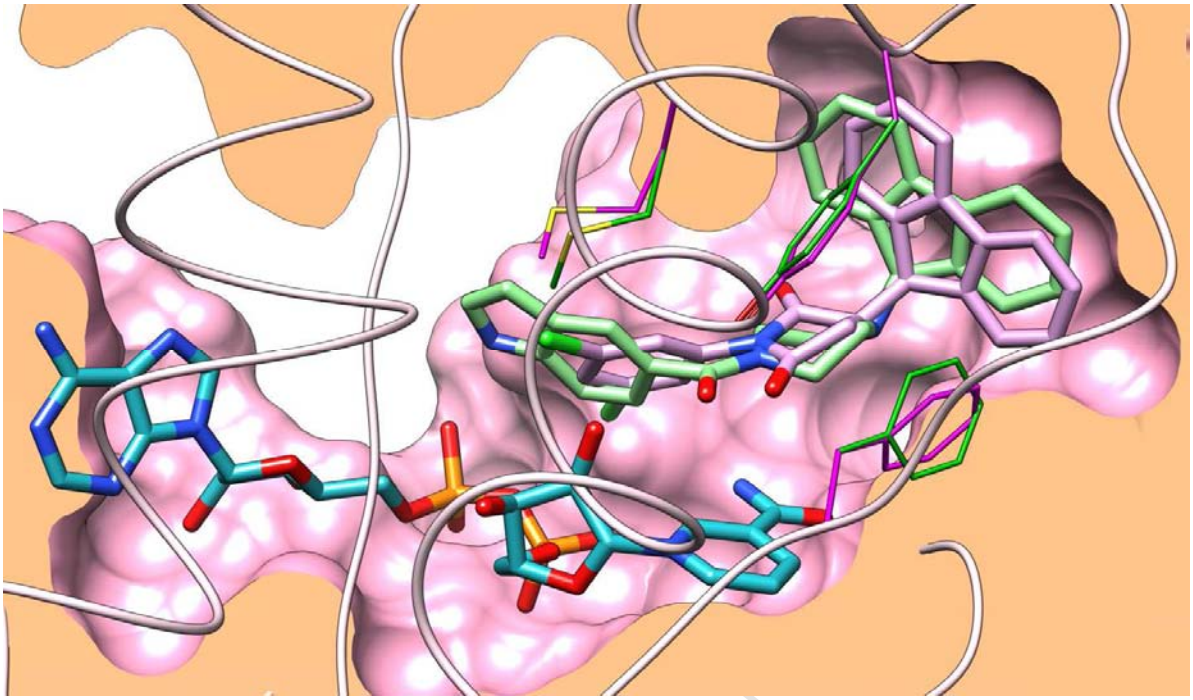

Figure 2. Superimposition of crystallographic conformation of GEQ (carbons in green stick representation) and simulated by docking binding mode of **11b** (carbons in violet stick representation) in the binding groove of InhA (1P44 PDB entry, chain A). Degree of residue flexibility (side chains of residues around the site, backbone) was applied in docking procedure. Residues Phe149, Tyr158 and Met161 colored in magenta (docked protein structure) and green (1P44 protein structure).

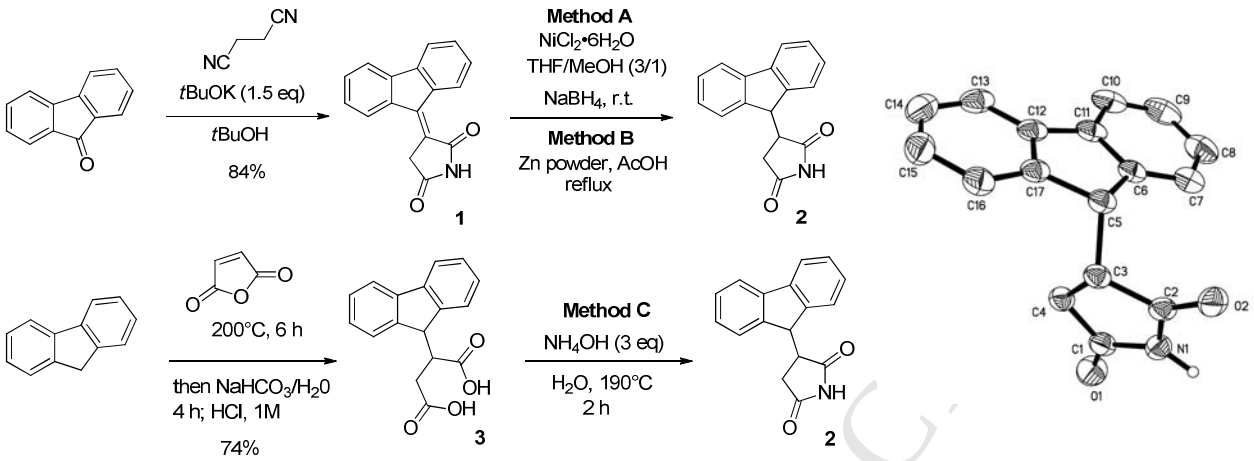

Scheme 1. Two routes to synthesize succinimide **2**; Molecular view of **2**. Thermal ellipsoids are drawn at the 50% probability level. Hydrogen atoms except for that on N1 are omitted for clarity

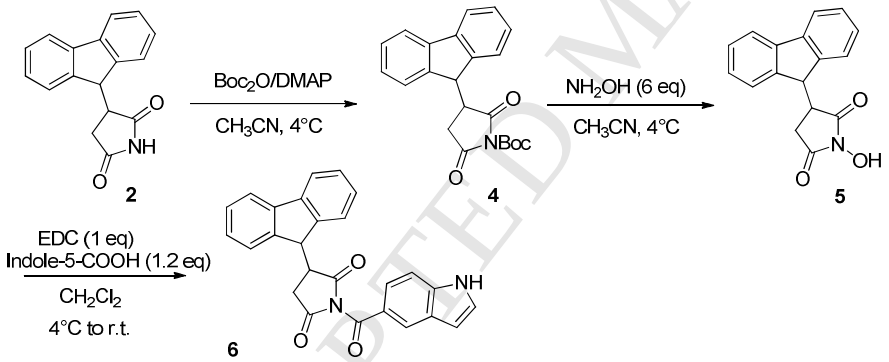

Scheme 2. Synthesis of derivative **6**.

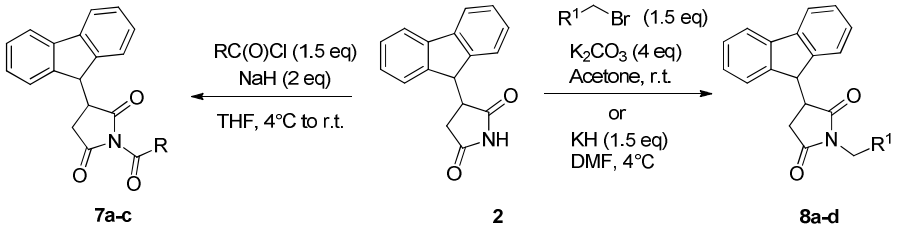

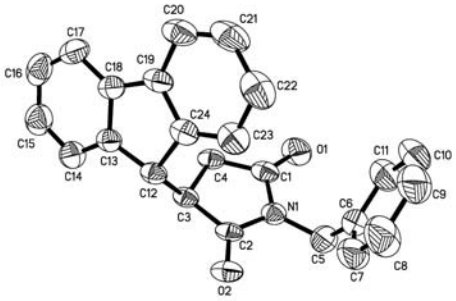

Scheme 3. Synthesis of compounds **7a-c** and **8a-d**; Molecular view of **8a**. Thermal ellipsoids are drawn at the 50% probability level. Hydrogen atoms are omitted for clarity

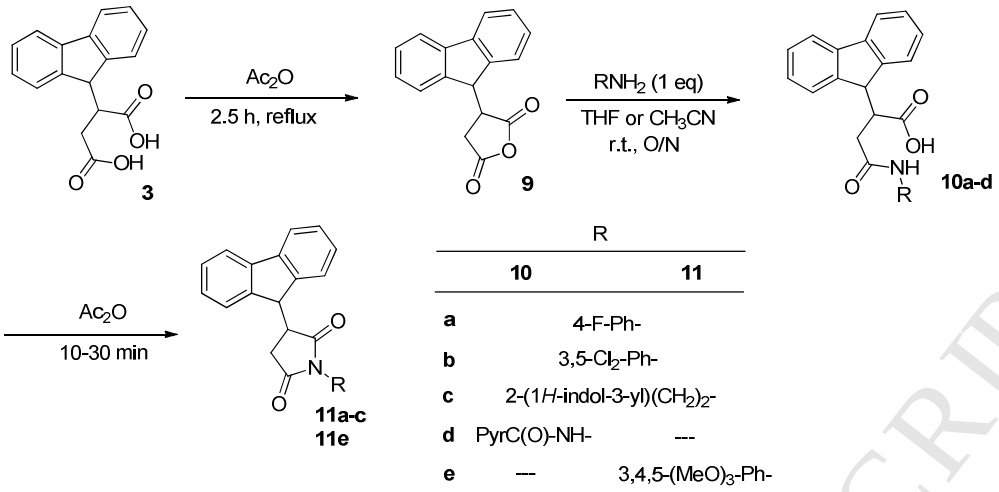

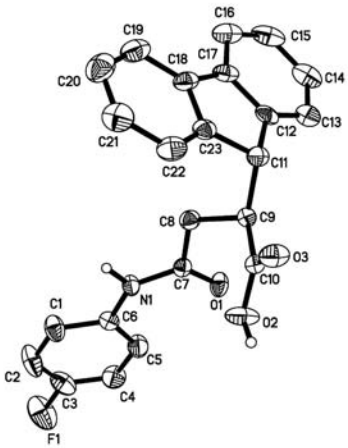

Scheme 4. Synthesis of derivatives **10a-d** and **11a-e.** Molecular view of compound **10a.** Thermal ellipsoids are drawn at the 50% probability level. Hydrogen atoms are omitted for clarity except for the H on N1 and O2.

Supporting information

Design, chemical synthesis of 3-(9*H*-fluoren-9-yl)pyrrolidine-2,5-dione derivatives and biological activity against enoyl-ACP reductase (InhA) and *Mycobacterium tuberculosis*

Tetiana Matviiuk,[a,b,d] Frédéric Rodriguez,[a,b] Nathalie Saffon,[c] Sonia Mallet-Ladeira,[c] Marian Gorichko,[e] Ana Luisa de Jesus Lopes Ribeiro,[d] Maria Rosalia Pasca,[d] Christian Lherbet,[a,b*] Zoia Voitenko,[e] Michel Baltas[a,b*]

[a] CNRS; Laboratoire de Synthèse et Physico-Chimie de Molécules d'Intérêt Biologique, LSPCMIB, UMR-5068; 118 Route de Narbonne, F-31062 Toulouse cedex 9, France

[b.] Université de Toulouse; UPS; Laboratoire de Synthèse et Physico-Chimie de Molécules d'Intérêt Biologique, LSPCMIB; 118 route de Narbonne, F-31062 Toulouse cedex 9, France

[c.] Université de Toulouse, UPS and CNRS, ICT FR2599, 118 route de Narbonne, 31062 Toulouse cedex 9, France

[d.] University of Pavia; Dipartimento di Biologia e Biotecnologie "Lazzaro Spallanzani", via Ferrata 1, 27100 Pavia, Italy.

[e.] Taras Shevchenko National University of Kyiv, Department of Chemistry, 64 str. Volodymyrska, Kyiv, 01033, Ukraine

Fax: 33 (0)5 61556011; Tel: 33 (0)5 61556289; E-mail : lherbet@chimie.ups-tlse.fr; baltas@chimie.ups-tlse.fr

I. NMR data for the compounds
II. Crystallographic data for compounds **2**, **8a** and **10a**
III. SFC separation

I. NMR data for the compounds

Compound 1:

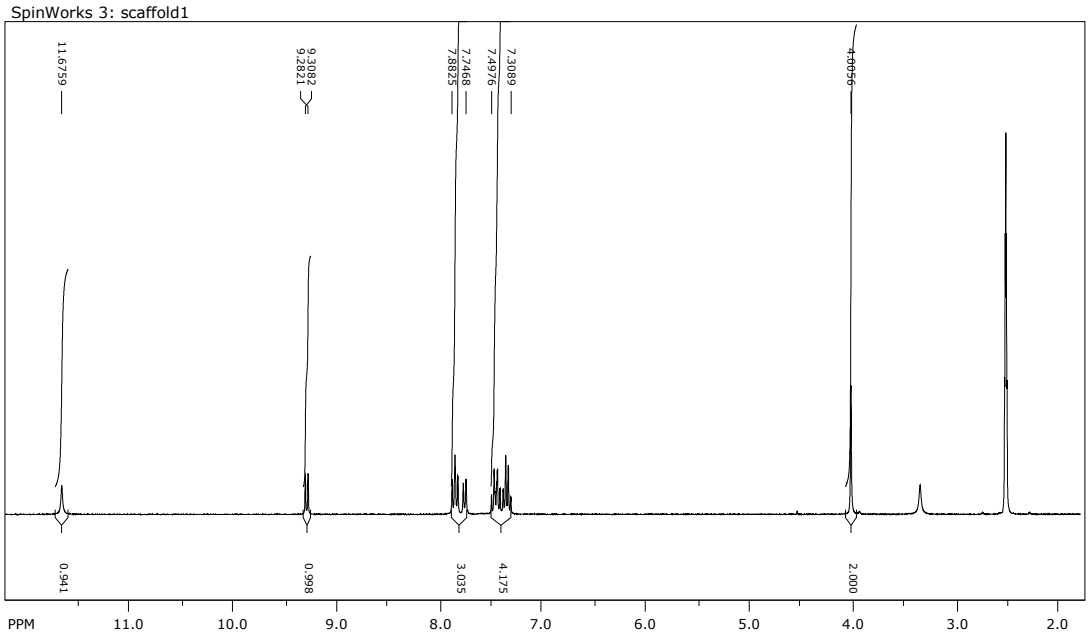

file: ...:\NMR\51_scaffold1_double_bond\fid expt: <zg30>
transmitter freq.: 300.181854 MHz
time domain size: 65536 points
width: 6188.12 Hz = 20.6146 ppm = 0.094423 Hz/pt
number of scans: 8

freq. of 0 ppm: 300.180006 MHz
processed size: 32768 complex points
LB: 0.000 GF: 0.0000
Hz/cm: 112.098 ppm/cm: 0.37344

Compound 2:

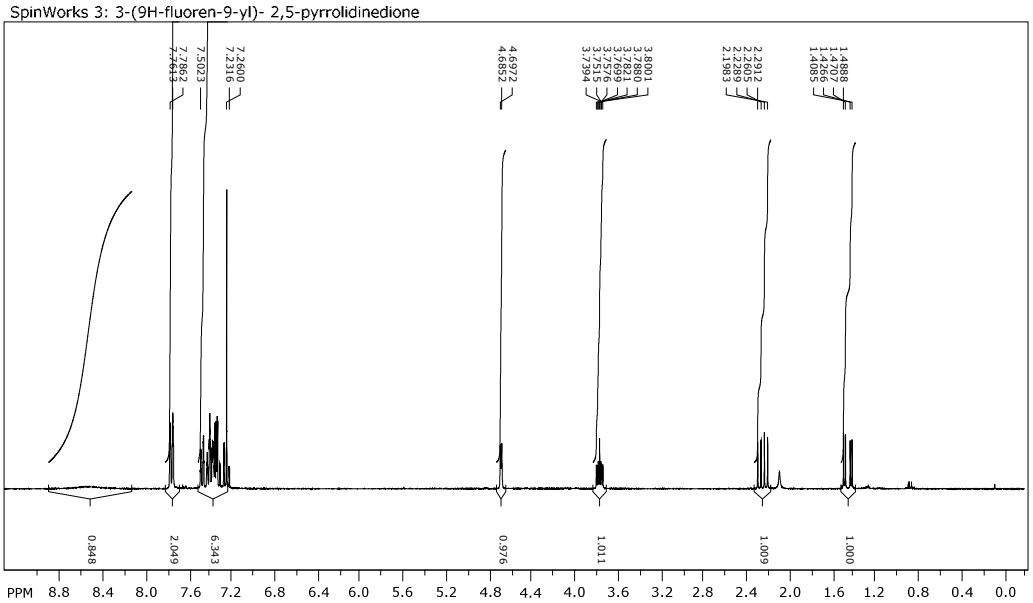
SpinWorks 3: 3-(9H-fluoren-9-yl)- 2,5-pyrrolidinedione
7.7862
7.7813
7.5023
7.2600
7.2316
4.6972
4.6852
3.8001
3.7880
3.7691
3.7576
3.7515
3.7394
2.2912
2.2605
2.2289
2.1983
1.4888
1.4707
1.4265
1.4085
0.848
2.049
6.343
0.976
1.011
1.009
1.000
PPM 8.8 8.4 8.0 7.6 7.2 6.8 6.4 6.0 5.6 5.2 4.8 4.4 4.0 3.6 3.2 2.8 2.4 2.0 1.6 1.2 0.8 0.4 0.0
file: E:\NMR\34_reduction_Zn\fid expt: <zg30>
transmitter freq.: 300.131853 MHz
time domain size: 65536 points
width: 6172.84 Hz = 20.5671 ppm = 0.094190 Hz/pt
number of scans: 24
freq. of 0 ppm: 300.130007 MHz
processed size: 65536 complex points
LB: 0.000 GF: 0.0000
Hz/cm: 102.267 ppm/cm: 0.34074

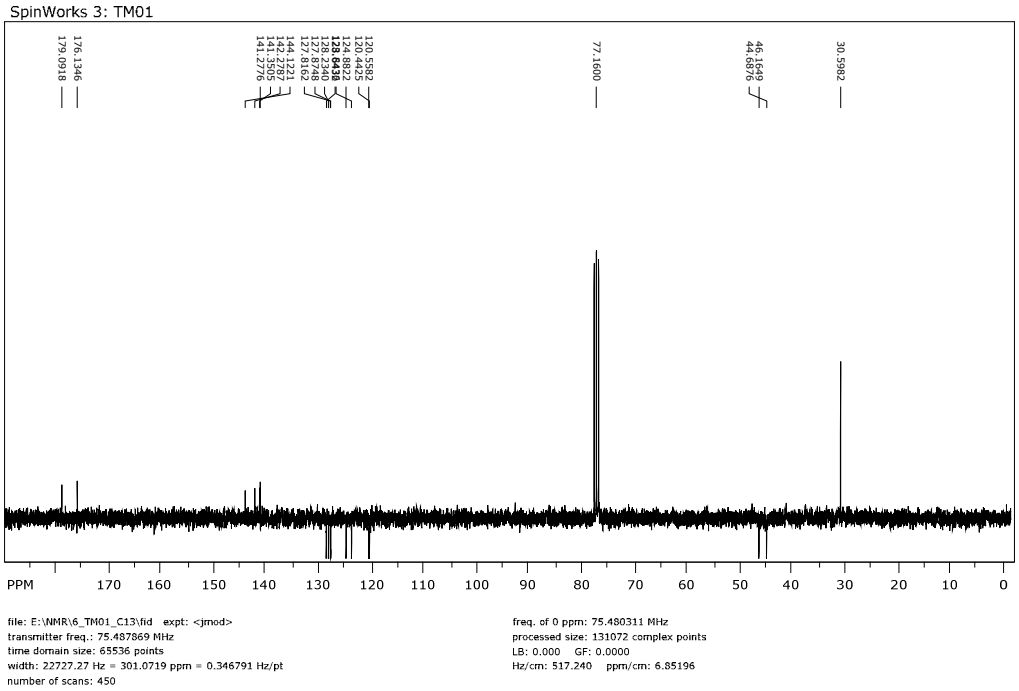
SpinWorks 3: TM01
179.0918
176.1346
141.2776
141.3505
141.5271
127.8162
127.8748
128.2340
120.4425
120.5582
77.1600
44.6876
46.1649
30.5982
PPM 170 160 150 140 130 120 110 100 90 80 70 60 50 40 30 20 10 0
file: E:\NMR\6_TM01_C13\fid expt: <jmod>
transmitter freq.: 75.487869 MHz
time domain size: 65536 points
width: 22727.27 Hz = 301.0719 ppm = 0.346791 Hz/pt
number of scans: 450
freq. of 0 ppm: 75.480311 MHz
processed size: 131072 complex points
LB: 0.000 GF: 0.0000
Hz/cm: 517.240 ppm/cm: 6.85196

Compound 3:

SpinWorks 3: 2-(9H-Fluoren-9-yl)succinic acid

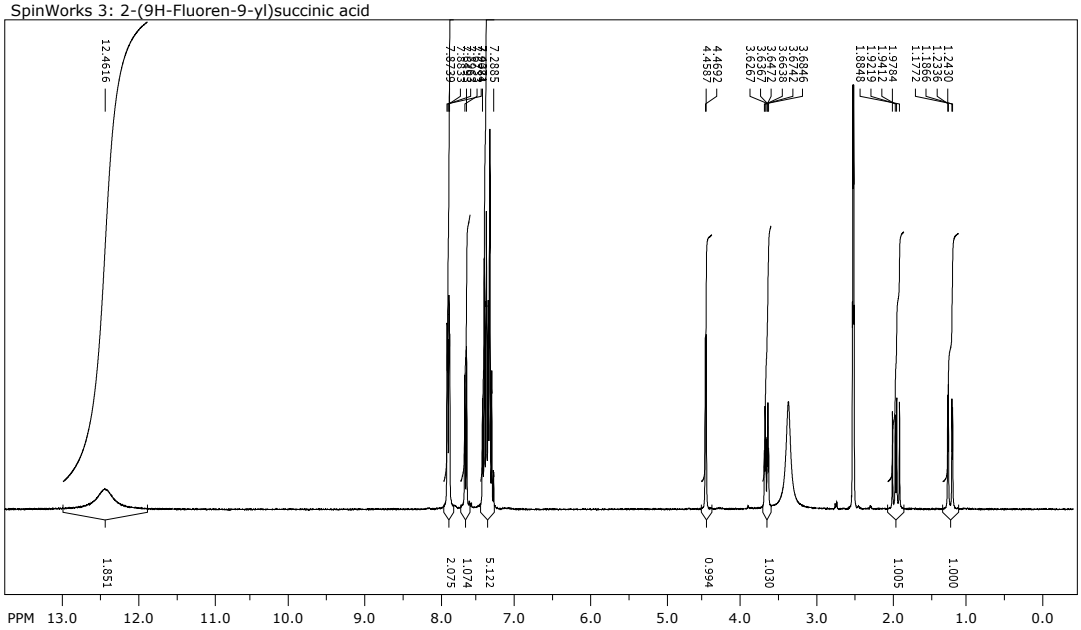

file: ...NMR\70_fluorensuccinic_acid_H1\fid expt: <zg30>
transmitter freq.: 300.181854 MHz
time domain size: 65536 points
width: 6188.12 Hz = 20.6146 ppm = 0.094423 Hz/pt
number of scans: 8

freq. of 0 ppm: 300.180006 MHz
processed size: 32768 complex points
LB: 0.000 GF: 0.0000
Hz/cm: 152.539 ppm/cm: 0.50816

SpinWorks 3: 2-(9H-Fluoren-9-yl)succinic acid

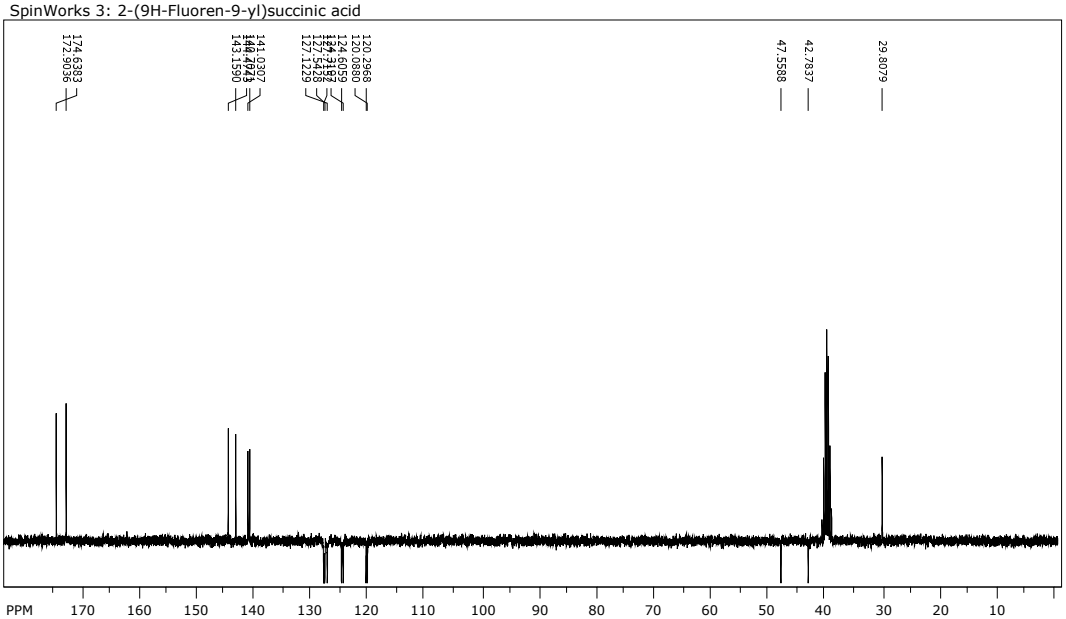

file: ...MR\71_fluorensuccinic_acid_C13\fid expt: <jmod>
transmitter freq.: 75.487869 MHz
time domain size: 65536 points
width: 22727.27 Hz = 301.0719 ppm = 0.346791 Hz/pt
number of scans: 256

freq. of 0 ppm: 75.480355 MHz
processed size: 131072 complex points
LB: 0.000 GF: 0.0000
Hz/cm: 498.348 ppm/cm: 6.60170

Compound 6:

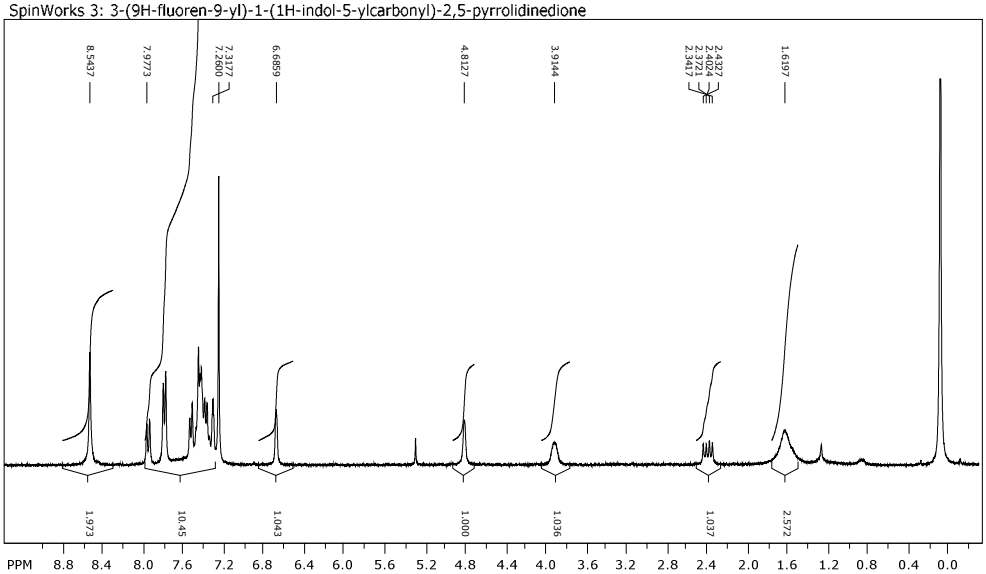
SpinWorks 3: 3-(9H-fluoren-9-yl)-1-(1H-indol-5-ylcarbonyl)-2,5-pyrrolidinedione
8.5437
7.9773
7.3177
7.2600
6.6859
4.8127
3.9144
2.4327
2.4024
2.3721
2.3417
1.6197
1.973
10.45
1.043
1.000
1.036
1.037
2.572
PPM 8.8 8.4 8.0 7.6 7.2 6.8 6.4 6.0 5.6 5.2 4.8 4.4 4.0 3.6 3.2 2.8 2.4 2.0 1.6 1.2 0.8 0.4 0.0
file: ...trum\Korolov_spectr\27_indole+\fid expt: <zg30>
transmitter freq.: 300.181854 MHz
time domain size: 65536 points
width: 6188.12 Hz = 20.6146 ppm = 0.094423 Hz/pt
number of scans: 8
freq. of 0 ppm: 300.180011 MHz
processed size: 32768 complex points
LB: 0.000 GF: 0.0000
Hz/cm: 104.117 ppm/cm: 0.34685

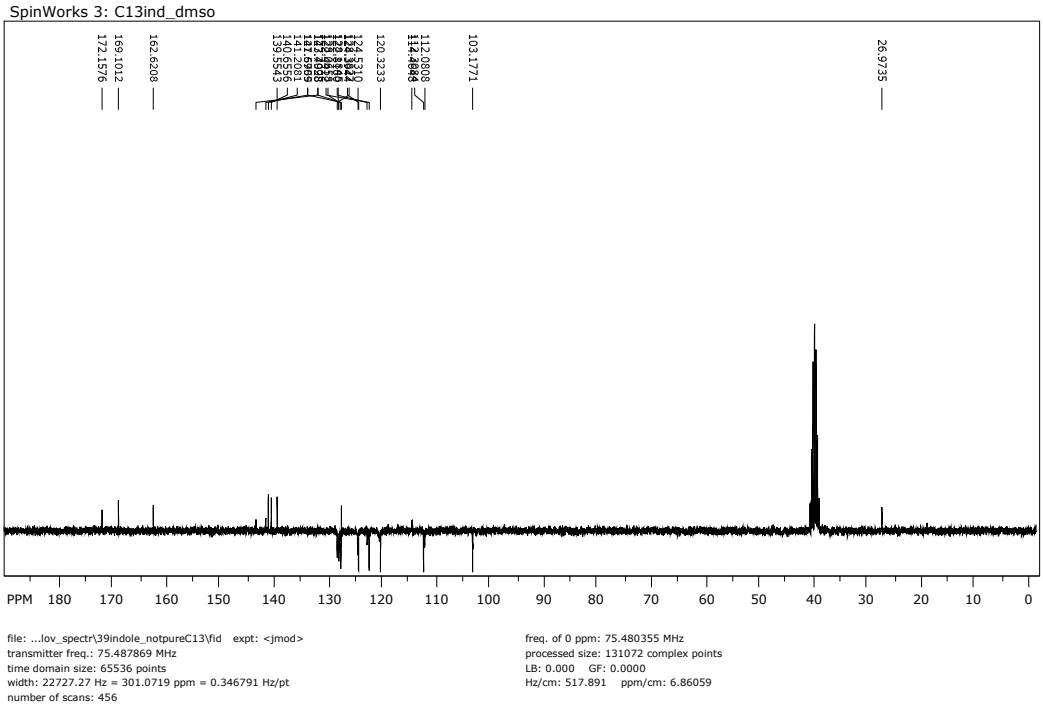
SpinWorks 3: C13ind_dmso
172.1576
169.1012
162.6208
139.5543
140.6556
120.3233
112.0808
103.1771
26.9735
PPM 180 170 160 150 140 130 120 110 100 90 80 70 60 50 40 30 20 10 0
file: ...lov_spectr\39indole_notpureC13\fid expt: <jmod>
transmitter freq.: 75.487869 MHz
time domain size: 65536 points
width: 22727.27 Hz = 301.0719 ppm = 0.346791 Hz/pt
number of scans: 456
freq. of 0 ppm: 75.480355 MHz
processed size: 131072 complex points
LB: 0.000 GF: 0.0000
Hz/cm: 517.891 ppm/cm: 6.86059

Compound 7a:

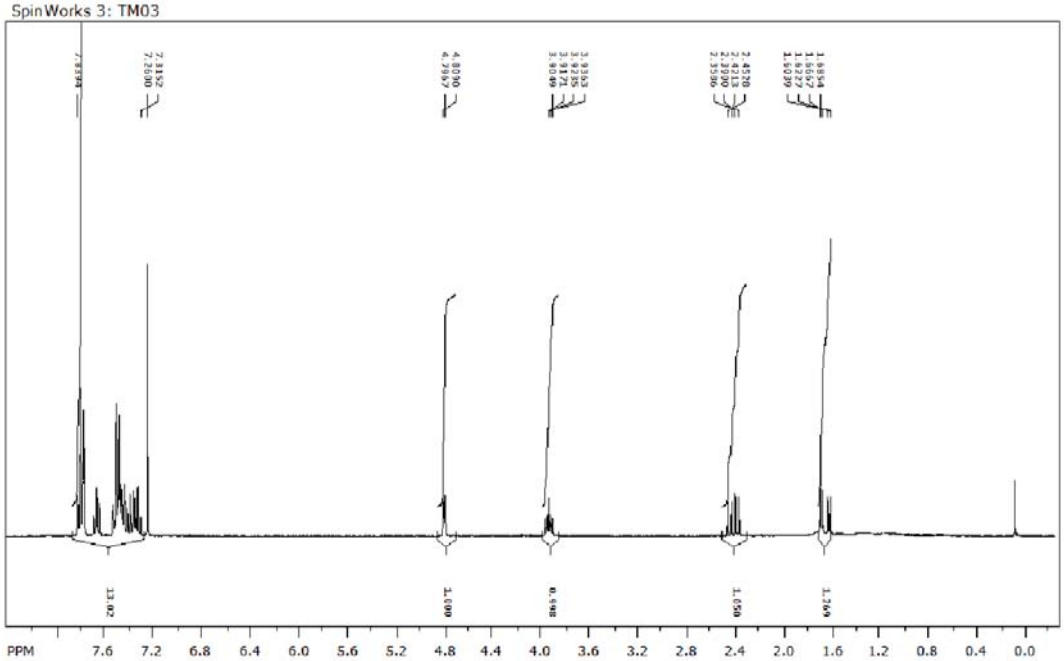
SpinWorks 3: TM03
PPM
file: ...nthesis\F02\spectrum\4300b_F02\fid expt: <zg30>
transmitter freq.: 300.181854 MHz
time domain size: 65536 points
width: 6188.12 Hz = 20.6146 ppm = 0.094423 Hz/pt
number of scans: 8
freq. of 0 ppm: 300.180011 MHz
processed size: 32768 complex points
LB: 0.000 GF: 0.0000
Hz/cm: 93.297 ppm/cm: 0.31080

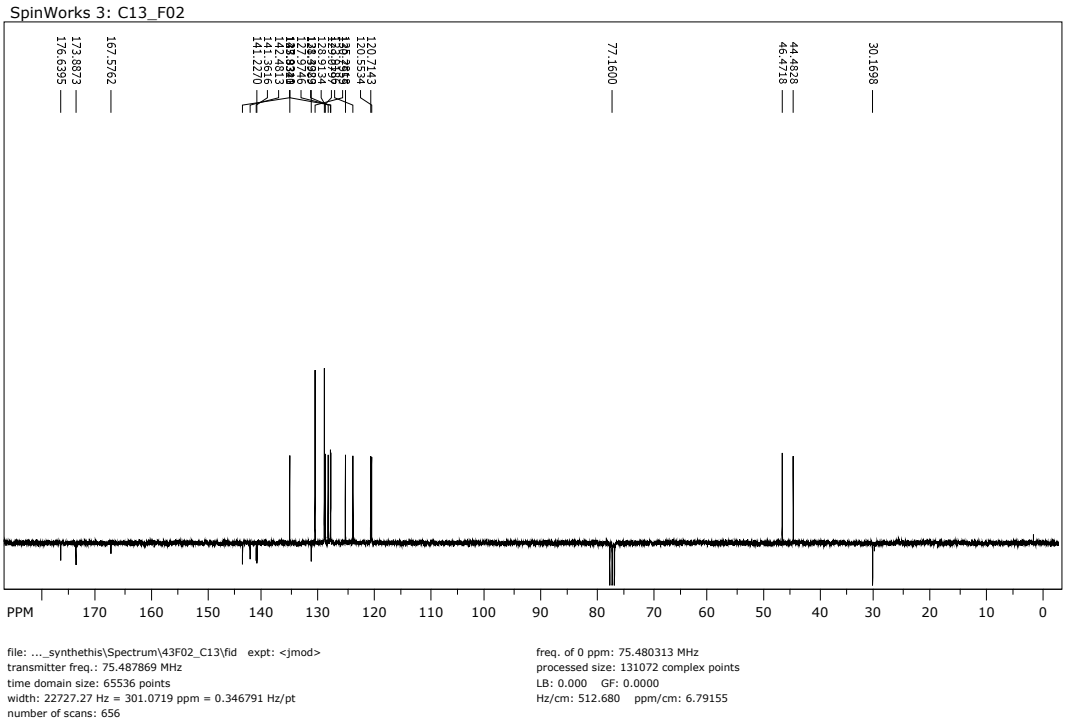
SpinWorks 3: C13_F02
PPM
file: ..._synthethis\Spectrum\43F02_C13\fid expt: <jmod>
transmitter freq.: 75.487869 MHz
time domain size: 65536 points
width: 22727.27 Hz = 301.0719 ppm = 0.346791 Hz/pt
number of scans: 656
freq. of 0 ppm: 75.480313 MHz
processed size: 131072 complex points
LB: 0.000 GF: 0.0000
Hz/cm: 512.680 ppm/cm: 6.79155

Compound 7b:

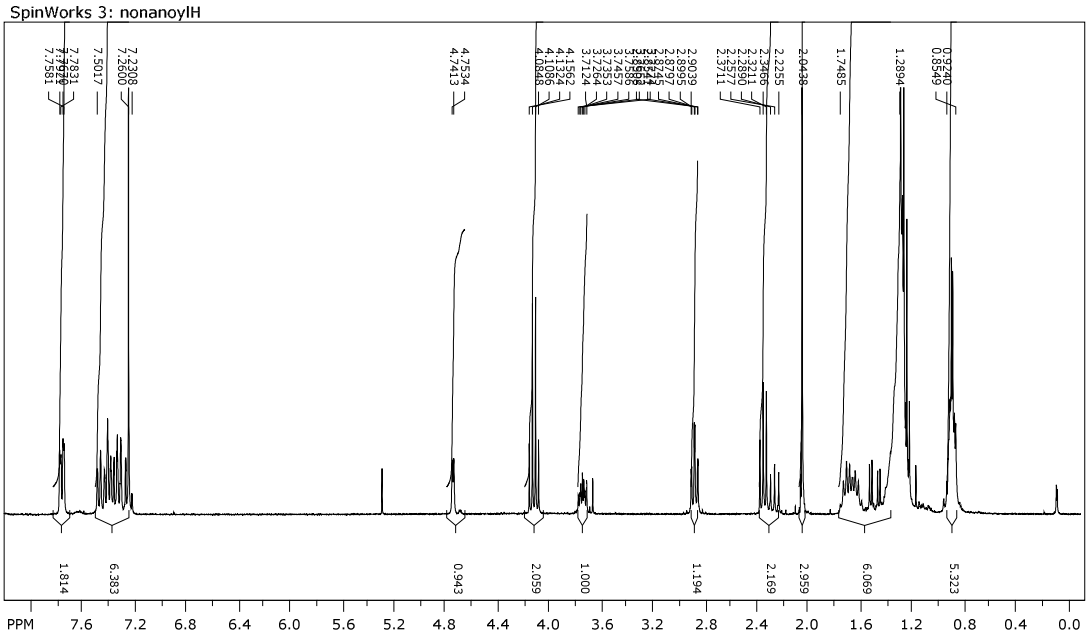

file: E:\NMR\54_acyl_C9_H1\fid expt: <zg30>
transmitter freq.: 300.181854 MHz
time domain size: 65536 points
width: 6188.12 Hz = 20.6146 ppm = 0.094423 Hz/pt
number of scans: 16

freq. of 0 ppm: 300.180011 MHz
processed size: 32768 complex points
LB: 0.000 GF: 0.0000
Hz/cm: 89.395 ppm/cm: 0.29780

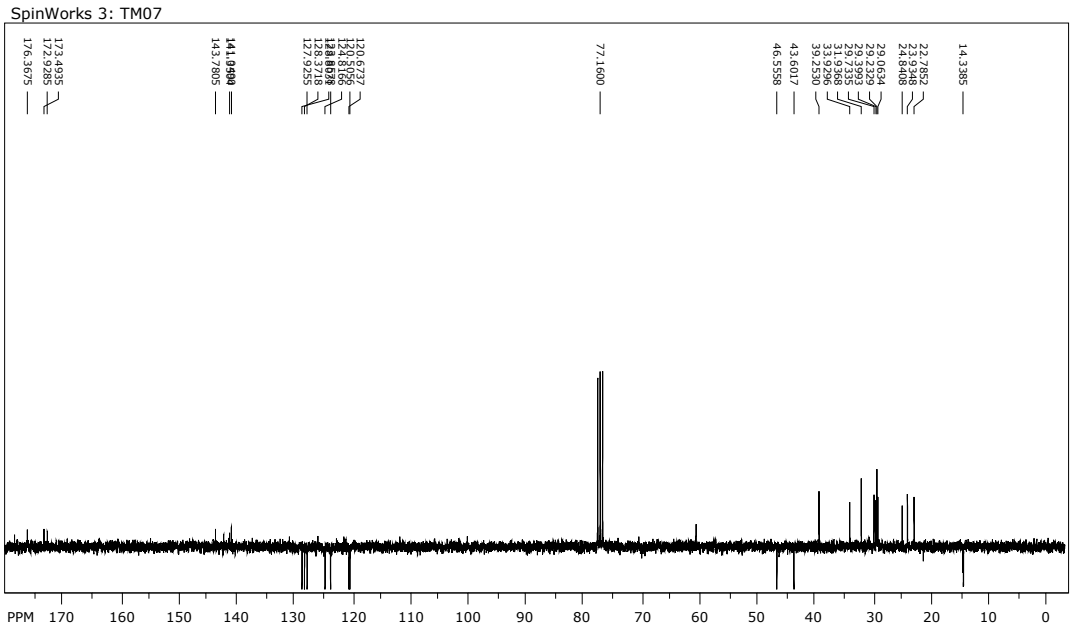

file: E:\NMR\55_acyl_C9_C13\fid expt: <jmod>
transmitter freq.: 75.487869 MHz
time domain size: 65536 points
width: 22727.27 Hz = 301.0719 ppm = 0.346791 Hz/pt
number of scans: 415

freq. of 0 ppm: 75.480311 MHz
processed size: 131072 complex points
LB: 0.000 GF: 0.0000
Hz/cm: 495.091 ppm/cm: 6.55855

Compound 8a:

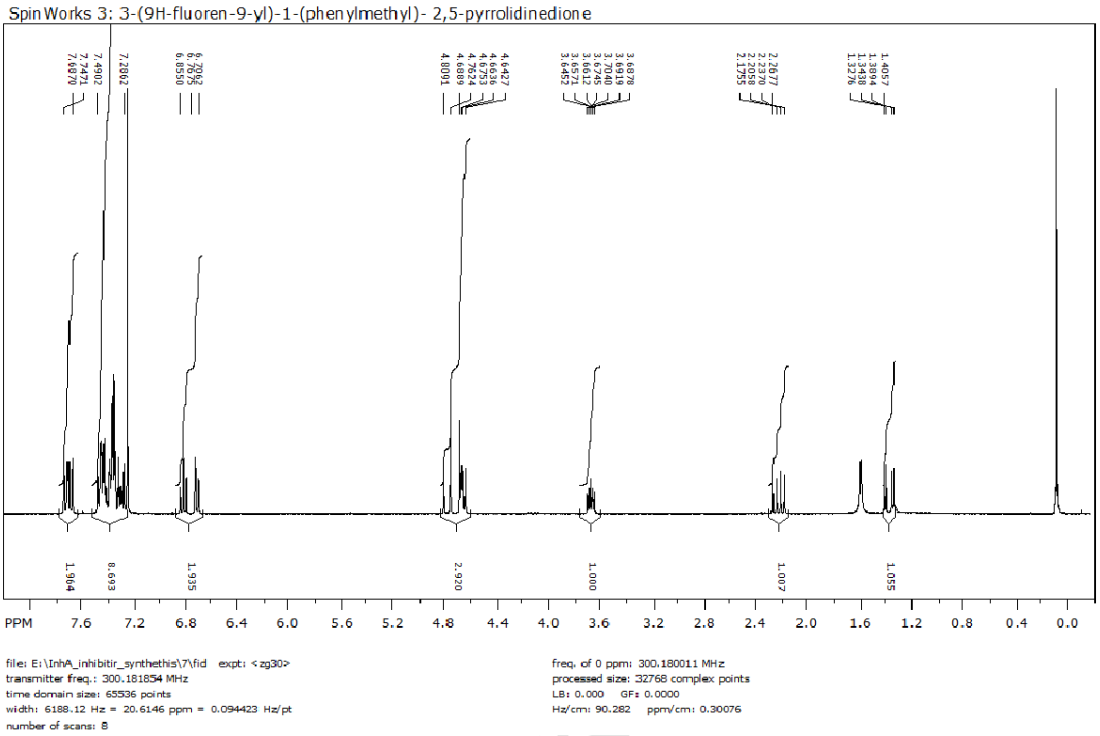

file: E:\InhA_inhibitir_synthethis\7\fid expt: <zg30>
transmitter freq.: 300.181854 MHz
time domain size: 65536 points
width: 6188.12 Hz = 20.6146 ppm = 0.094423 Hz/pt
number of scans: 8

freq. of 0 ppm: 300.180011 MHz
processed size: 32768 complex points
LB: 0.000 GF: 0.0000
Hz/cm: 90.282 ppm/cm: 0.30076

Compound 8b:

SpinWorks 3: TM05

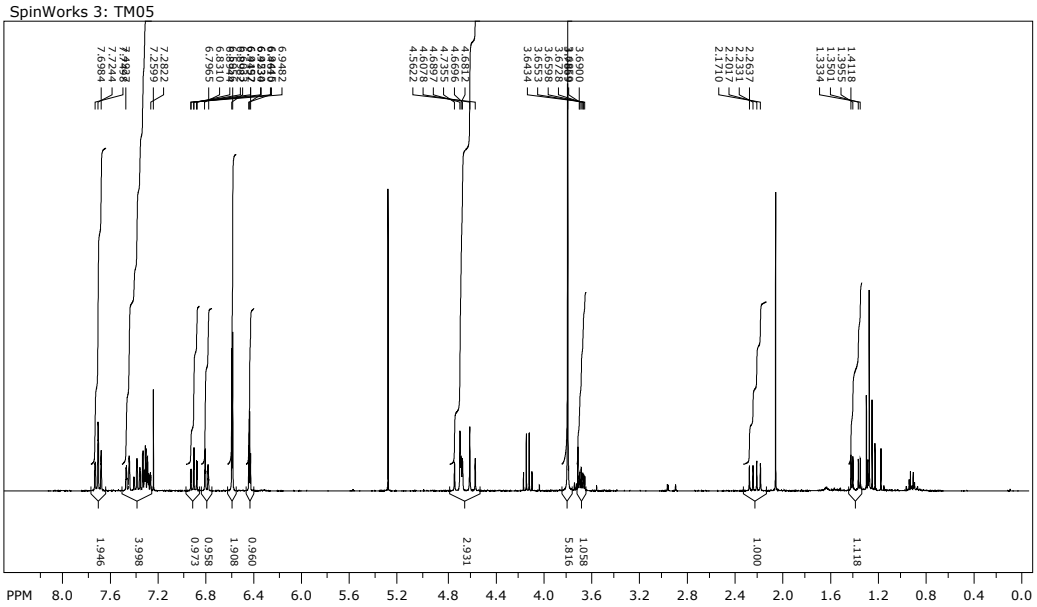

file: E:\NMR\41_CH2Ph(OCH3)2\fid expt: <zg30>
transmitter freq.: 300.131853 MHz
time domain size: 65536 points
width: 6172.84 Hz = 20.5671 ppm = 0.094190 Hz/pt
number of scans: 20

freq. of 0 ppm: 300.130006 MHz
processed size: 65536 complex points
LB: 0.000 GF: 0.0000
Hz/cm: 92.146 ppm/cm: 0.30702

SpinWorks 3: CH2Ph(OCH3)2

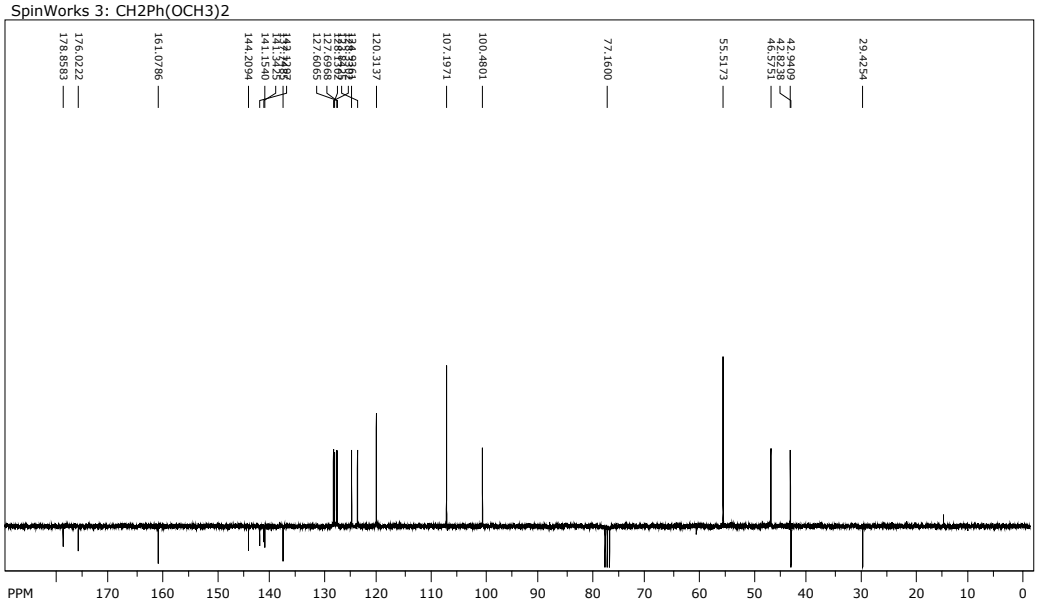

file: ...!RMN_2013\66_CH2Ph(OCH3)2_TM05\fid expt: <jmod>
transmitter freq.: 75.487869 MHz
time domain size: 65536 points
width: 22727.27 Hz = 301.0719 ppm = 0.346791 Hz/pt
number of scans: 256

freq. of 0 ppm: 75.480313 MHz
processed size: 131072 complex points
LB: 0.000 GF: 0.0000
Hz/cm: 516.588 ppm/cm: 6.84333

Compound 8c:

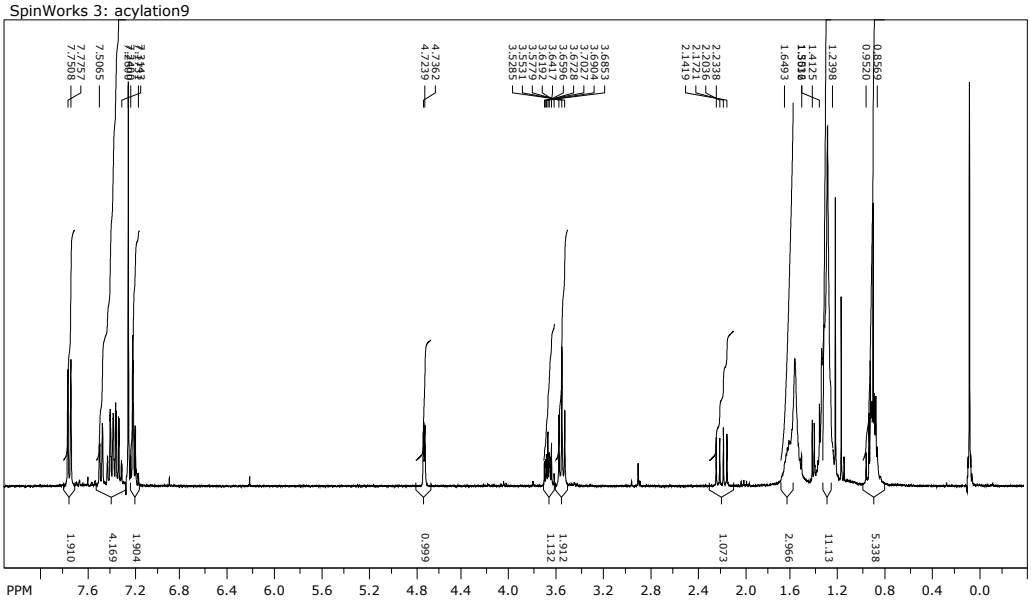

file: E:\NMR\52_alkylated_C9\fid expt: <zg30>
transmitter freq.: 300.181854 MHz
time domain size: 65536 points
width: 6188.12 Hz = 20.6146 ppm = 0.094423 Hz/pt
number of scans: 16

freq. of 0 ppm: 300.180011 MHz
processed size: 32768 complex points
LB: 0.000 GF: 0.0000
Hz/cm: 93.475 ppm/cm: 0.31139

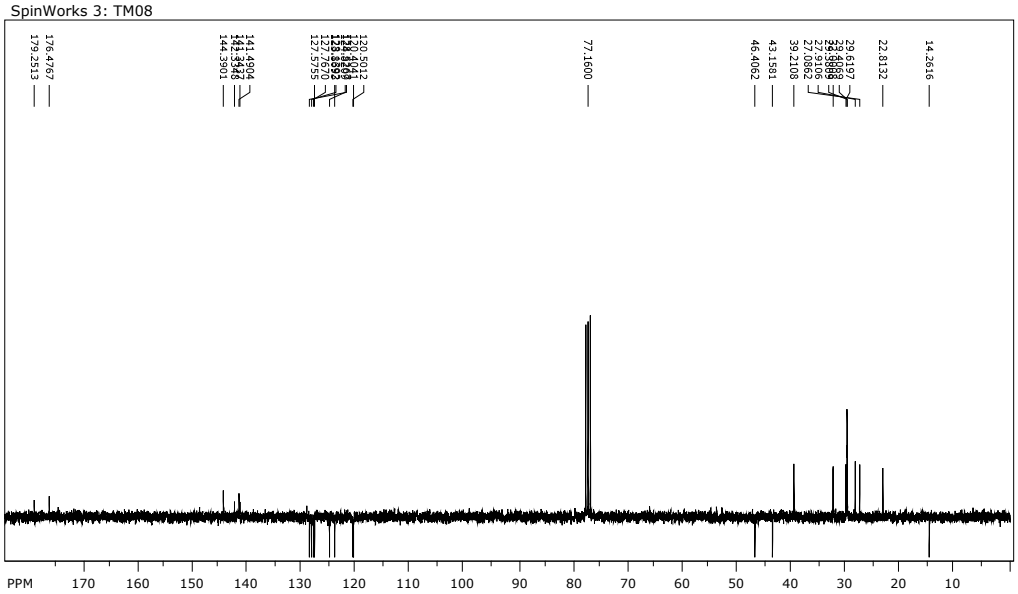

file: ...RMN_2013\300b_2013\28_TM08_C13\fid expt: <jmod>
transmitter freq.: 75.487869 MHz
time domain size: 65536 points
width: 22727.27 Hz = 301.0719 ppm = 0.346791 Hz/pt
number of scans: 600

freq. of 0 ppm: 75.480311 MHz
processed size: 131072 complex points
LB: 0.000 GF: 0.0000
Hz/cm: 499.651 ppm/cm: 6.61896

Compounds 8d:

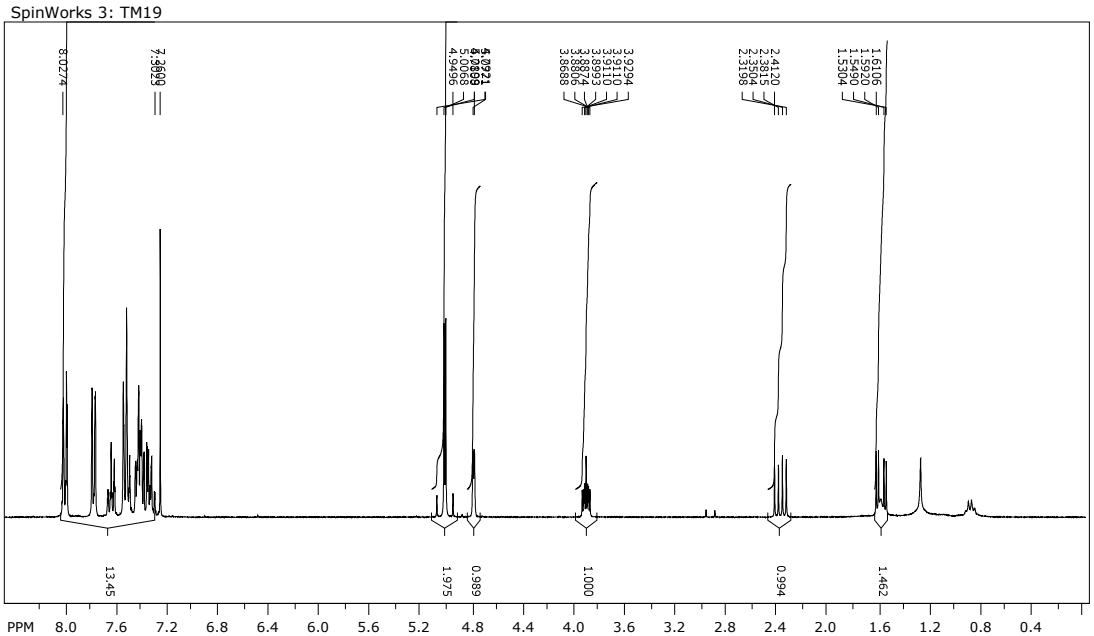

file: E:\NMR\!!RMN_2013\10_TM19_H1\fid expt: <zg30>
transmitter freq.: 300.181854 MHz
time domain size: 65536 points
width: 6188.12 Hz = 20.6146 ppm = 0.094423 Hz/pt
number of scans: 8

freq. of 0 ppm: 300.180011 MHz
processed size: 32768 complex points
LB: 0.000 GF: 0.0000
Hz/cm: 91.456 ppm/cm: 0.30467

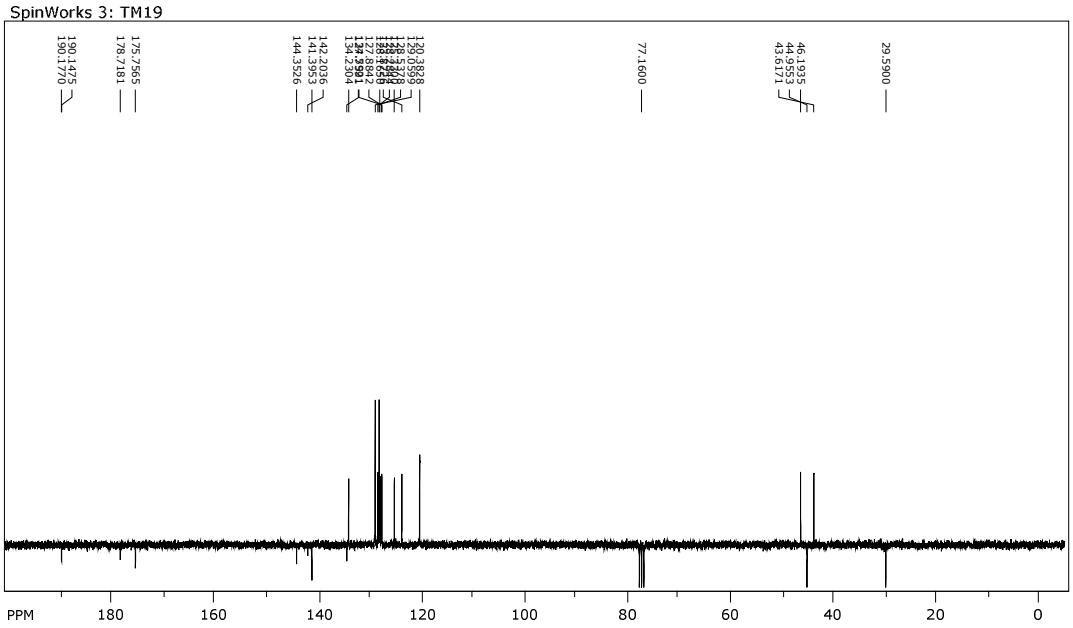

file: E:\NMR\!!RMN_2013\11_TM19_C13\fid expt: <jmod>
transmitter freq.: 75.487869 MHz
time domain size: 65536 points
width: 22727.27 Hz = 301.0719 ppm = 0.346791 Hz/pt
number of scans: 420

freq. of 0 ppm: 75.480311 MHz
processed size: 131072 complex points
LB: 0.000 GF: 0.0000
Hz/cm: 556.883 ppm/cm: 7.37712

Compound 9:

SpinWorks 3: fluorensuccinic anhydride (9)

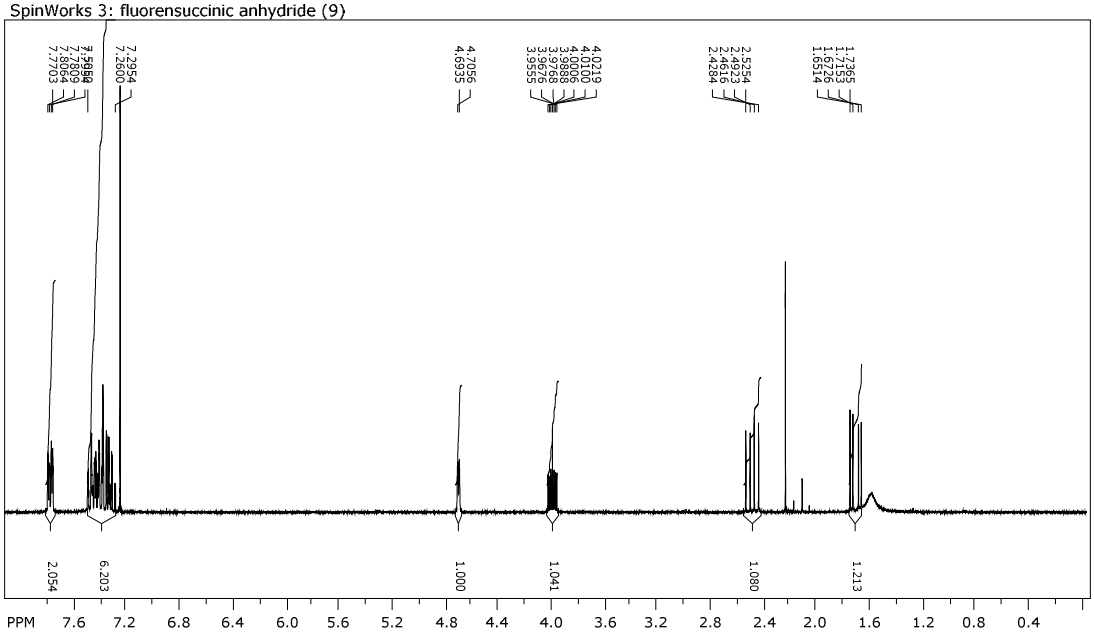

file: ...3\28_fluorensuccinic_anhydride\fid expt: <zg30>
transmitter freq.: 300.131853 MHz
time domain size: 65536 points
width: 6172.84 Hz = 20.5671 ppm = 0.094190 Hz/pt
number of scans: 16

freq. of 0 ppm: 300.130006 MHz
processed size: 65536 complex points
LB: 0.000 GF: 0.0000
Hz/cm: 87.759 ppm/cm: 0.29240

Compound 10a:

SpinWorks 3: amidoacid

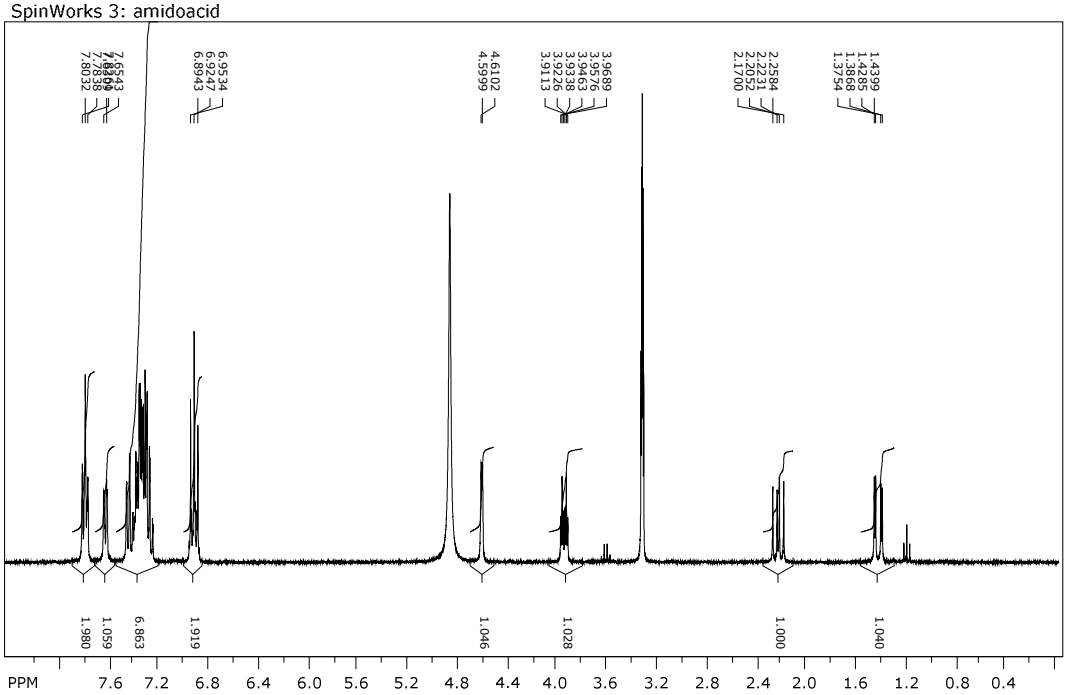

file: E:\NMR\45_amido_acid_pFaniline\fid expt: <zg30>
transmitter freq.: 300.131853 MHz
time domain size: 65536 points
width: 6172.84 Hz = 20.5671 ppm = 0.094190 Hz/pt
number of scans: 8

freq. of 0 ppm: 300.130005 MHz
processed size: 65536 complex points
LB: 0.000 GF: 0.0000
Hz/cm: 102.055 ppm/cm: 0.34003

SpinWorks 3: fluoren_maleamic_acid_carbon

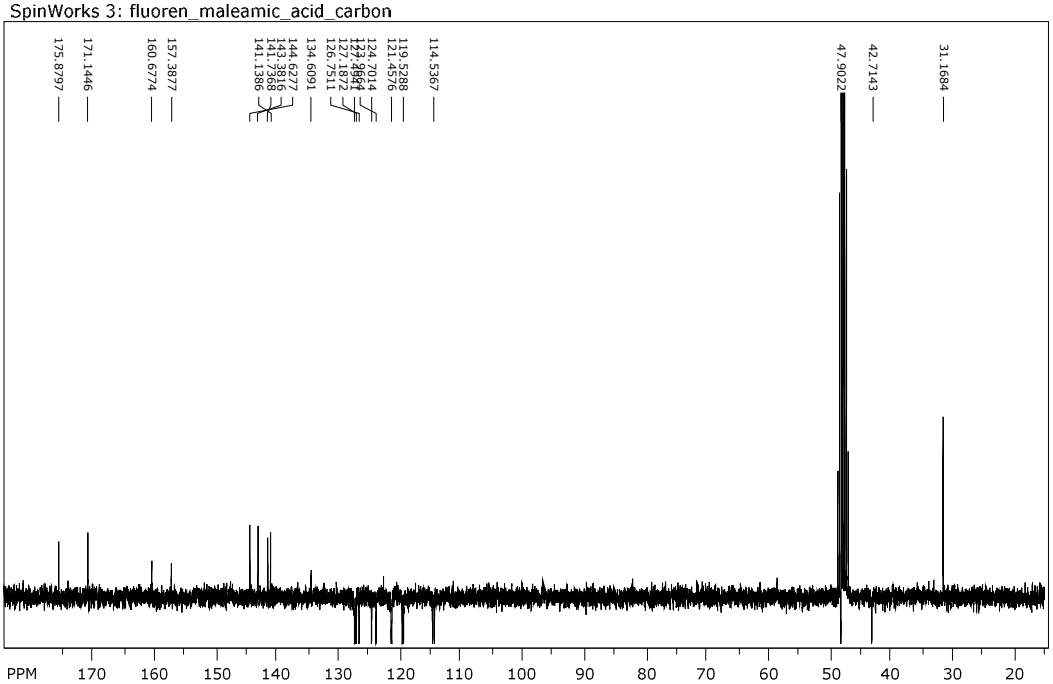

file: ...75_maleamic_acid_pFaniline_C13\fid expt: <jmod>
transmitter freq.: 75.487869 MHz
time domain size: 65536 points
width: 22727.27 Hz = 301.0719 ppm = 0.346791 Hz/pt
number of scans: 400

freq. of 0 ppm: 75.480321 MHz
processed size: 131072 complex points
LB: 0.000 GF: 0.0000
Hz/cm: 513.644 ppm/cm: 6.80432

Compound 10b:

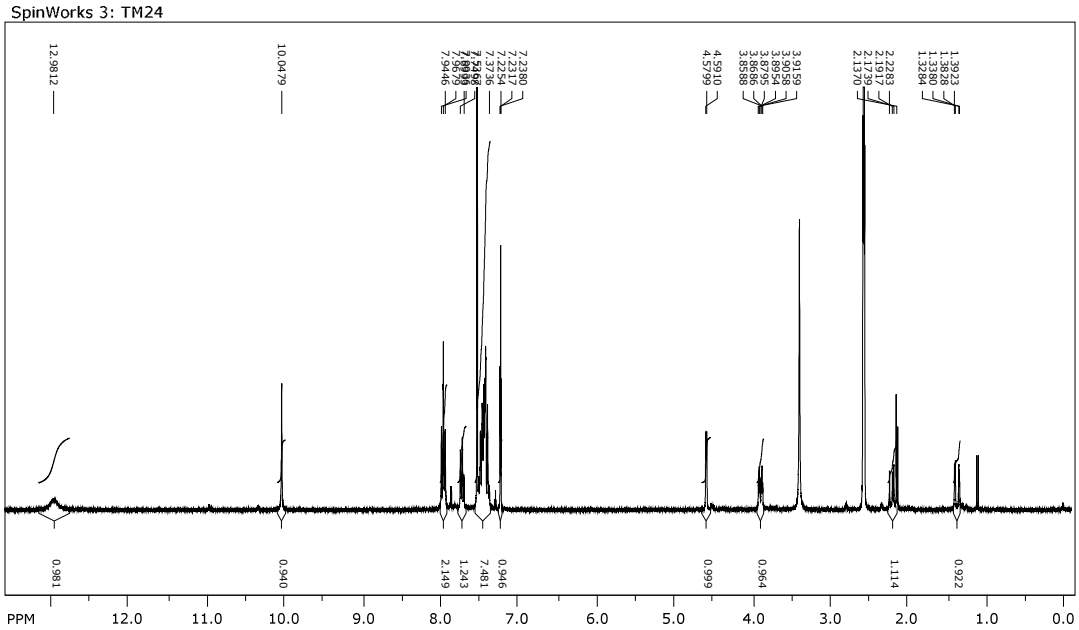

file: ...dichloraniline_succinamik_acid\fid expt: <zg30>
transmitter freq.: 300.131853 MHz
time domain size: 65536 points
width: 6172.84 Hz = 20.5671 ppm = 0.094190 Hz/pt
number of scans: 8

freq. of 0 ppm: 300.129983 MHz
processed size: 65536 complex points
LB: 0.000 GF: 0.0000
Hz/cm: 147.031 ppm/cm: 0.48989

Compound 10c:

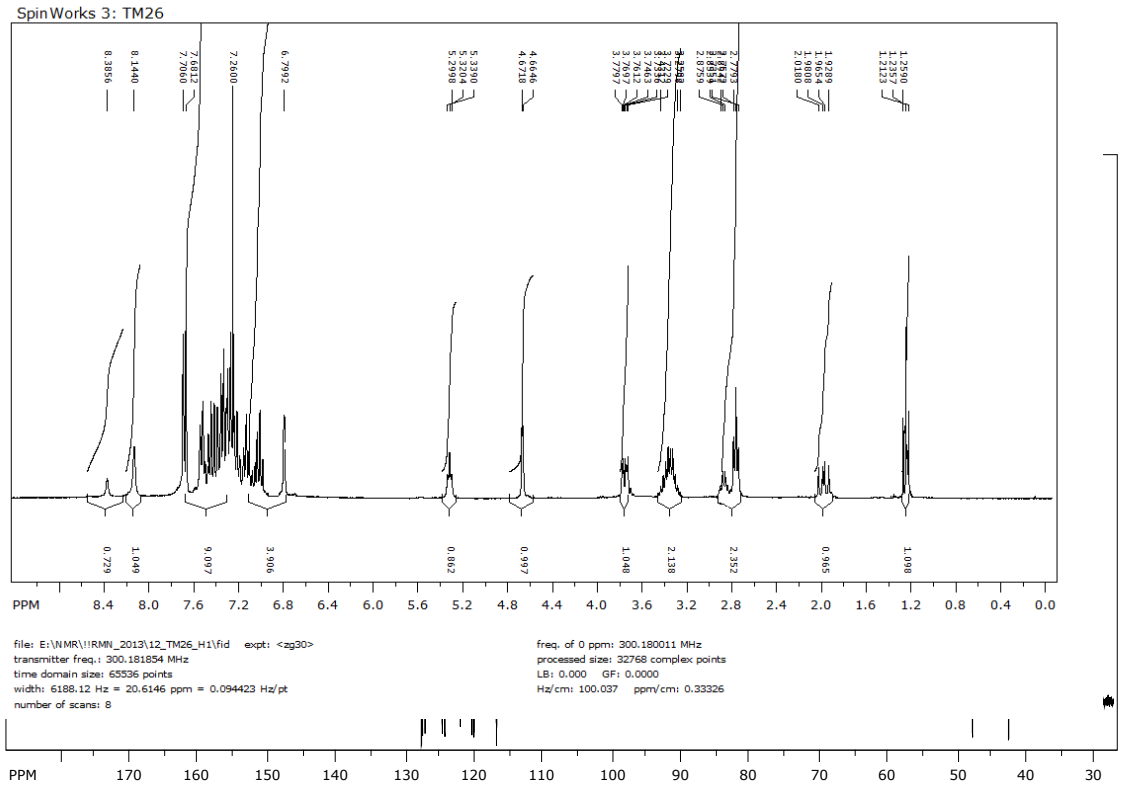

file: E:\NMR\!!RMN_2013\12_TM26_H1\fid expt: <zg30>
transmitter freq.: 300.181854 MHz
time domain size: 65536 points
width: 6188.12 Hz = 20.6146 ppm = 0.094423 Hz/pt
number of scans: 8

freq. of 0 ppm: 300.180011 MHz
processed size: 32768 complex points
LB: 0.000 GF: 0.0000
Hz/cm: 100.037 ppm/cm: 0.33326

file: ...3,5dichloranilin_succinic_acid\fid expt: <jmod>
transmitter freq.: 75.487869 MHz
time domain size: 65536 points
width: 22727.27 Hz = 301.0719 ppm = 0.346791 Hz/pt
number of scans: 320

freq. of 0 ppm: 75.480357 MHz
processed size: 131072 complex points
LB: 0.000 GF: 0.0000
Hz/cm: 434.507 ppm/cm: 5.75599

Compound 10d:

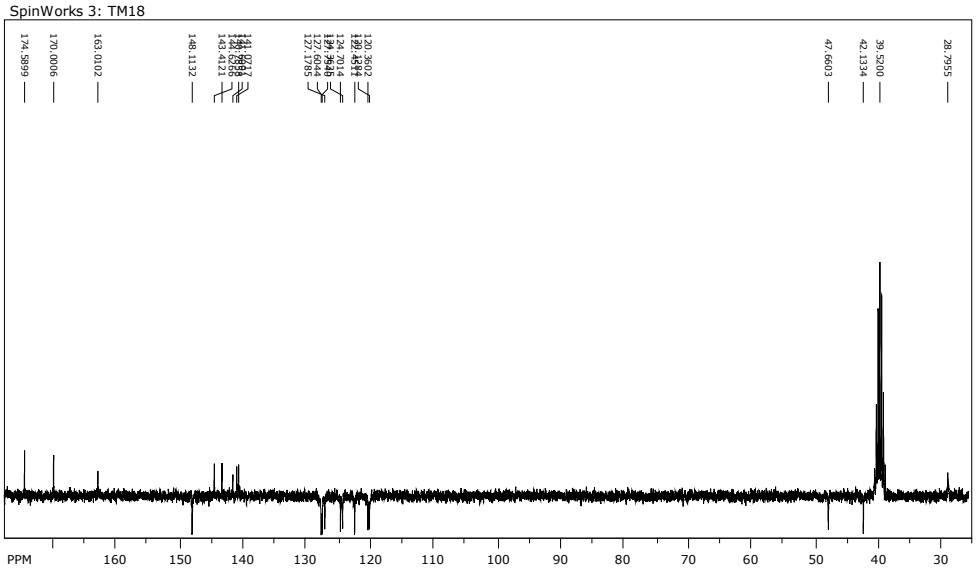

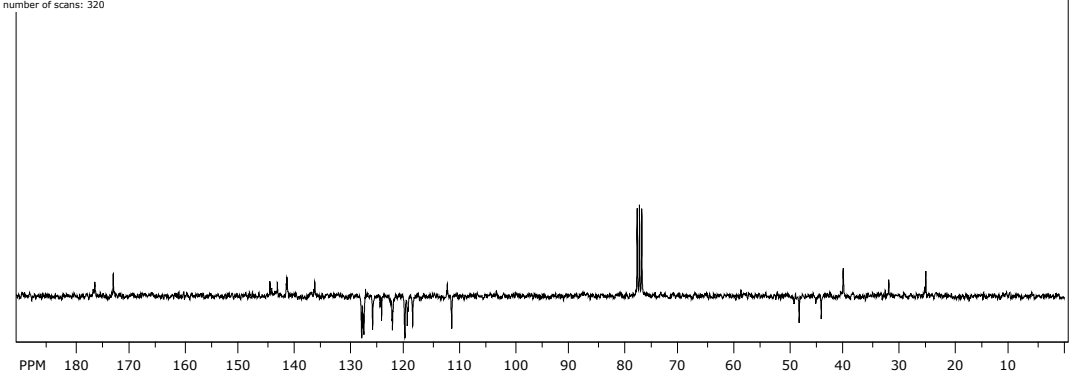

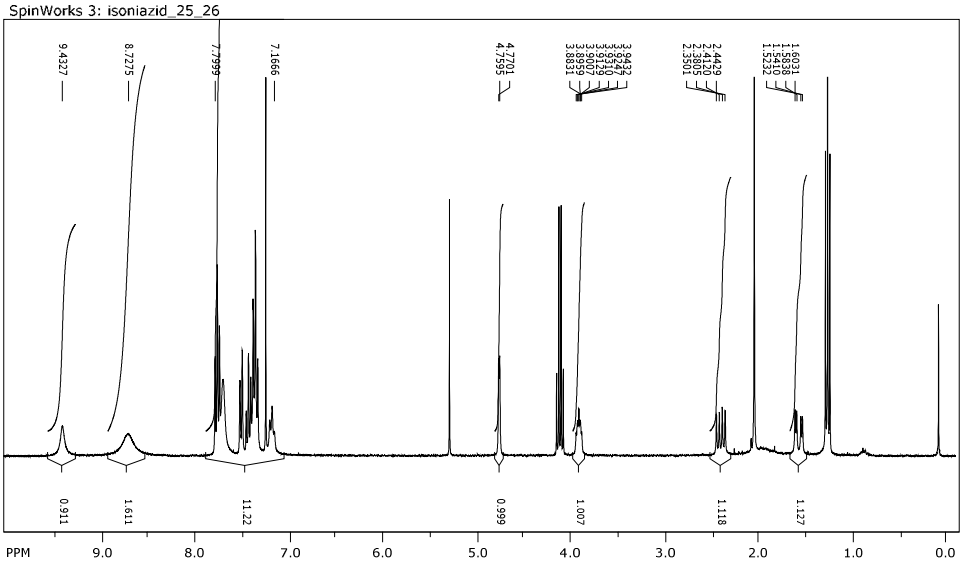

Compound 11a:

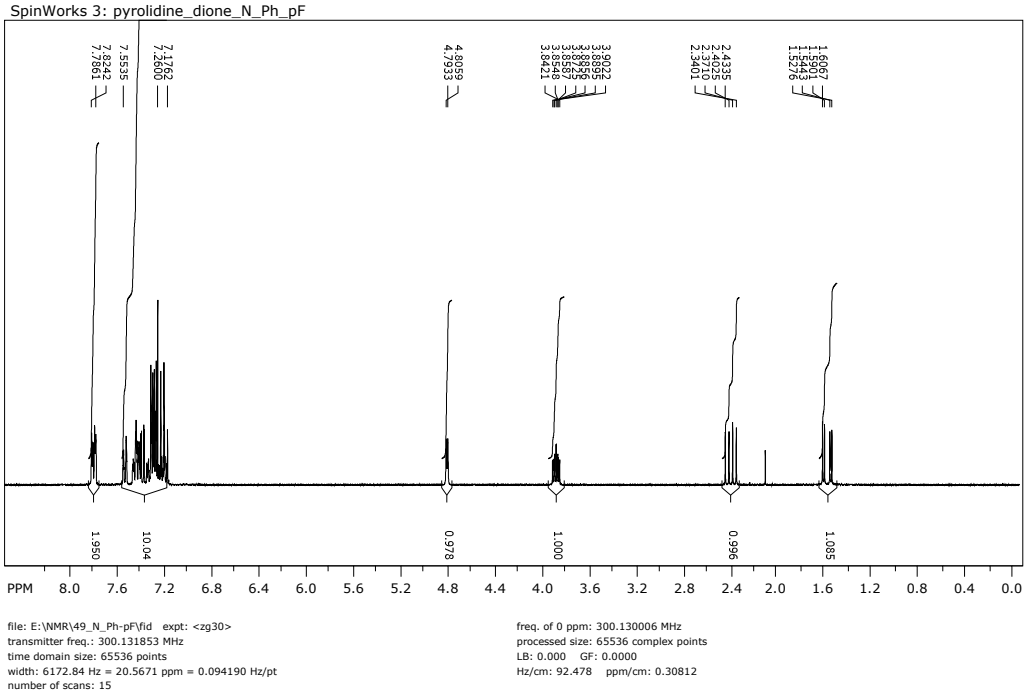

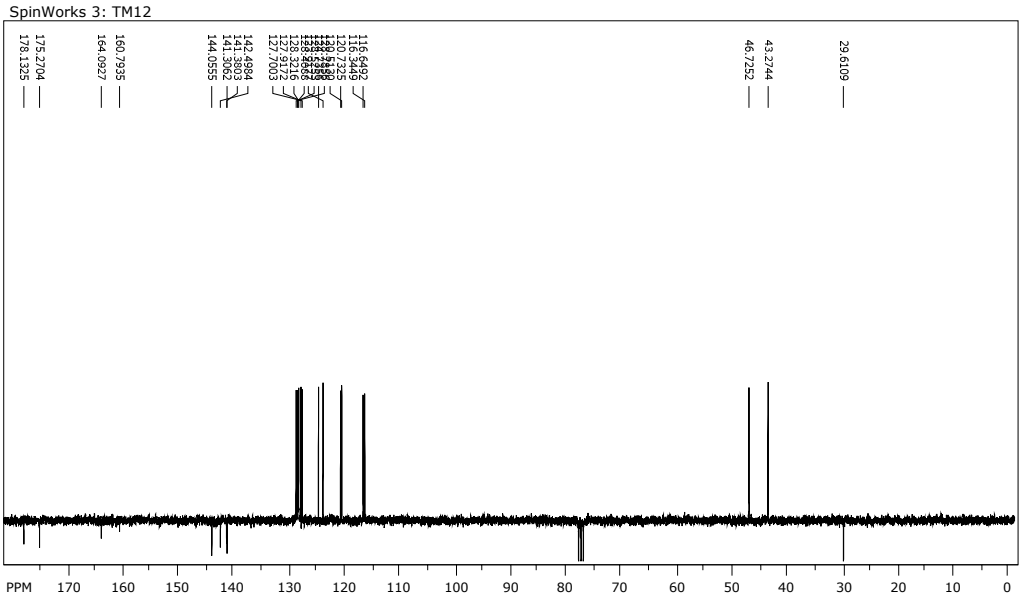

file: E:\NMR\!!RMN_2013\300b_2013\33\fid expt: <jmod>
transmitter freq.: 75.487869 MHz
time domain size: 65536 points
width: 22727.27 Hz = 301.0719 ppm = 0.346791 Hz/pt
number of scans: 340

freq. of 0 ppm: 75.480312 MHz
processed size: 131072 complex points
LB: 0.000 GF: 0.0000
Hz/cm: 493.788 ppm/cm: 6.54129

Compound 11b:

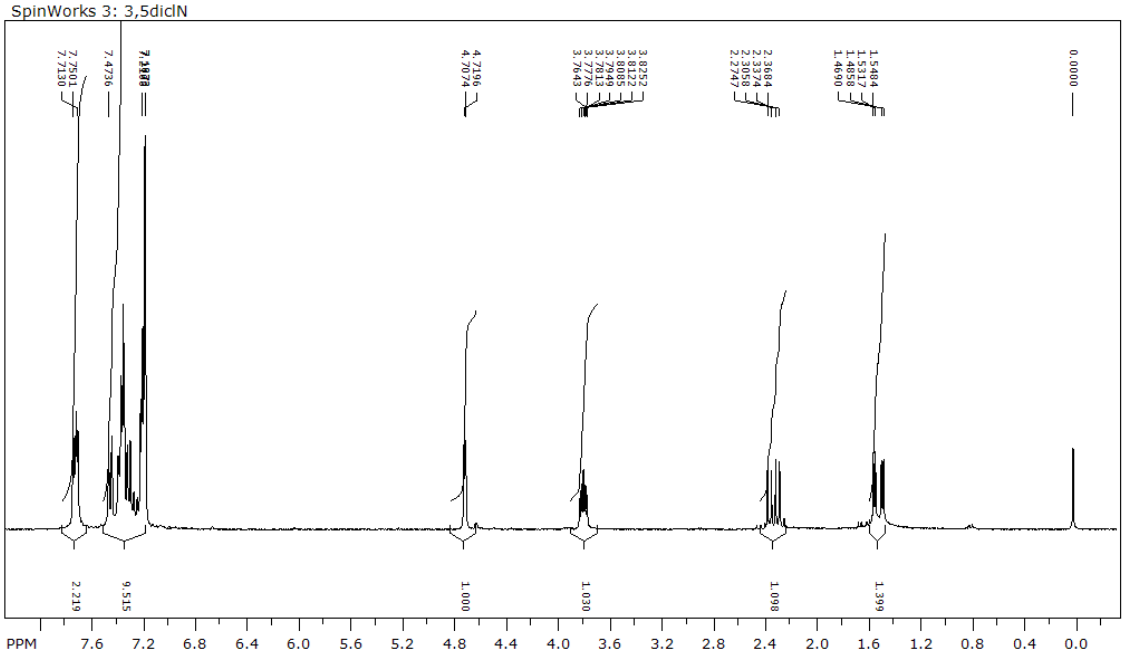

file: E:\NMR\83\fid expt: <zg30>
transmitter freq.: 300.181854 MHz
time domain size: 65536 points
width: 6188.12 Hz = 20.6146 ppm = 0.094423 Hz/pt
number of scans: 8

freq. of 0 ppm: 300.180033 MHz
processed size: 32768 complex points
LB: 0.000 GF: 0.0000
Hz/cm: 92.410 ppm/cm: 0.30785

SpinWorks 3: N-dichlorosuccinimide

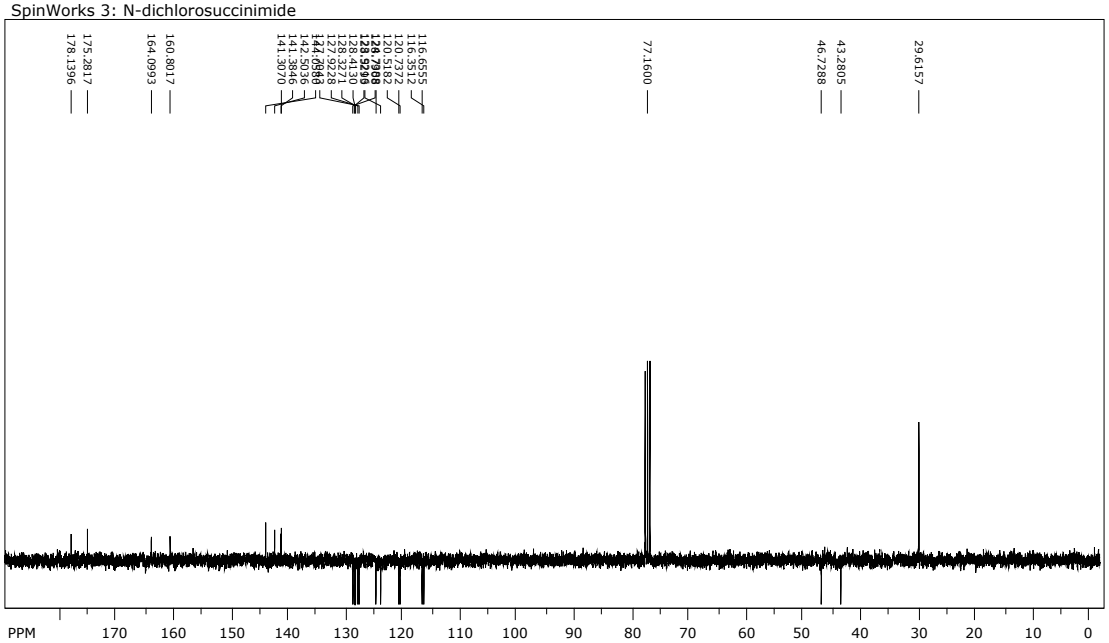

file: ...MR\95_C13_N-diClPh_succinimide\fid expt: <jmod>
transmitter freq.: 75.487869 MHz
time domain size: 65536 points
width: 22727.27 Hz = 301.0719 ppm = 0.346791 Hz/pt
number of scans: 310

freq. of 0 ppm: 75.480312 MHz
processed size: 131072 complex points
LB: 0.000 GF: 0.0000
Hz/cm: 517.240 ppm/cm: 6.85196

Compound 11c:

SpinWorks 3: TM17

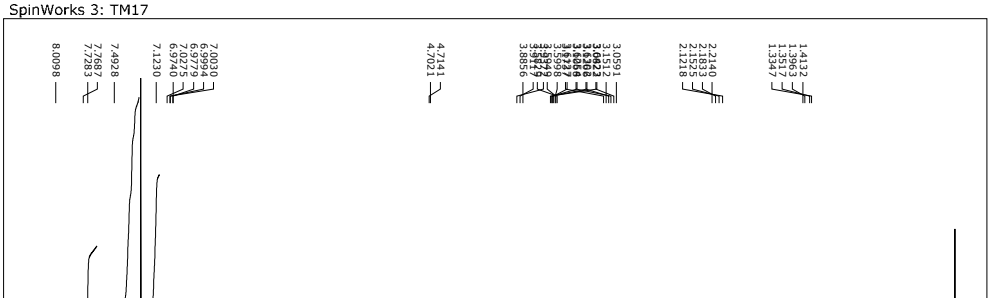

SpinWorks 3: trp_cyclization

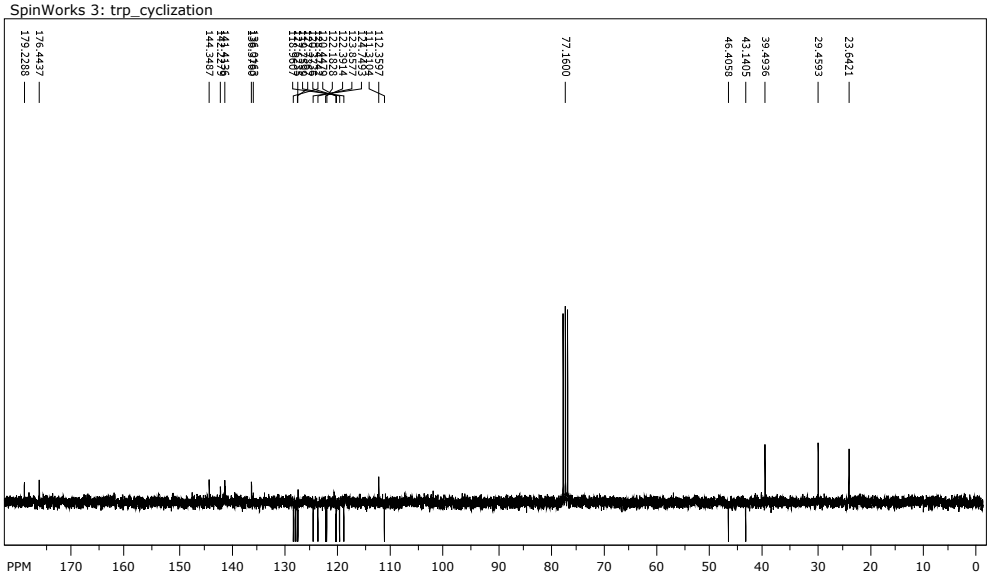

file: E:\NMR\102_Trp_cyclization_C13\fid expt: <jmod>
transmitter freq.: 75.487869 MHz
time domain size: 65536 points
width: 22727.27 Hz = 301.0719 ppm = 0.346791 Hz/pt
number of scans: 420

freq. of 0 ppm: 75.480311 MHz
processed size: 131072 complex points
LB: 0.000 GF: 0.0000
Hz/cm: 497.697 ppm/cm: 6.59307

Compound 11d:

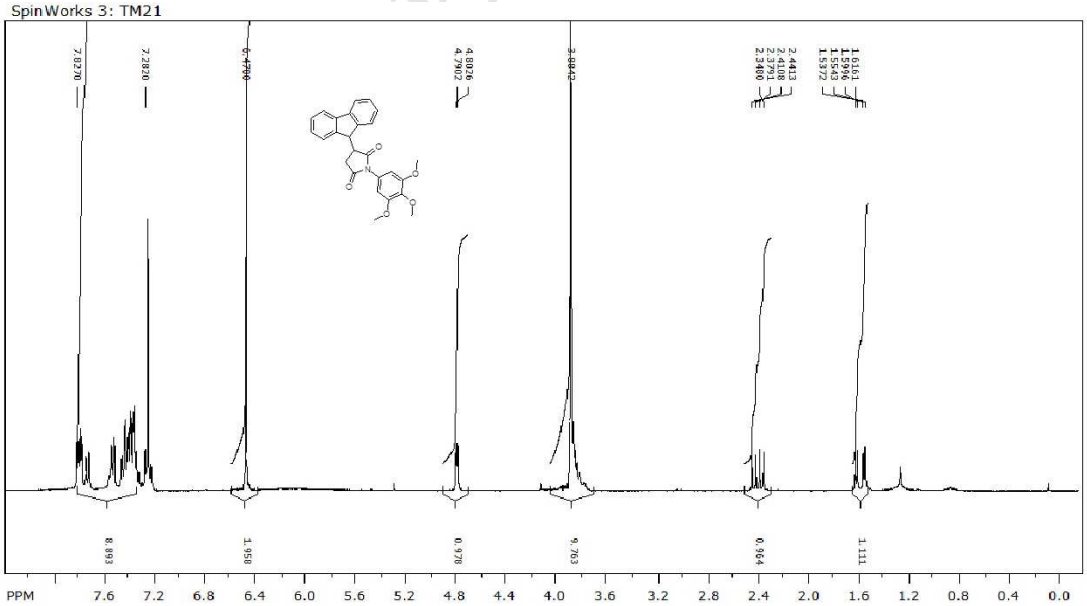

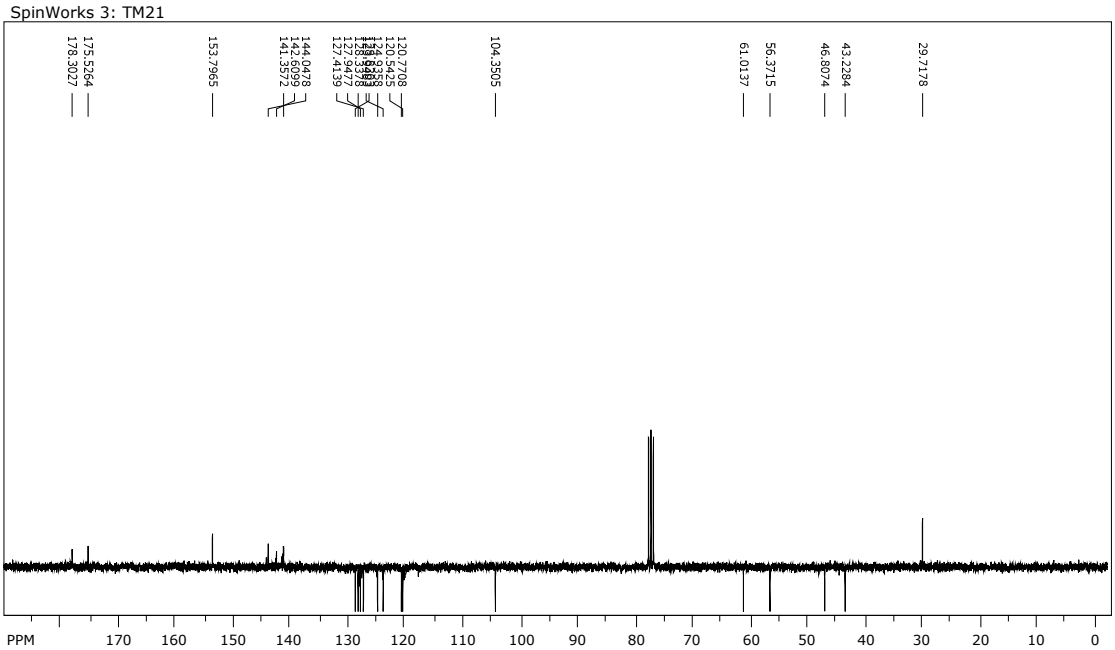

file: E:\NMR\!!RMN_2013\18_TM21_C13\fid expt: <jmod>
transmitter freq.: 75.487869 MHz
time domain size: 65536 points
width: 22727.27 Hz = 301.0719 ppm = 0.346791 Hz/pt
number of scans: 520

freq. of 0 ppm: 75.480312 MHz
processed size: 131072 complex points
LB: 0.000 GF: 0.0000
Hz/cm: 519.845 ppm/cm: 6.88648

II. Crystallographic data

Compound 2

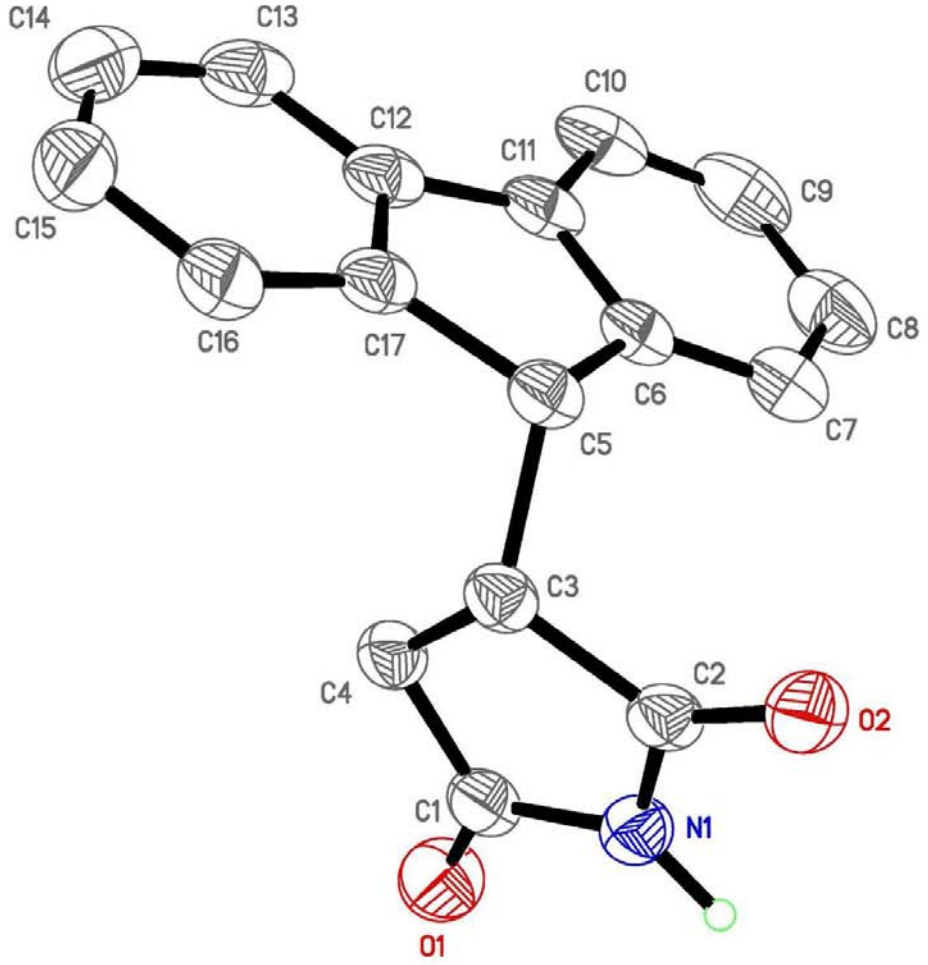

Table 1. Crystal data and structure refinement for tetiana3m.

Identification code	tetiana3m
Empirical formula	C17 H13 N O2
Formula weight	263.28
Temperature	193(2) K

Wavelength	0.71073 Å	
Crystal system	Monoclinic	
Space group	P2(1)/n	
Unit cell dimensions	a = 5.5615(4) Å	α= 90°.
	b = 10.8405(8) Å	β= 96.163(5)°.
	c = 21.6241(18) Å	γ = 90°.
Volume	1296.17(17) $Å^3$	
Z	4	
Density (calculated)	1.349 Mg/m^3	
Absorption coefficient	0.089 mm^{-1}	
F(000)	552	
Crystal size	0.35 x 0.10 x 0.04 mm^3	
Theta range for data collection	5.24 to 27.88°.	
Index ranges	-7<=h<=6, -14<=k<=14, -28<=l<=28	
Reflections collected	19411	
Independent reflections	3075 [R(int) = 0.0672]	
Completeness to theta = 27.88°	99.2 %	
Absorption correction	Semi-empirical from equivalents	
Max. and min. transmission	0.9965 and 0.9695	
Refinement method	Full-matrix least-squares on F^2	
Data / restraints / parameters	3075 / 0 / 185	
Goodness-of-fit on F^2	0.999	
Final R indices [I>2sigma(I)]	R1 = 0.0498, wR2 = 0.0985	
R indices (all data)	R1 = 0.0995, wR2 = 0.1173	
Largest diff. peak and hole	0.187 and -0.185 $e.Å^{-3}$	

Table 2. Atomic coordinates (x 10^4) and equivalent isotropic displacement parameters ($Å^2$x 10^3) for tetiana3m. U(eq) is defined as one third of the trace of the orthogonalized U^{ij} tensor.

	x	y	z	U(eq)
O(1)	-764(2)	-1616(1)	626(1)	51(1)
O(2)	5900(2)	843(1)	700(1)	40(1)
N(1)	2643(3)	-465(1)	531(1)	35(1)
C(1)	767(3)	-903(2)	844(1)	35(1)
C(2)	4152(3)	325(2)	878(1)	31(1)
C(3)	3332(3)	430(1)	1519(1)	30(1)
C(4)	992(3)	-321(2)	1475(1)	33(1)
C(5)	3129(3)	1769(1)	1740(1)	30(1)
C(6)	1318(3)	2570(2)	1347(1)	32(1)
C(7)	1226(4)	2869(2)	723(1)	41(1)
C(8)	-618(4)	3641(2)	466(1)	53(1)
C(9)	-2284(4)	4127(2)	829(1)	55(1)
C(10)	-2195(3)	3841(2)	1451(1)	45(1)
C(11)	-402(3)	3042(2)	1710(1)	35(1)
C(12)	110(3)	2559(2)	2341(1)	34(1)
C(13)	-1104(4)	2689(2)	2867(1)	44(1)
C(14)	-231(4)	2104(2)	3412(1)	51(1)
C(15)	1838(4)	1383(2)	3436(1)	48(1)
C(16)	3051(3)	1239(2)	2915(1)	38(1)
C(17)	2193(3)	1823(2)	2370(1)	31(1)

Table 3. Bond lengths [Å] and angles [°] for tetiana3m.

O(1)-C(1)	1.207(2)
O(2)-C(2)	1.2205(19)
N(1)-C(2)	1.365(2)
N(1)-C(1)	1.386(2)
C(1)-C(4)	1.497(3)
C(2)-C(3)	1.509(2)
C(3)-C(4)	1.529(2)
C(3)-C(5)	1.536(2)
C(5)-C(17)	1.511(2)
C(5)-C(6)	1.519(2)
C(6)-C(7)	1.383(3)
C(6)-C(11)	1.397(3)
C(7)-C(8)	1.392(3)
C(8)-C(9)	1.380(3)
C(9)-C(10)	1.376(3)
C(10)-C(11)	1.392(3)
C(11)-C(12)	1.463(3)
C(12)-C(13)	1.390(3)
C(12)-C(17)	1.402(2)
C(13)-C(14)	1.379(3)
C(14)-C(15)	1.388(3)
C(15)-C(16)	1.383(3)
C(16)-C(17)	1.378(3)
C(2)-N(1)-C(1)	113.42(16)
O(1)-C(1)-N(1)	124.43(18)
O(1)-C(1)-C(4)	127.72(17)
N(1)-C(1)-C(4)	107.84(15)
O(2)-C(2)-N(1)	125.36(17)
O(2)-C(2)-C(3)	125.78(16)
N(1)-C(2)-C(3)	108.86(14)
C(2)-C(3)-C(4)	103.98(14)
C(2)-C(3)-C(5)	113.30(14)
C(4)-C(3)-C(5)	115.60(13)
C(1)-C(4)-C(3)	105.58(14)
C(17)-C(5)-C(6)	102.13(13)

C(17)-C(5)-C(3)	111.12(13)
C(6)-C(5)-C(3)	115.70(14)
C(7)-C(6)-C(11)	120.39(16)
C(7)-C(6)-C(5)	129.23(16)
C(11)-C(6)-C(5)	110.38(16)
C(6)-C(7)-C(8)	118.6(2)
C(9)-C(8)-C(7)	120.9(2)
C(10)-C(9)-C(8)	120.91(19)
C(9)-C(10)-C(11)	118.8(2)
C(10)-C(11)-C(6)	120.43(19)
C(10)-C(11)-C(12)	131.09(18)
C(6)-C(11)-C(12)	108.47(15)
C(13)-C(12)-C(17)	119.54(18)
C(13)-C(12)-C(11)	131.66(18)
C(17)-C(12)-C(11)	108.78(16)
C(14)-C(13)-C(12)	119.65(19)
C(13)-C(14)-C(15)	120.37(19)
C(16)-C(15)-C(14)	120.5(2)
C(17)-C(16)-C(15)	119.39(18)
C(16)-C(17)-C(12)	120.52(17)
C(16)-C(17)-C(5)	129.23(16)
C(12)-C(17)-C(5)	110.21(15)

Symmetry transformations used to generate equivalent atoms:

Table 4. Anisotropic displacement parameters ($Å^2 x 10^3$) for tetiana3m. The anisotropic displacement factor exponent takes the form: $-2\pi^2[h^2 a^{*2} U^{11} + ... + 2 h k a^* b^* U^{12}]$

	U^{11}	U^{22}	U^{33}	U^{23}	U^{13}	U^{12}
O(1)	49(1)	47(1)	56(1)	-11(1)	9(1)	-18(1)
O(2)	32(1)	39(1)	52(1)	-5(1)	16(1)	-3(1)
N(1)	35(1)	32(1)	39(1)	-4(1)	10(1)	-2(1)
C(1)	34(1)	26(1)	44(1)	0(1)	6(1)	0(1)
C(2)	26(1)	26(1)	43(1)	-1(1)	9(1)	4(1)
C(3)	25(1)	25(1)	39(1)	1(1)	6(1)	2(1)
C(4)	32(1)	28(1)	40(1)	0(1)	11(1)	-1(1)
C(5)	25(1)	24(1)	40(1)	-1(1)	6(1)	0(1)
C(6)	30(1)	21(1)	43(1)	-1(1)	2(1)	-3(1)
C(7)	45(1)	29(1)	49(1)	1(1)	2(1)	0(1)
C(8)	63(1)	36(1)	56(2)	8(1)	-9(1)	0(1)
C(9)	48(1)	30(1)	82(2)	6(1)	-13(1)	4(1)
C(10)	33(1)	25(1)	76(2)	-5(1)	2(1)	2(1)
C(11)	27(1)	22(1)	55(1)	-5(1)	3(1)	-3(1)
C(12)	28(1)	24(1)	50(1)	-9(1)	9(1)	-7(1)
C(13)	36(1)	35(1)	65(2)	-17(1)	19(1)	-8(1)
C(14)	55(1)	49(1)	52(1)	-17(1)	25(1)	-21(1)
C(15)	58(1)	46(1)	41(1)	-2(1)	9(1)	-17(1)
C(16)	39(1)	32(1)	44(1)	-2(1)	4(1)	-4(1)
C(17)	28(1)	24(1)	41(1)	-6(1)	6(1)	-5(1)

Table 5. Hydrogen coordinates (x 10^4) and isotropic displacement parameters ($Å^2$x 10^3) for tetiana3m.

	x	y	z	U(eq)
H(3)	4552	0	1818	36
H(4A)	1078	-961	1804	39
H(4B)	-411	221	1521	39
H(5)	4760	2166	1767	36
H(7)	2396	2555	475	50
H(8)	-732	3837	36	63
H(9)	-3508	4665	646	66
H(10)	-3337	4183	1700	54
H(13)	-2527	3177	2851	53
H(14)	-1050	2197	3772	61
H(15)	2425	984	3813	57
H(16)	4464	742	2933	46
H(1)	2890(40)	-673(19)	110(11)	57(6)

Compound 8a

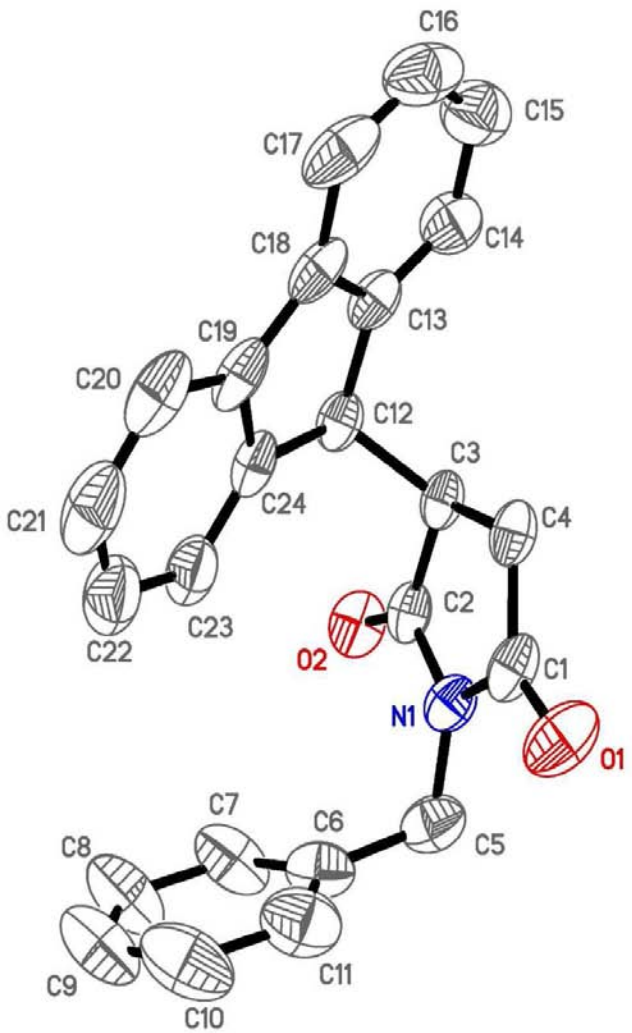

Table 1. Crystal data and structure refinement for tetiana2m.

Identification code	tetiana2m	
Empirical formula	C24 H19 N O2	
Formula weight	353.40	
Temperature	193(2) K	
Wavelength	0.71073 Å	
Crystal system	Monoclinic	
Space group	P2(1)	
Unit cell dimensions	a = 6.2750(4) Å	α= 90°.
	b = 11.4164(6) Å	β= 93.845(2)°.
	c = 13.0178(8) Å	γ = 90°.
Volume	930.47(10) $Å^3$	
Z	2	

Density (calculated)	1.261 Mg/m^3
Absorption coefficient	0.080 mm^{-1}
F(000)	372
Crystal size	0.40 x 0.22 x 0.10 mm^3
Theta range for data collection	5.15 to 24.71°.
Index ranges	-7<=h<=7, -13<=k<=12, -15<=l<=15
Reflections collected	17683
Independent reflections	3054 [R(int) = 0.0294]
Completeness to theta = 24.71°	98.6 %
Absorption correction	Semi-empirical from equivalents
Max. and min. transmission	0.9920 and 0.9687
Refinement method	Full-matrix least-squares on F^2
Data / restraints / parameters	3054 / 1 / 245
Goodness-of-fit on F^2	1.074
Final R indices [I>2sigma(I)]	R1 = 0.0324, wR2 = 0.0747
R indices (all data)	R1 = 0.0380, wR2 = 0.0773
Largest diff. peak and hole	0.113 and -0.092 $e.Å^{-3}$

Table 2. Atomic coordinates (x 10^4) and equivalent isotropic displacement parameters ($Å^2$x 10^3) for tetia2m. U(eq) is defined as one third of the trace of the orthogonalized U^{ij} tensor.

	x	y	z	U(eq)
O(1)	8887(2)	6846(1)	2724(1)	66(1)
O(2)	14576(2)	4888(1)	1576(1)	50(1)
N(1)	11992(2)	5921(1)	2348(1)	40(1)
C(1)	9907(3)	6296(2)	2127(2)	44(1)
C(2)	12791(3)	5306(1)	1549(1)	37(1)
C(3)	11107(3)	5242(1)	677(1)	35(1)
C(4)	9212(3)	5911(2)	1064(1)	39(1)
C(5)	13250(3)	6151(2)	3316(2)	55(1)
C(6)	13176(3)	5121(2)	4039(1)	54(1)
C(7)	14741(4)	4265(2)	4061(2)	70(1)
C(8)	14623(4)	3278(3)	4673(2)	88(1)
C(9)	12931(4)	3149(3)	5279(2)	83(1)
C(10)	11391(4)	3989(3)	5286(2)	84(1)
C(11)	11489(4)	4979(2)	4668(2)	70(1)
C(12)	10612(3)	3965(1)	351(1)	37(1)
C(13)	8969(3)	3919(2)	-556(1)	41(1)
C(14)	8996(3)	4467(2)	-1506(2)	54(1)
C(15)	7270(4)	4337(2)	-2216(2)	66(1)
C(16)	5539(4)	3664(2)	-1989(2)	68(1)
C(17)	5490(3)	3108(2)	-1051(2)	61(1)
C(18)	7211(3)	3245(2)	-311(2)	44(1)
C(19)	7589(3)	2809(2)	742(2)	46(1)
C(20)	6332(4)	2111(2)	1334(2)	60(1)
C(21)	7076(4)	1838(2)	2320(2)	70(1)
C(22)	9040(4)	2242(2)	2726(2)	68(1)
C(23)	10326(4)	2928(2)	2138(2)	54(1)
C(24)	9577(3)	3218(1)	1147(1)	41(1)

Table 3. Bond lengths [Å] and angles [°] for tetia2m.

O(1)-C(1)	1.215(2)
O(2)-C(2)	1.216(2)
N(1)-C(2)	1.377(2)
N(1)-C(1)	1.388(2)
N(1)-C(5)	1.465(3)
C(1)-C(4)	1.488(3)
C(2)-C(3)	1.500(2)
C(3)-C(4)	1.526(2)
C(3)-C(12)	1.544(2)
C(5)-C(6)	1.509(3)
C(6)-C(7)	1.385(3)
C(6)-C(11)	1.390(3)
C(7)-C(8)	1.384(4)
C(8)-C(9)	1.373(3)
C(9)-C(10)	1.362(4)
C(10)-C(11)	1.392(4)
C(12)-C(13)	1.515(3)
C(12)-C(24)	1.521(2)
C(13)-C(14)	1.387(3)
C(13)-C(18)	1.399(2)
C(14)-C(15)	1.384(3)
C(15)-C(16)	1.378(3)
C(16)-C(17)	1.378(3)
C(17)-C(18)	1.407(3)
C(18)-C(19)	1.462(3)
C(19)-C(20)	1.391(3)
C(19)-C(24)	1.402(3)
C(20)-C(21)	1.372(4)
C(21)-C(22)	1.387(4)
C(22)-C(23)	1.391(3)
C(23)-C(24)	1.384(3)
C(2)-N(1)-C(1)	112.71(14)
C(2)-N(1)-C(5)	122.59(15)
C(1)-N(1)-C(5)	124.70(15)
O(1)-C(1)-N(1)	123.76(18)

O(1)-C(1)-C(4)	127.86(18)
N(1)-C(1)-C(4)	108.38(14)
O(2)-C(2)-N(1)	124.06(16)
O(2)-C(2)-C(3)	127.13(16)
N(1)-C(2)-C(3)	108.82(14)
C(2)-C(3)-C(4)	104.53(14)
C(2)-C(3)-C(12)	111.89(13)
C(4)-C(3)-C(12)	114.63(13)
C(1)-C(4)-C(3)	105.55(14)
N(1)-C(5)-C(6)	111.08(15)
C(7)-C(6)-C(11)	118.2(2)
C(7)-C(6)-C(5)	120.81(18)
C(11)-C(6)-C(5)	120.9(2)
C(8)-C(7)-C(6)	121.4(2)
C(9)-C(8)-C(7)	119.5(3)
C(10)-C(9)-C(8)	120.3(3)
C(9)-C(10)-C(11)	120.6(2)
C(6)-C(11)-C(10)	120.0(2)
C(13)-C(12)-C(24)	102.21(13)
C(13)-C(12)-C(3)	111.18(14)
C(24)-C(12)-C(3)	115.39(14)
C(14)-C(13)-C(18)	120.49(18)
C(14)-C(13)-C(12)	129.09(16)
C(18)-C(13)-C(12)	110.38(16)
C(15)-C(14)-C(13)	119.5(2)
C(16)-C(15)-C(14)	120.6(2)
C(15)-C(16)-C(17)	120.8(2)
C(16)-C(17)-C(18)	119.5(2)
C(13)-C(18)-C(17)	119.12(19)
C(13)-C(18)-C(19)	108.62(16)
C(17)-C(18)-C(19)	132.26(18)
C(20)-C(19)-C(24)	120.4(2)
C(20)-C(19)-C(18)	130.73(19)
C(24)-C(19)-C(18)	108.87(15)
C(21)-C(20)-C(19)	118.6(2)
C(20)-C(21)-C(22)	121.3(2)
C(21)-C(22)-C(23)	120.7(2)
C(24)-C(23)-C(22)	118.4(2)

C(23)-C(24)-C(19)	120.58(17)
C(23)-C(24)-C(12)	129.50(17)
C(19)-C(24)-C(12)	109.92(16)

Symmetry transformations used to generate equivalent atoms:

Table 4. Anisotropic displacement parameters ($Å^2 x 10^3$) for tetia2m. The anisotropic displacement factor exponent takes the form: $-2\pi^2[h^2 a^{*2} U^{11} + ... + 2 h k a^* b^* U^{12}]$

	U^{11}	U^{22}	U^{33}	U^{23}	U^{13}	U^{12}
O(1)	58(1)	64(1)	79(1)	-26(1)	22(1)	8(1)
O(2)	29(1)	50(1)	70(1)	-2(1)	10(1)	0(1)
N(1)	38(1)	35(1)	47(1)	-5(1)	8(1)	-5(1)
C(1)	39(1)	30(1)	63(1)	-6(1)	17(1)	-4(1)
C(2)	29(1)	28(1)	54(1)	3(1)	12(1)	-6(1)
C(3)	33(1)	26(1)	48(1)	1(1)	12(1)	-2(1)
C(4)	32(1)	28(1)	58(1)	0(1)	10(1)	-1(1)
C(5)	56(1)	55(1)	55(1)	-12(1)	5(1)	-11(1)
C(6)	47(1)	69(1)	44(1)	-5(1)	4(1)	-8(1)
C(7)	54(1)	103(2)	54(1)	22(1)	6(1)	9(1)
C(8)	82(2)	118(2)	63(2)	35(2)	9(1)	24(2)
C(9)	79(2)	111(2)	58(1)	34(1)	2(1)	-1(2)
C(10)	66(2)	132(3)	55(1)	20(2)	18(1)	-10(2)
C(11)	63(1)	93(2)	57(1)	-2(1)	15(1)	5(1)
C(12)	33(1)	29(1)	50(1)	-2(1)	12(1)	0(1)
C(13)	37(1)	33(1)	54(1)	-12(1)	12(1)	1(1)
C(14)	53(1)	54(1)	56(1)	-6(1)	6(1)	0(1)
C(15)	63(1)	73(2)	60(1)	-9(1)	-1(1)	12(1)
C(16)	55(1)	79(2)	71(2)	-32(1)	-7(1)	16(1)
C(17)	37(1)	56(1)	90(2)	-37(1)	11(1)	-2(1)
C(18)	37(1)	32(1)	65(1)	-21(1)	14(1)	0(1)
C(19)	43(1)	28(1)	69(1)	-15(1)	25(1)	-4(1)
C(20)	59(1)	38(1)	87(2)	-16(1)	33(1)	-13(1)
C(21)	86(2)	40(1)	90(2)	-4(1)	46(2)	-19(1)
C(22)	100(2)	42(1)	67(1)	5(1)	27(1)	-6(1)
C(23)	67(1)	33(1)	62(1)	0(1)	14(1)	-5(1)
C(24)	46(1)	23(1)	57(1)	-5(1)	17(1)	1(1)

Table 5. Hydrogen coordinates (x 10^4) and isotropic displacement parameters ($Å^2$x 10^3) for tetia2m.

	x	y	z	U(eq)
H(3)	11631	5672	74	42
H(4A)	8855	6595	618	47
H(4B)	7941	5398	1071	47
H(5A)	12681	6855	3649	66
H(5B)	14750	6311	3170	66
H(7)	15920	4356	3648	84
H(8)	15705	2696	4673	105
H(9)	12834	2470	5696	100
H(10)	10239	3898	5717	101
H(11)	10403	5558	4675	84
H(12)	11957	3578	157	45
H(14)	10188	4928	-1667	65
H(15)	7279	4714	-2866	79
H(16)	4367	3583	-2485	82
H(17)	4301	2634	-906	73
H(20)	4987	1828	1062	72
H(21)	6228	1365	2733	85
H(22)	9513	2047	3414	82
H(23)	11685	3191	2410	65

Compound 10a:

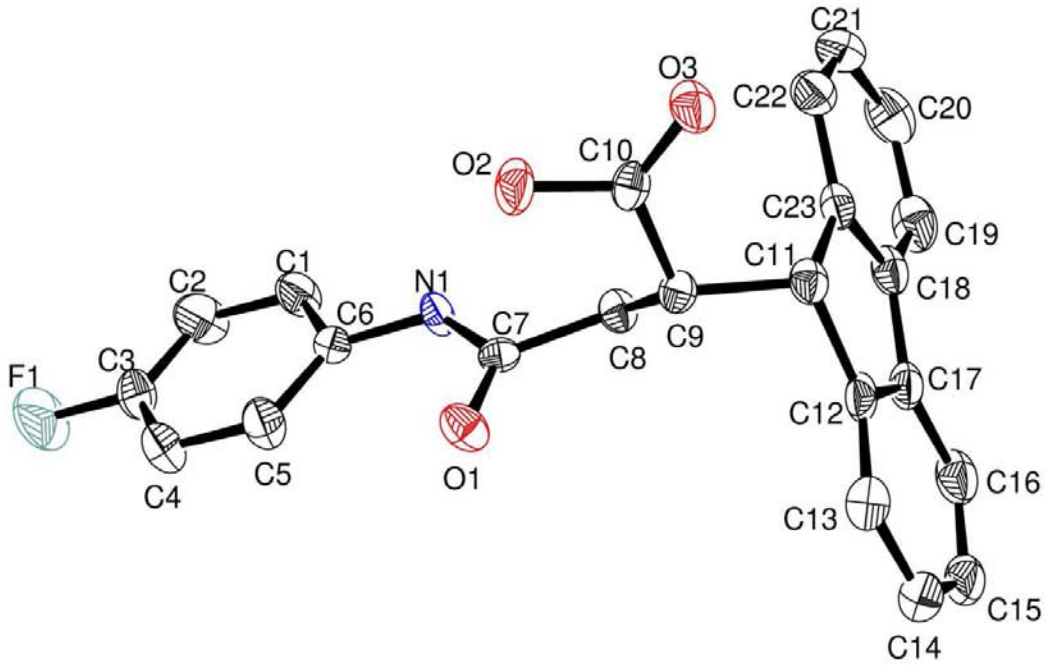

Table 1. Crystal data and structure refinement for tetiana2m.

Identification code	Tetiana2
Empirical formula	C23 H18 F N O3
Formula weight	375.38
Temperature	193(2) K
Wavelength	0.71073 A
Crystal system, space group	monoclinic, P 21/c
Unit cell dimensions	a = 10.201(2) A alpha = 90 deg. b = 18.495(4) A beta = 90.485(9) deg. c = 9.6175(17) A gamma = 90 deg.
Volume	1814.5(6) A^3
Z, Calculated density	4, 1.374 Mg/m^3
Absorption coefficient	0.098 mm^-1
F(000)	784

Crystal size	0.4 x 0.16 x 0.04 mm
Theta range for data collection	2.97 to 24.71 deg.
Limiting indices	-12<=h<=11, -21<=k<=21, -11<=l<=11
Reflections collected / unique	19817 / 2951 [R(int) = 0.1349]
Completeness to theta = 24.71	95.3 %
Max. and min. transmission	0.996 and 0.981
Refinement method	Full-matrix least-squares on F^2
Data / restraints / parameters	2951 / 2 / 261
Goodness-of-fit on F^2	1.021
Final R indices [I>2sigma(I)]	R1 = 0.0537, wR2 = 0.1195
R indices (all data)	R1 = 0.1320, wR2 = 0.1494
Largest diff. peak and hole	0.281 and -0.278 e.A^-3

Table 2. Atomic coordinates (x 10^4) and equivalent isotropic displacement parameters (A^2 x 10^3) for tetiana2m. U(eq) is defined as one third of the trace of the orthogonalized Uij tensor.

	x	y	z	U(eq)
C(1)	5401(3)	3848(2)	4615(3)	34(1)
C(2)	6228(4)	4413(2)	4933(4)	47(1)
C(3)	6587(3)	4519(2)	6284(4)	38(1)
C(4)	6173(3)	4085(2)	7322(3)	36(1)
C(5)	5354(3)	3515(2)	7007(3)	34(1)
C(6)	4961(3)	3392(2)	5648(3)	24(1)
C(7)	3484(3)	2331(2)	6000(3)	21(1)
C(8)	2519(3)	1887(2)	5173(3)	25(1)
C(9)	2352(3)	1103(2)	5628(3)	22(1)
C(10)	3517(3)	635(2)	5300(3)	24(1)
C(11)	1085(3)	778(2)	5011(3)	25(1)
C(12)	-135(3)	1103(2)	5661(3)	27(1)
C(13)	-526(3)	1075(2)	7031(4)	36(1)
C(14)	-1700(4)	1407(2)	7394(4)	43(1)
C(15)	-2467(3)	1751(2)	6389(4)	44(1)
C(16)	-2075(3)	1780(2)	5026(4)	39(1)
C(17)	-901(3)	1450(2)	4652(3)	29(1)
C(18)	-265(3)	1374(2)	3306(3)	29(1)
C(19)	-616(4)	1641(2)	2009(4)	40(1)
C(20)	175(4)	1493(2)	889(4)	45(1)
C(21)	1298(4)	1082(2)	1058(3)	41(1)
C(22)	1651(3)	811(2)	2351(3)	35(1)
C(23)	872(3)	964(2)	3480(3)	26(1)
N(1)	4121(2)	2826(2)	5227(2)	24(1)
O(1)	3628(2)	2265(1)	7265(2)	30(1)
O(2)	4640(2)	913(1)	5730(3)	40(1)
O(3)	3443(2)	51(1)	4739(2)	34(1)
F(1)	7397(2)	5082(1)	6617(2)	65(1)

Table 3. Bond lengths [A] and angles [deg] for tetiana2m.

C(1)-C(2)	1.376(5)
C(1)-C(6)	1.381(5)
C(1)-H(1)	0.9500
C(2)-C(3)	1.361(5)
C(2)-H(2)	0.9500
C(3)-C(4)	1.351(5)
C(3)-F(1)	1.366(4)
C(4)-C(5)	1.378(5)
C(4)-H(4)	0.9500
C(5)-C(6)	1.383(4)
C(5)-H(5)	0.9500
C(6)-N(1)	1.411(4)
C(7)-O(1)	1.231(3)
C(7)-N(1)	1.349(4)
C(7)-C(8)	1.504(4)
C(8)-C(9)	1.525(4)
C(8)-H(8A)	0.9900
C(8)-H(8B)	0.9900
C(9)-C(10)	1.505(4)
C(9)-C(11)	1.540(4)
C(9)-H(9)	1.0000
C(10)-O(3)	1.210(4)
C(10)-O(2)	1.319(4)
C(11)-C(12)	1.521(4)
C(11)-C(23)	1.526(4)
C(11)-H(11)	1.0000
C(12)-C(13)	1.381(4)
C(12)-C(17)	1.397(4)
C(13)-C(14)	1.393(5)
C(13)-H(13)	0.9500
C(14)-C(15)	1.392(5)
C(14)-H(14)	0.9500
C(15)-C(16)	1.375(5)
C(15)-H(15)	0.9500
C(16)-C(17)	1.394(5)
C(16)-H(16)	0.9500
C(17)-C(18)	1.460(5)
C(18)-C(19)	1.385(5)
C(18)-C(23)	1.395(4)
C(19)-C(20)	1.379(5)
C(19)-H(19)	0.9500
C(20)-C(21)	1.383(5)
C(20)-H(20)	0.9500
C(21)-C(22)	1.386(5)
C(21)-H(21)	0.9500
C(22)-C(23)	1.381(5)
C(22)-H(22)	0.9500
N(1)-H(101)	0.884(10)
O(2)-H(102)	0.848(10)
C(2)-C(1)-C(6)	120.4(3)
C(2)-C(1)-H(1)	119.8
C(6)-C(1)-H(1)	119.8

C(3)-C(2)-C(1)	118.7(3)
C(3)-C(2)-H(2)	120.7
C(1)-C(2)-H(2)	120.7
C(4)-C(3)-C(2)	122.5(3)
C(4)-C(3)-F(1)	118.1(3)
C(2)-C(3)-F(1)	119.4(3)
C(3)-C(4)-C(5)	119.0(3)
C(3)-C(4)-H(4)	120.5
C(5)-C(4)-H(4)	120.5
C(4)-C(5)-C(6)	120.2(3)
C(4)-C(5)-H(5)	119.9
C(6)-C(5)-H(5)	119.9
C(1)-C(6)-C(5)	119.1(3)
C(1)-C(6)-N(1)	116.6(3)
C(5)-C(6)-N(1)	124.3(3)
O(1)-C(7)-N(1)	123.9(3)
O(1)-C(7)-C(8)	122.7(3)
N(1)-C(7)-C(8)	113.3(3)
C(7)-C(8)-C(9)	116.2(2)
C(7)-C(8)-H(8A)	108.2
C(9)-C(8)-H(8A)	108.2
C(7)-C(8)-H(8B)	108.2
C(9)-C(8)-H(8B)	108.2
H(8A)-C(8)-H(8B)	107.4
C(10)-C(9)-C(8)	113.3(3)
C(10)-C(9)-C(11)	110.9(3)
C(8)-C(9)-C(11)	110.8(2)
C(10)-C(9)-H(9)	107.1
C(8)-C(9)-H(9)	107.1
C(11)-C(9)-H(9)	107.1
O(3)-C(10)-O(2)	122.6(3)
O(3)-C(10)-C(9)	124.1(3)
O(2)-C(10)-C(9)	113.3(3)
C(12)-C(11)-C(23)	101.4(2)
C(12)-C(11)-C(9)	112.0(3)
C(23)-C(11)-C(9)	113.4(3)
C(12)-C(11)-H(11)	109.9
C(23)-C(11)-H(11)	109.9
C(9)-C(11)-H(11)	109.9
C(13)-C(12)-C(17)	121.0(3)
C(13)-C(12)-C(11)	128.4(3)
C(17)-C(12)-C(11)	110.6(3)
C(12)-C(13)-C(14)	118.6(3)
C(12)-C(13)-H(13)	120.7
C(14)-C(13)-H(13)	120.7
C(15)-C(14)-C(13)	120.5(4)
C(15)-C(14)-H(14)	119.8
C(13)-C(14)-H(14)	119.8
C(16)-C(15)-C(14)	120.9(3)
C(16)-C(15)-H(15)	119.5
C(14)-C(15)-H(15)	119.5
C(15)-C(16)-C(17)	119.1(3)
C(15)-C(16)-H(16)	120.5
C(17)-C(16)-H(16)	120.5
C(16)-C(17)-C(12)	119.9(3)
C(16)-C(17)-C(18)	131.3(3)
C(12)-C(17)-C(18)	108.8(3)
C(19)-C(18)-C(23)	120.7(3)

C(19)-C(18)-C(17)	130.6(3)
C(23)-C(18)-C(17)	108.7(3)
C(20)-C(19)-C(18)	118.9(3)
C(20)-C(19)-H(19)	120.5
C(18)-C(19)-H(19)	120.5
C(19)-C(20)-C(21)	120.5(3)
C(19)-C(20)-H(20)	119.8
C(21)-C(20)-H(20)	119.8
C(20)-C(21)-C(22)	120.9(3)
C(20)-C(21)-H(21)	119.6
C(22)-C(21)-H(21)	119.6
C(23)-C(22)-C(21)	119.0(3)
C(23)-C(22)-H(22)	120.5
C(21)-C(22)-H(22)	120.5
C(22)-C(23)-C(18)	120.1(3)
C(22)-C(23)-C(11)	129.4(3)
C(18)-C(23)-C(11)	110.5(3)
C(7)-N(1)-C(6)	129.8(2)
C(7)-N(1)-H(101)	115(2)
C(6)-N(1)-H(101)	114(2)
C(10)-O(2)-H(102)	109(3)

Symmetry transformations used to generate equivalent atoms:

Table 4. Anisotropic displacement parameters (A^2 x 10^3) for tetiana2m.
The anisotropic displacement factor exponent takes the form:
-2 pi^2 [h^2 a*^2 U11 + ... + 2 h k a* b* U12]

	U11	U22	U33	U23	U13	U12
C(1)	45(2)	32(3)	26(2)	-2(2)	4(2)	-12(2)
C(2)	65(3)	38(3)	37(2)	-2(2)	15(2)	-24(2)
C(3)	35(2)	29(2)	50(3)	-12(2)	3(2)	-16(2)
C(4)	41(2)	34(3)	33(2)	-7(2)	-7(2)	-6(2)
C(5)	38(2)	35(3)	29(2)	2(2)	-4(2)	-10(2)
C(6)	22(2)	24(2)	24(2)	-3(2)	1(1)	-1(2)
C(7)	22(2)	18(2)	22(2)	0(2)	3(1)	5(2)
C(8)	25(2)	24(2)	25(2)	0(2)	-3(1)	-1(2)
C(9)	21(2)	21(2)	24(2)	2(1)	0(1)	-1(2)
C(10)	20(2)	26(2)	26(2)	6(2)	-3(1)	-2(2)
C(11)	23(2)	17(2)	34(2)	-2(2)	-3(1)	1(2)
C(12)	21(2)	20(2)	41(2)	-4(2)	-1(2)	-8(2)
C(13)	30(2)	38(3)	40(2)	-2(2)	-1(2)	-6(2)
C(14)	32(2)	46(3)	50(2)	-14(2)	8(2)	-9(2)
C(15)	23(2)	42(3)	65(3)	-24(2)	2(2)	-1(2)
C(16)	28(2)	32(3)	56(3)	-11(2)	-10(2)	3(2)
C(17)	19(2)	26(2)	41(2)	-7(2)	-5(2)	-1(2)
C(18)	25(2)	25(2)	37(2)	-3(2)	-10(2)	0(2)
C(19)	34(2)	34(3)	51(2)	-2(2)	-14(2)	4(2)
C(20)	54(3)	44(3)	36(2)	-2(2)	-13(2)	-4(2)
C(21)	41(2)	49(3)	32(2)	-13(2)	3(2)	-1(2)
C(22)	31(2)	38(3)	34(2)	-9(2)	-4(2)	3(2)

C(23)	24(2)	23(2)	31(2)	-3(2)	-5(2)	-5(2)
N(1)	29(2)	25(2)	17(2)	1(1)	-3(1)	-11(1)
O(1)	43(2)	27(2)	20(1)	2(1)	-2(1)	-5(1)
O(2)	19(1)	32(2)	68(2)	-16(1)	-7(1)	3(1)
O(3)	28(1)	23(2)	50(2)	-10(1)	-7(1)	5(1)
F(1)	77(2)	52(2)	65(2)	-17(1)	8(1)	-39(1)

Table 5. Hydrogen bonds for tetiana2m [A and deg.].

D-H...A	d(D-H)	d(H...A)	d(D...A)	<(DHA)
N(1)-H(101)...O(1)#1	0.884(10)	2.020(12)	2.893(3)	169(3)
O(2)-H(102)...O(3)#2	0.848(10)	1.839(11)	2.688(3)	179(4)

Symmetry transformations used to generate equivalent atoms:
#1 x,-y+1/2,z-1/2 #2 -x+1,-y,-z+1

III.SFC separation

Le 30 mai 2011 **Projet : Lherbet**

Préparation des échantillons

Produit 1 : TE1, 1.05 mg sont dilués dans 1 mL de CH3OH. [TE1] = 1.05 mg/mL

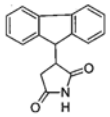

Screening sur 4 colonnes différentes avec différents % de CH3OH comme co-solvant.

Colonne Chiralpak OJH 5µm (4.6x250)mm (cellulose tris(4-methylbenzoate) avec 20 % CH3OH :

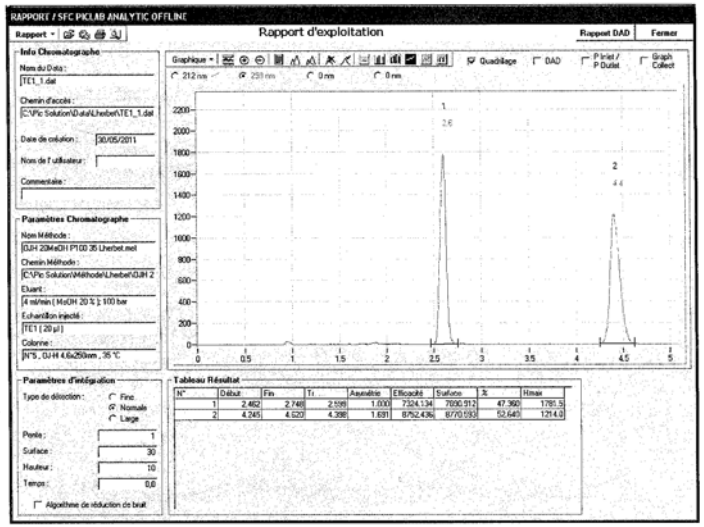

=(4.398-0.941)/(2.599-0.941)=2.085

Séparation facile transposable en chromatographie préparative !

Colonne Chiralpak OJH 5µm (4.6x250)mm (cellulose tris(4-methylbenzoate) avec 15 % CH3OH :

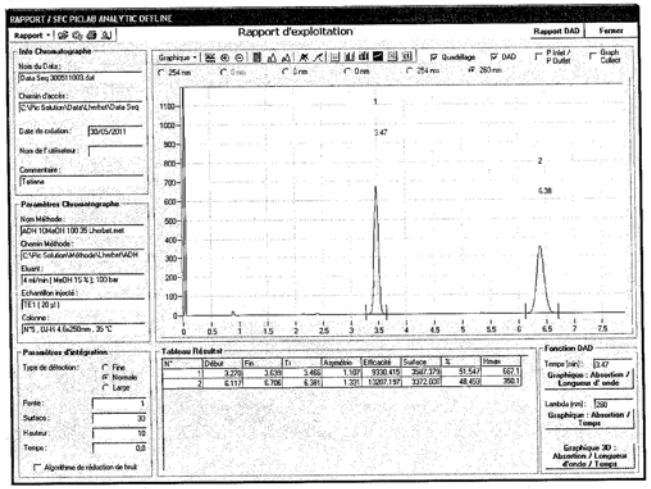

α=(6.38-0.94)/(3.47-0.94)=2.15

Ces conditions peuvent être essayées pour la chromatographie préparative si nécessaire.

Colonne Chiralpak ASH 5µm (4.6x250)mm (amylose tris[(S)-methylbenzyl carbamate]) avec 10 % CH3OH :

L'injection de 10 µL de TE1 donne 2 pics séparés à 11.5 et 15.5 min.

Colonne Chiralpak ODH 5µm (4.6x250)mm (cellulose tris(3,5-dimethylphenylcarbamate)avec 15% CH3OH :

L'injection de 10 µL de TE1 donne 2 pics confondus à 12 et 13.2 min.

Colonne Chiralpak ADH 5µm (4.6x250)mm (amylose tris(3,5-dimethylphenylcarbamate) avec 20 % CH3OH :

L'injection de 10 µL de TE1 donne 2 pics séparés à 5.8 et 13.4 min.

Le 01 juin 2011 **Projet : Lherbet**

Préparation des échantillons

Produit 1 : F02, 30 mg sont dilués dans 1 mL de CH3CN. [F02] = 30mg/mL

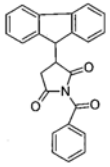

Colonne analytique Chiralpak OJH 5µm (4.6x250) mm (cellulose tris(4-methylbenzoate) avec 20 % CH3CN, boucle d'injection 50 µL :

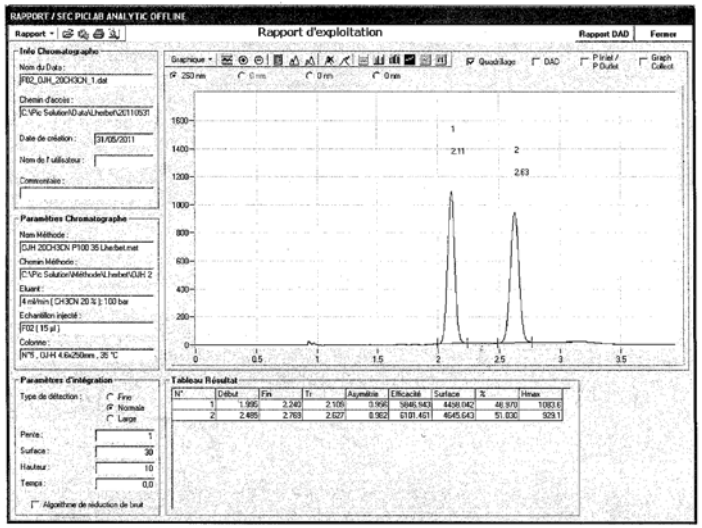

Colonne préparative Chiralpak OJH 5µm (10x250) mm (cellulose tris(4-methylbenzoate) avec 15 % CH3CN, 40 °C, Pout=120 bar :

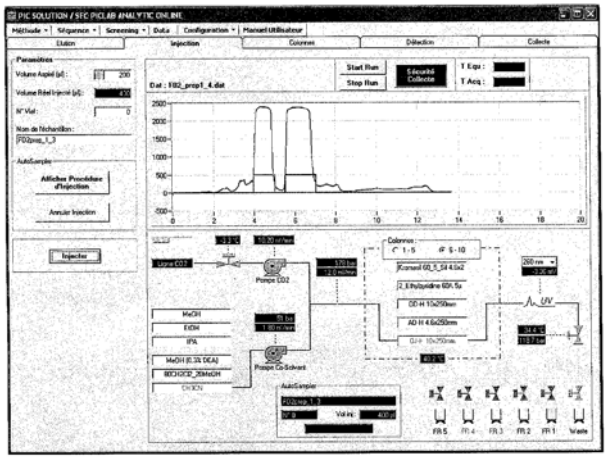

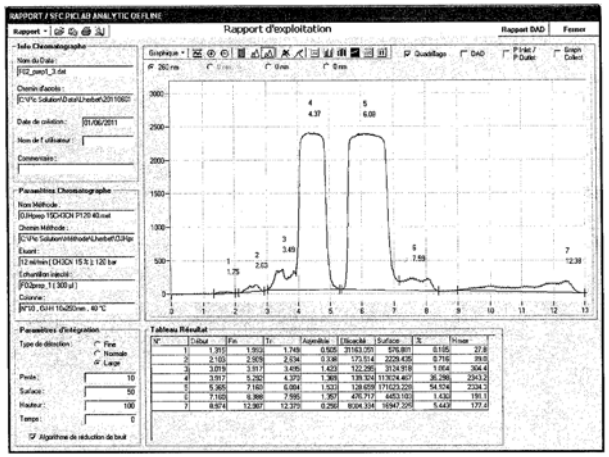

Le 15 juin 2011 **Projet : Lherbet**

Préparation des échantillons

Produit 1 : F02X, 40 mg sont dilués dans 1.5 mL de CH3CN. [F02X] = 26.6 mg/mL

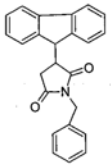

Colonne analytique Chiralpak OJH 5µm (4.6x250) mm (cellulose tris(4-methylbenzoate) avec 20 % CH3CN, boucle d'injection 400 µL :